Charles University in Prague
Faculty of Mathematics and Physics

DIPLOMA THESIS

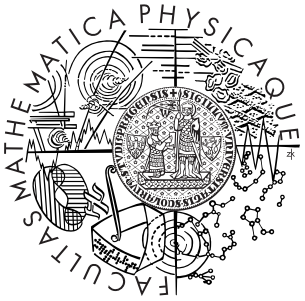

Viktor Holubec

Nonequilibrium Thermodynamics of Small Systems

Nerovnovážná termodynamika malých systémů

Institute of Theoretical Physics

Supervisor: Doc. RNDr. Petr Chvosta, CSc.,
Study programme: Physics, Theoretical physics

2009

I would like to thank my supervisor Doc. RNDr. Petr Chvosta CSc. for his generous help with this work. Also I would like to thank my family and friends for their support and tolerance during the preparation of the manuscript.

I hereby declare that I have written the diploma thesis myself, using only cited sources. I agree with lending and distribution of the thesis.

Prague, April 15, 2009 Viktor Holubec

Contents

Název práce: Nerovnovážná termodynamika malých systémů
Autor: Viktor Holubec
Katedra (ústav): Ústav teoretické fyziky
Vedoucí diplomové práce: Doc. RNDr. Petr Chvosta, CSc., Katedra makromolekulární fyziky
e-mail vedoucího: Petr.Chvosta@mff.cuni.cz

Abstrakt: Cílem našeho zkoumání je mikroskopický motor založený na dvouhladinovém systému udržovaném vnějším působením v nerovnovážném stavu. Operační cyklus tohoto motoru se skládá ze dvou taktů, během nichž se energie obou hladin mění lineárně s časem. Pravděpodobnosti obsazení jednotlivých hladin, odrážející (zpožděnou) reakci systému na vnější působení, se řídí Pauliho rovnicí. V práci uvádíme přesné řešení této pohybové rovnice a s jeho pomocí diskutujeme termodynamické vlastnosti motoru. Zkoumáme například účinnost a výkon motoru v závislosti na parametrech modelu. Dále představujeme složený stochastický proces, který sleduje v daném čase jak pravděpodobnosti obsazení hladin, tak práci vykonanou na systému během předchozího vývoje. Uvádíme přesný výpočet evolučního operátoru pro složený proces a s jeho pomocí diskutujeme hustotu pravděpodobnosti pro práci vykonanou během operačního cyklu motoru. Při silně nevratném průběhu cyklu vykazuje tato hustota značné odlišnosti od běžného gaussovského tvaru.

Klíčová slova: termodynamika malých systémů, hustota pravděpodobnosti pro práci

Title: Nonequilibrium Thermodynamics of Small Systems
Author: Viktor Holubec
Department: Institute of Theoretical Physics
Supervisor: Doc. RNDr. Petr Chvosta, CSc., Department of Macromolecular Physics
Supervisor's e-mail address: Petr.Chvosta@mff.cuni.cz

Abstract: We investigate a microscopic engine based on an externally controlled two-level system. One cycle of the engine operation consists of two strokes. Within each stroke, the two energy levels are driven with a time-independent rate. The occupation probabilities of the two levels are controlled by the underlying Pauli rate equation and they represent the (delayed) system response in respect to the external driving. We give the exact solution of the dynamical equation and discuss its thermodynamical consequences. In between, we investigate the engine's efficiency, the power output, and the performance dependence on the control parameters. Secondly, we introduce an augmented stochastic process which reflects, at a given time, both the occupation probabilities for the two levels and the work done on the system during the previous evolution. Our exact calculation of the evolution operator for the augmented process allows for a detailed discussion of the probability density for the work done during the cycle of the engine operation. In the strongly irreversible regime, the density exhibits important qualitative differences with respect to the common gaussian shape.

Keywords: thermodynamics of small systems, work probability density

List of symbols

T	Temperature.
$\beta = 1/(k_{\mathrm{B}}T)$	Inverse temperature.
k_{B}	Boltzmann constant. $k_{\mathrm{B}} \doteq 1.38\,10^{-23}\,\mathrm{JK}^{-1}$.
N	Number of levels of the system, usually $N = 2$.
$E_i(t)$, $i = 1, 2, \ldots, N$	Energies of the individual levels of the system.
$\{\mathsf{X}_n\}_{n=i_0}^{i_{\max}}$	Set of random variables X_n.
$\{\mathsf{T}_n\}_{n=0}^{\infty}$	Attempt times.
$\{\mathsf{T}_n - \mathsf{T}_{n-1}\}_{n=1}^{\infty}$	Inter-attempt times.
$\mathsf{D}(t)$	State of the system at a time t.
$\mathsf{D}(t, t_0)$	Time nonhomogeneous Markov process which runs within time interval (t_0, t).
$\{\mathsf{D}(t_n), \ldots, \mathsf{D}(t_1), \mathsf{D}(t_0)\}$	Trajectory of the Markov process.
$\mathsf{W}(t, t_0)$	Accepted work within a time interval (t, t_0).
$\mathsf{Q}(t, t_0)$	Accepted heat within a time interval (t, t_0)
$\{\mathsf{D}(t, t_0), \mathsf{W}(t, t_0)\}$	Augmented process.
$\mathsf{U}(t)$	Internal energy of the system at an instant t.
$\langle \mathsf{X}(t) \rangle$	Mean value of a random variable $\mathsf{X}(t)$ over the trajectories.
$\sigma(\mathsf{X}(t))$	Dispersion of a random variable $\mathsf{X}(t)$.
$\phi(t) = \nu \mathrm{e}^{-\nu t}$	Probability density for the inter-attempt times.
ν	Frequency for the inter-attempt times.
$\mathbb{K}(t_n)$	Transition probabilities matrix.
$k_{ij}(t_n) = \langle i \vert \, \mathbb{K}(t_n) \, \vert j \rangle$	Elements of the transition probabilities matrix.
$\nu\mathbb{L}(t)$, $\mathbb{M}(t)$	Transition rate matrix.
Prob $\{\ldots\}$	Probability that an event … occurs.
$P(t, n; \ldots) \prod_{k=1}^{n} \mathrm{d}t_k$	Probability of a single path described by ….
$W(t, n; \ldots)$	Accepted work along a trajectory described by ….
$\vert p(t) \rangle$	Occupation probability vector at a time t.
$p_i(t) = \langle i \vert p(t) \rangle$	Occupation probability of the ith state.

$\lvert p(t,t_0)\rangle$	State of the system at an instant t, under the condition that the system evolves from a state $\lvert p(t_0)\rangle$ at a time t_0.
$\lvert \pi(t)\rangle$	Gibbs equilibrium state corresponding to the temperature of the contact reservoir and to the position of the energy levels at an instant t.
$\lvert p^{\mathrm{stat}}\rangle$	Initial occupation probability vector of the limit cycle.
$\mathbb{R}(t,t_0)$	Propagator for Pauli equation.
$\langle i\rvert\, \mathbb{R}(t,t_0)\, \lvert j\rangle$	Prob $\{\mathsf{D}(t)=i \mid \mathsf{D}(t_0)=j\}$.
$\mathbb{R}_+(t)$	Propagator $\mathbb{R}(t,t_0)$ within the first stroke.
$\mathbb{R}_-(t)$	Propagator $\mathbb{R}(t,t_0)$ within the second stroke.
$\mathbb{R}_{\mathrm{p}}(t)$	Propagator $\mathbb{R}(t,t_0)$ within the limit cycle.
$\mathbb{G}(w,w_0,t,t_0)$	Propagator for the augmented process.
$\langle i\rvert\, \mathbb{G}(w,w_0,t,t_0)\, \lvert j\rangle\, \mathrm{d}w$	Prob $\big\{\mathsf{W}(t,0)\in(w,w+\mathrm{d}w)\ \wedge\ \mathsf{D}(t)=i \mid \mathsf{W}(t_0,0)=w_0\ \wedge\ \mathsf{D}(t_0)=j\big\}$.
$\mathbb{G}_+(w',0;t_+,0)$	Propagator $\mathbb{G}(w,w_0,t,t_0)$ within the first stroke.
$\mathbb{G}_-(w,w';t_{\mathrm{p}},t_+)$	Propagator $\mathbb{G}(w,w_0,t,t_0)$ within the second stroke.
$\mathbb{G}_{\mathrm{p}}(w,t_{\mathrm{p}})$	Propagator $\mathbb{G}(w,w_0,t,t_0)$ within the limit cycle.
$\rho(w,w_0,t,t_0)$	Probability density for the accepted work $\mathsf{W}(t,t_0)=w-w_0$.
$\rho_{\mathrm{p}}(t,w)$	Work probability density within the limit cycle.
$\chi_{\mathrm{p}}(t,\omega)$	Heat probability density within the limit cycle.
h	Initial energy of the first level in generic scenario.
v	Velocity of the first level in generic scenario.
h_1	Energy of the first state at the beginning of the first stroke of the limit cycle.
h_2	Energy of the first state at the end of the first stroke of the limit cycle.
t_+	Duration of the first stroke of the limit cycle.
t_-	Duration of the second stroke of the limit cycle.
t_{p}	Duration of the limit cycle.
T_+	Temperature of the reservoir during the first stroke.
T_-	Temperature of the reservoir during the second stroke.
$U(t)$	Mean internal energy of the system at a time t.
$S_{\mathrm{s}}(t)$	Entropy of the two-level system at a time t.
$S_{\mathrm{r}}(t_0)$	Entropy of the reservoir at a time t.
$S_{\mathrm{tot}}(t_0)$	Entropy of the whole system at a time t.
$F(t)$	Helmholtz free energy of the system at a time t.
$Q(t,t_0)$	Mean heat accepted by the system within a time period $t-t_0$.

$W(t, t_0)$	Mean work accepted by the system within a time period $t - t_0$.
$W(t)$	Mean work accepted by the engine within the limit cycle.
$Q(t)$	Mean heat accepted by the engine within the limit cycle.
W_{out}	Mean work done by the engine on the environment per cycle.
P_{out}	Power output of the engine.
μ	Efficiency of the engine.
$\mu_{\max}$	Maximum efficiency of the engine for given $T_+ < T_-$, h_1 and h_2.
μ_{C}	Carnot efficiency of an engine. If $T_+ > T_-$, then $\mu_{\text{C}} = 1 - T_+/T_-$.
μ_{CA}	Curzon-Ahlborn efficiency of an engine at maximum power. If $T_+ > T_-$, then $\mu_{\text{CA}} = 1 - \sqrt{T_+/T_-}$.
u	Laplace variable conjugated to the work variable w.
$\rho(u, t, t_0)$	Direct Laplace transformation of $\rho(w, w_0, t, t_0)$.
$\eta = 2\beta(w - w_0)$	Dimensionless work.
s	Laplace variable conjugated to the dimensionless work variable η.
Ω	$\Omega = 2\beta\lvert v\rvert$.
c	$c = \exp(-2\beta h\lvert v\rvert/v)$.
a	Reversibility parameter. $a = \nu/\Omega$.
$\tau = \Omega(t - t_0)$	Dimensionless time.
z	Laplace variable conjugated to the dimensionless time variable τ.
$H(a; \eta, \tau)$	Auxiliary function for calculation of $\mathbb{G}(w, w_0, t, t_0)$.
${}_2\text{F}_1\,(a, b; c; z)$	Gauss hypergeometric function.
$\Theta(t)$	Unit step function.
$\delta(t)$	Delta function.
δ_{ij}	Kronecker delta.

Transformations of functions: In the whole work, we shall recognise transformed and untransformed functions only through their variables. For example, if z is the Laplace variable conjugated to t, then $f(t)$ is the untransformed function and $f(z)$ is the transformed one. Moreover, we shall use similar notation also using substitutions. For example, the substitution $t \to \tau(t)$ changes the function $f(t)$ into a function $f(\tau)$. Note that, of course, $f(t) \neq f(z) \neq f(\tau)$.

Chapter 1

Introduction

Non-equilibrium phenomena in the presence of time-varying external fields, where in particular the systems are in contact with a thermal reservoir, are of vital interest in many areas of current research [1, 2, 3]. Examples are ageing and rejuvenation effects in the rheology of soft-matter systems and in the dynamics of spin glasses, relaxation and transport processes in biological systems such as molecular motors, ion diffusion through membranes, or stretching of DNA molecules, driven diffusion systems with time-dependent bias, and Nano-engines. Along with minimisation of the system size, thermal fluctuations become relevant and the non-equilibrium behavior of such systems depends strongly on the driving forces and the changes of one system state to another, which is inherently finite in time. As a consequence, thermodynamic quantities like heat and work are now random but still fullfill a stochastic energy balance. General features of such systems are reflected in fundamental fluctuation theorems [4, 5, 6, 7, 8, 9, 10, 11, 12, 13, 14], based on the probability distributions of work and heat. In this context, the formulation of mesoscopic engines as a class of Nano-engines, which operate between two different heat baths under non-equilibrium conditions, have received an increasing attention. The variety of models of mesoscopic engines can be roughly classified according to their underlying dynamics of the used working medium like classical stochastic heat engines, where the state space can either be discrete or continuously (see for example [15, 16, 17] and references therein), and quantum heat engines [18, 19]. A essential point of mesoscopic heat engines, where thermal fluctuations are important, is that these machines operates within a finite time cycle. An evaluation of such heat engines with respect to their significance can be carried out be the efficiency.

Note, the traditional (ideally) efficiency consideration of heat engines working in the thermodynamic limit between two heat baths at temperatures $T_2 > T_1$ leads

to a maximal efficiency bound given by the Carnot limit $\eta_C = 1 - T_1/T_2$. However this bound is achieved under reversible conditions, where state changes require infinite time and the power output tends to zero. Real heat engines are designed to have a finite power output $P_{\text{out}} = W_{\text{out}}/t$, i.e., to perform work in an finite time associated with an finite heat flow Q/t. In this context, the most appropriate way is to characterize the engines, which operate in finite time on mesoscopic level as well as macroscopic level, by their efficiency at maximum power. On the macroscopic level the efficiency at maximum power is bounded by the Curzon-Ahlborn efficiency $\eta_{CA} = 1 - \sqrt{T_1/T_2}$, where $\eta_{CA} < \eta_C$ [20]. Recently, for a large class of mesoscopic heat engines an expression differing from the Curzon-Ahlborn limit was found [17].

For a deeper understanding of the finite time performance of mesoscopic heat engines operating between two different heat baths under non-equilibrium conditions, where the work is inherently a fluctuating quantity, one has to estimate the work distributions as function of the driving parameters. If one is able the calculate the work distribution exactly, it is possible to deduce fully the energetic features of the heat engine like the mean work done as well as the fluctuations of the work, the mean power output and the efficiency within a finite-time cycle. Moreover, in modern experiments, the histogram of work done on biomolecules within the stretching experiments is measurable [2]. These molecules are often modeled as two state systems.

To keep the analysis conceptual simple, our heat engine consists of just two isothermal branches, where the working medium is a standard two-level system. We impose a periodic, time-dependent external driving of the energy levels and the dynamics of the working medium is governed by a master equation with time-depending transition rates. Selected form of the transition rates guarantees that, provided the two energies are frozen at two definite values, the system simply relaxes towards the Gibbs canonical equilibrium state compatible with the frozen energies. However, during the engine operation, this case never happens and the system (the horse) dynamics just reflects the instantaneous values of the energy levels (the carrot) as it is depicted in FIG. 1.1. Models of this kind are often applied to describe non-equilibrium phenomena on a coarse-grained level, where activated transitions dominate the slow dynamics. After a transient regime the engine settle in an uniquely defined *limit cycle*, where the working medium is for a finite time in contact with a hot and cold temperature reservoir, respectively. Note that our engine operates in an inherently irreversible regime, due to the instantaneous changing of the bath temperature after a certain contact period. That means, if the driving period goes to infinity, we cannot reach a fully reversible cycle. But in this quasi-static limit, the irreversible cycle approaches arbitrary close to the

reversible isotherms. In a sense, our setting represents the simplest microscopically based heat engine and it is worthy a detailed analysis.

The work is organised as follows. In CHAP. 2 we describe theoretical background suitable for analyses of time nonhomogeneous Markov processes. In CHAP. 3 we specify the model and its main properties. The main results of the work are contained in chapters 4 and 5. In the fourth chapter we calculate the engine performance characteristics. In the fifth chapter we view the work and the heat per cycle as a fluctuating quantities and we calculate its probability densities. Interesting results are also contained in Appendix B, where we present in detail two methods of simulation of a time nonhomogeneous Markov process.

FIG. 1.1: The horse chasing the carrot. Selected form of the transition rates guarantees that, provided the two energies are frozen at two definite values, the system simply relaxes towards the Gibbs canonical equilibrium state. However, due to the periodical driving, during the engine operation this case never happens and the system (the horse – actually the donkey in the picture) dynamics just reflects the instantaneous position of the energy levels (the carrot).

Chapter 2

Theoretical background

2.1 Path decomposition of a Markov process

Let us consider a general N level quantum system in contact with a thermal reservoir. We shall designate the energies of the individual levels $E_i(t)$, $i = 1, 2, \ldots, N$. The time dependence of the energies reflects the external driving. At an arbitrary fixed time t, the state of the system is specified by the state vector $|p(t)\rangle$. Components of this vector $\langle i|p(t)\rangle = p_i(t)$, $i = 1, \ldots, N$ are the occupation probabilities of the individual energy levels. Here and below, we use the bracket notation for the components of the probability vectors and matrices.

In many experimentally important situations, the time evolution of the system is described as a Markov process. Such process is governed by the Pauli master equation [21]. The transition rates in the equation depend on the temperature of the bath and on the external parameters which influence the energy levels of the system. Since the energies of the energy levels depend on time, the rates must be time dependent as well. The underlying Markov process is time nonhomogeneous.

One possible probabilistic approach [22, 23] to the analysis of a continuous time Markov process uses its decomposition into discrete time Markov chain and a system of random points on the time axis. The transitions between the states of the Markov chain occur just at random instants. Usually, the time intervals between individual transitions are taken as independent exponentially distributed random variables. This decomposition can be used for simple and fast simulations of time nonhomogeneous Markov processes. The details are discussed in Appendix B. We will now describe main features of the decomposition.

Let $\{\mathsf{D}_n\}_{n=0}^{\infty}$ be the conventional *time nonhomogeneous* N-state Markov chain [24]. Usually, the random variables D_n, $n = 0, 1 \ldots$, describe the state of the system

at equally spaced time instants. However, in anticipating the transitions towards continuous time, we assume that the nth transition occurs at the time t_n, $n = 0, 1 \ldots$, and we designate the random variables which form the chain as $\{\mathsf{D}(t_n)\}_{n=0}^{\infty}$. Notice that the intervals $(t_n - t_{n-1})$, $n = 0, 1, \ldots$, are not necessarily of the same duration. We shall call the time instants t_n as the *attempt times*.

An arbitrary fixed random variable $\mathsf{D}(t_n)$ assumes the values from the state space $\{i\}_{i=1}^{N}$. The complete description of the Markov chain $\{\mathsf{D}(t_n)\}_{n=0}^{\infty}$ requires the specification of the initial condition and the prescription for the transition probabilities. As for the initial condition, we must prescribe the probabilities $p_i(t_0) = \langle i|p(t_0)\rangle = \mathrm{Prob}\{\mathsf{D}(t_0) = i\}$, $i = 1, \ldots, N$. Here and below, we use the bracket notation for the components of the probability vector. As for the transition probabilities, we must define the sequence of the matrixes $\mathbb{K}(t_n)$, $n = 1, 2, \ldots$, with the matrix elements $k_{ij}(t_n) = \langle i|\mathbb{K}(t_n)|j\rangle = \mathrm{Prob}\{\mathsf{D}(t_n) = i|\mathsf{D}(t_{n-1}) = j\}$, $i, j = 1, \ldots, N$. Differently speaking, $k_{ij}(t)$ is the probability of the transition from the j-th state to the i-th one, provided the transition occurs at the time t. The transition probabilities reflect the instantaneous tendency to change the state. The specific way they depend on the time variable reflects the *driving* and *transition* scenarios and it will be specified in Sec. 3.1.

Having described the Markov chain, we now assume that the attempt times form a random sequence $\{\mathsf{T}_n\}_{n=0}^{\infty}$ on the time axis. More precisely, we identify the attempt times with the so-called Poisson points [25, 26]: the time intervals between the neighboring attempt times are independent and exponentially distributed random variables. We designate $\phi(t) = \nu \exp(-\nu t)$ the generic probability density for the inter-attempt times $(\mathsf{T}_n - \mathsf{T}_{n-1})$, $n = 1, 2, \ldots$. The parameter ν represents the mean frequency with which the attempt times occur, i.e., $1/\nu$ is the mean duration of the time interval between the neighboring attempt times.

As mentioned above, the process which originates from allowing the state transitions just at the random attempt times is a time nonhomogeneous Markov process; we shall designate it as $\mathsf{D}(t, t_0)$. Here we use two-time notation to stress that the process depends on the initial condition $|p(t_0)\rangle$ given at the time t_0. However, for sake of brevity, we shall still use the abbreviation $\mathsf{D}(t)$ for a state of the system at a time t in the cases when will be clear what the initial condition is.

We should be able to derive the dynamical equation for the occupation probabilities $\langle i|p(t, t_0)\rangle = \mathrm{Prob}\{\mathsf{D}(t, t_0) = i\}$, $i = 1, \ldots, N$. More importantly for the present work, the construction allows for a transparent probabilistic description of the individual path (trajectories) of the process $\mathsf{D}(t, t_0)$. Let us make this idea explicit.

A trajectory of the process $\mathsf{D}(t, t_0)$ is actually a set of states of the Markov pro-

cess at some attempt times, for example $\{\mathsf{D}(t_n), \ldots, \mathsf{D}(t_1), \mathsf{D}(t_0)\}$. We designate as $P(t, n; j_n, j_{n-1}, \ldots, j_1, j_0; t_n, t_{n-1}, \ldots, t_1, t_0) \prod_{k=1}^{n} \mathrm{d}t_k$ the probability of a path including exactly n attempt times within the interval (t_0, t) which, moreover, evolves as follows. It departs with probability $p_j(t_0)$ from the state j_0 at the time t_0 and the first attempt time is localised within the interval $(t_1, t_1 + \mathrm{d}t)$. Having reached it, the trajectory jumps from the state j_0 to the state j_1. Note that the new state can coincide with the old one, i.e., that for the states j_0 and j_1 may hold $j_0 = j_1$. Similarly at other attempt times localised at the intervals $(t_k, t_k + \mathrm{d}t)$, $k = 2, 3, \ldots, n$. Afterwards, the state variable remains j_n up to the time t. For transparency, we summarise the above described path's properties in Tab. 2.1.

Probability that the inter-attempt time is localised within the interval $(t_k - t_{k-1}, t_k - t_{k-1} + \mathrm{d}t)$ is $\phi(t_k - t_{k-1})\,\mathrm{d}t$ and the probability that the system jumps from the level j_{k-1} to the level j_k at the time t_k equals $k_{j_k j_{k-1}}(t_k)$. Finally, the probability that no further attempt time occurs during the interval (t, t_n) is $f(t - t_n) = \exp[-\nu(t - t_n)]$. Collecting the probabilities of all individual events, the probability of the whole trajectory is

$$P(t, n; j_n, j_{n-1}, \ldots, j_1, j_0; t_n, t_{n-1}, \ldots, t_1, t_0) \prod_{k=1}^{n} \mathrm{d}t_k$$
$$= f(t - t_n) \prod_{k=1}^{n} \left[k_{j_k j_{k-1}}(t_k) \phi(t_k - t_{k-1})\,\mathrm{d}t_k\right] p_{j_0}(t_0)\ , \quad (2.1)$$

For $n = 0$, we define $P(t, 0; j_0, t_0) = f(t - t_0) p_{j_0}(t_0)$.

Eq. (2.1) contains whole information about the path. By various reductions of this information, we shall be able to derive both the Pauli equation and equation for the work probability density [27]. First we shall focus on the derivation of the Pauli equation.

Inter-attempt time	$t_1 - t_0$	$t_2 - t_1$	$\ldots$	$t_n - t_{n-1}$	$t - t_n$
State	j_0	j_1	$\ldots$	j_{n-1}	j_n
Attempt time	t_0	t_1	$\ldots$	t_{n-1}	t_n
Transition	$j_0 \to j_1$	$j_1 \to j_2$	$\ldots$	$j_{n-2} \to j_{n-1}$	$j_{n-1} \to j_n$

Tab. 2.1: Example of a path of the Markov process $\mathsf{D}(t, t_0)$. The first two lines show the state of the process within the time periods between the attempt times, i.e., within the inter-attempt times. The third and the fourth line show which transitions occur at the individual attempt times.

2.2 Pauli equation

Let us consider all possible trajectories which depart at a time t_0 with probability 1 from a state i and which are found at the time t with certainty in the state j. The sum of the probabilities of all such path is simply the conditional probability Prob $\{\mathsf{D}(t) = i \mid \mathsf{D}(t_0) = j\}$. We shall designate it as

$$r_{ij}(t, t_0) = \langle i| \, \mathbb{R}(t, t_0) \, |j\rangle = \text{Prob} \, \{\mathsf{D}(t) = i \mid \mathsf{D}(t_0) = j\} \ . \tag{2.2}$$

In other words, $(N \times N)$ matrix $\mathbb{R}(t, t_0)$ is the time-evolution operator (the propagator) for the state probabilities in the sense that the state vector $|p(t, t_0)\rangle$ can be calculated by the simple multiplication $|p(t, t_0)\rangle = \mathbb{R}(t, t_0)|p(t_0)\rangle$. Therefore the matrix $\mathbb{R}(t, t_0)$ is the propagator for the process $\mathsf{D}(t, t_0)$.

Considering simultaneously all N^2 pairs of the initial and final states and summing up the probabilities of the paths, the evolution operator emerges in the form

$$\mathbb{R}(t, t_0) = f(t - t_0) \, \mathbb{I} + \sum_{n=1}^{\infty} \int_{t_0}^{t} \mathrm{d}t_n \ldots \int_{t_0}^{t_2} \mathrm{d}t_1 \, f(t - t_n) \mathbb{K}(t_n) \phi(t_n - t_{n-1}) \\ \times \mathbb{K}(t_{n-1}) \ldots \phi(t_2 - t_1) \mathbb{K}(t_1) \phi(t_1 - t_0) \ . \tag{2.3}$$

The individual terms in the summation on the right-hand side of the last formula are the conditional averages, the condition being a fixed number n of the attempt times. The multiple integration takes into account all possible localisations of the attempt times, and the matrix multiplication in the integrated expression incorporates the summation over all possible sequences of the states.

Finally, if we perform the time derivative on this equation, we obtain the Pauli equation in the form

$$\frac{\mathrm{d}}{\mathrm{d}t} \mathbb{R}(t, t_0) = -\nu \mathbb{L}(t) \mathbb{R}(t, t_0), \qquad \mathbb{R}(t_0, t_0) = \mathbb{I} \ . \tag{2.4}$$

Here the matrix $\nu\mathbb{L}(t) = \nu \, [\mathbb{I} - \mathbb{K}(t)]$ contains the transition rates. The Pauli equation is the dynamical equation for the process $\mathsf{D}(t, t_0)$.

From perspective of Eq. (2.4), the matrix $\mathbb{R}(t, t_0)$, as it is given in Eq. (2.3), is a perturbative decomposition of the time-ordered exponential [27]

$$\mathbb{R}(t, t_0) = \exp_{\leftarrow} \left(-\nu \int_{t_0}^{t} \mathrm{d}t' \, \mathbb{L}(t') \right) \ , \tag{2.5}$$

which provides the formal solution of the Pauli equation.

Note that due to its above described probabilistic interpretation (cf Eq. (2.2)), the propagator $\mathbb{R}(t, t_0)$ must fulfil certain normalisation condition. Specifically, the following equation holds

$$\sum_{i=1}^{N} \langle i| \, \mathbb{R}(t, t_0) \, |j\rangle = 1, \quad \forall \, j \ . \tag{2.6}$$

Very important property of Markov processes is that the so-called Chapman-Kolmogorov equation holds for them. For the propagator $\mathbb{R}(t, t_0)$ it is

$$\mathbb{R}(t, t_0) = \mathbb{R}(t, t')\mathbb{R}(t', t_0), \quad \forall \, t' \ . \tag{2.7}$$

In closing this section, let us introduce another form of the Pauli equation. We get it immediately if we consider the, above written, relation between the propagator and the state vector $|p(t, t_0)\rangle = \mathbb{R}(t, t_0)|p(t_0)\rangle$. After its insertion into the Eq. (2.4), we obtain the Pauli equation in the form

$$\frac{\mathrm{d}}{\mathrm{d}t}|p(t, t_0)\rangle = -\nu\mathbb{L}(t)|p(t, t_0)\rangle, \qquad |p(t_0, t_0)\rangle = |p(t_0)\rangle \ . \tag{2.8}$$

2.3 Work functional

Let us now concentrate on the work done by an external agent on the system (*the accepted work*) along the above described trajectory. Within the inter-attempt times, the changes of the system state are, by their very construction, excluded. The work is done on the system by changing its energy levels while the occupation of the states remains fixed [28]. For example if the system is during the time interval (t_j, t_{j+1}) on the level j, the work done on it during this time interval is $E_j(t_{j+1}) - E_j(t_j)$. Similarly, if the state of the system evolves along the above described trajectory, the work done on the system during the time interval (t_0, t) is

$$\begin{aligned} &W(t, n; j_n, \ldots, j_0; t_n, \ldots, t_0) \\ &\qquad = [E_{j_n}(t) - E_{j_n}(t_n)] + \sum_{k=1}^{n} [E_{j_{k-1}}(t_k) - E_{j_{k-1}}(t_{k-1})] \ . \end{aligned} \tag{2.9}$$

Let $\mathsf{W}(t, t_0)$ be the random variable which detects the work done on the system during a time interval (t_0, t). Now, we are able to write for any given path the probability of this path and also the value of the work $\mathsf{W}(t, t_0)$ accepted by the system

along this path. The work probability density can be defined as the mean value $\rho(w,t,t_0) = \langle \delta(\mathsf{W}(t,t_0) - w) \rangle$, where the averaging runs over all possible trajectories. Due to computational reasons we shall focus on the Laplace transformation of this quantity with respect to the work variable w. Thus we would like to calculate the function $\rho(u,t,t_0) = \langle \exp\left[-u\mathsf{W}(t,t_0)\right] \rangle$, where u is the Laplace variable conjugated to the work variable w. From the definition of the mean value — $\langle A(t) \rangle = \sum_{\text{trajectories}} (\text{probability of the trajectory}) \cdot (\text{value of } A(t) \text{ for this trajectory})$ — we have

$$\rho(u,t,t_0) = \sum_{n=0}^{\infty} \int_{t_0}^{t} \mathrm{d}t_n \ldots \int_{t_0}^{t_2} \mathrm{d}t_1 \sum_{j_n=1}^{N} \cdots \sum_{j_0=1}^{N} \exp\left[-uW(t,n;j_n,\ldots,j_0;t_n,\ldots,t_0)\right] \times P(t,n;j_n,\ldots,j_0;t_n,\ldots,t_0) \ . \quad (2.10)$$

Let us now introduce the *augmented process* $\{\mathsf{D}(t,t_0), \mathsf{W}(t,t_0)\}$ which detects both the state of the system at the time t and the work accepted by the system during the time interval (t_0,t). It should be stressed that this process is again time nonhomogeneous Markov process (i.e., the evolution of the process from the time t depends just on the state of the system at that time). Similarly as in the derivation of the Pauli equation (Sec. 2.2), by pinning down the initial and the final state, we can again treat separately the N^2 subgroups of trajectories. We arrange the conditional averages over the subgroups into the matrix $\mathbb{G}(u,t,t_0)$ with the elements $g_{ij}(u,t,t_0) = \langle i | \, \mathbb{G}(u,t,t_0) \, | j \rangle$. The subscript (ij) reflects that the conditional average is taken over all the trajectories which depart from the state j at the time t_0, and reside in the state i at the time t. Let us now derive the dynamical equation for the matrix $\mathbb{G}(u,t,t_0)$, then we shall discuss its meaning.

If we insert the specific expression for the path probability (Eq. (2.1)) and for the trajectory-dependent work (Eq. (2.9)) into Eq. (2.10), we obtain, after a rather extensive rearrangement, the expression

$$\mathbb{G}(u,t,t_0) = \mathbb{E}(u,t) \Bigg[f(t-t_0) + \sum_{n=1}^{\infty} \int_{t_0}^{t} \mathrm{d}t_n \ldots \int_{t_0}^{t_2} \mathrm{d}t_1 \, f(t-t_n) \mathbb{M}(u,t_n) \phi(t_n - t_{n-1}) \times \mathbb{M}(u,t_{n-1}) \ldots \phi(t_2 - t_1) \mathbb{M}(u,t_1) \phi(t_1 - t_0) \Bigg] \mathbb{E}^{-1}(u,t_0) \ . \quad (2.11)$$

Here we have introduced the diagonal matrices $\mathbb{E}(u,t) = \exp[-u\mathbb{H}(t)]$ and $\mathbb{H}(t) = \mathrm{diag}\{E_1(t), E_2(t), \ldots, E_N(t)\}$. Further the matrix $\mathbb{M}(u,t)$ stands for the product $\mathbb{E}^{-1}(u,t)\mathbb{K}(t)\mathbb{E}(u,t)$. Similarly to Eq. (2.3), the individual terms in the summation

on the right-hand side of the last formula are the conditional averages, the condition being a fixed number n of the attempt times. The multiple integration takes into account all possible localisations of the attempt times, and the matrix multiplication in the integrated expression incorporates the summation over all possible sequences of the states.

Performing the time derivative on Eq. (2.11) and rearranging arising terms, we finally get the dynamical equation for the matrix $\mathbb{G}(u,t,t_0)$

$$\frac{\mathrm{d}}{\mathrm{d}t}\mathbb{G}(u,t,t_0) = -\left[u\frac{\mathrm{d}}{\mathrm{d}t}\mathbb{H}(t) + \nu\mathbb{L}(t)\right]\mathbb{G}(u,t,t_0), \qquad \mathbb{G}(u,t_0,t_0) = \mathbb{I}\ . \tag{2.12}$$

Similarly as in the preceding section, the solution of this equation can be written in the form of the time-ordered exponential. The form of the matrix $\mathbb{G}(u,t,t_0)$ given in Eq. (2.11) is again perturbative decomposition of this time-ordered exponential.

The meaning of the matrix $\mathbb{G}(u,t,t_0)$ could be seen easily in the work variable w (i.e., after its inverse Laplace transformation with respect to the variable u). Then the functions $g_{ij}(w,t,t_0)$ describe the one-time properties of the augmented process $\{\mathsf{D}(t,t_0),\mathsf{W}(t,t_0)\}$. More precisely, the function $g_{ij}(w,t,t_0)\,\mathrm{d}w$ equals the probability that, during the process which departs at the time t_0 from the state j and resides at the time t in the state i, the system accepts amount of work which belongs to the infinitesimal interval $(w, w+\mathrm{d}w)$. Mathematically

$$\begin{aligned} g_{ij}(w,w_0;t,t_0)\,\mathrm{d}w &= \langle i|\,\mathbb{G}(w,w_0,t,t_0)\,|j\rangle\,\mathrm{d}w \\ &= \mathrm{Prob}\left\{\mathsf{W}(t,0)\in(w,w+\mathrm{d}w)\ \wedge\ \mathsf{D}(t)=i\ |\ \mathsf{W}(t_0,0)=w_0\ \wedge\ \mathsf{D}(t_0)=j\right\}\ . \end{aligned} \tag{2.13}$$

Here we have, moreover, supposed that the initial work done on the system is with certainty w_0 and thus the work done on the system within the time interval (t_0,t) is $w-w_0$. These extended functions come from the functions $g_{ij}(w,t,t_0)$, where the initial value of the work is with certainty 0, by the simple substitution $w\to w-w_0$

$$g_{ij}(w,w_0,t,t_0) = g_{ij}(w-w_0,t,t_0), \quad \mathsf{W}(t_0,0)=w_0\ . \tag{2.14}$$

Comparing Eq. (2.2) and Eq. (2.13), we see that the propagator $\mathbb{G}(w,w_0,t,t_0)$ plays the same role for the augmented process $\{\mathsf{D}(t,t_0),\mathsf{W}(t,t_0)\}$ as the propagator $\mathbb{R}(t,t_0)$ plays for the process $\mathsf{D}(t,t_0)$. If we perform the inverse Laplace transformation with respect to the variable u (but now conjugated to the variable $w-w_0$) on the whole Eq. (2.12), we get the dynamical equation which plays the same role for the augmented process as plays the Pauli equation (2.4) for the process $\mathsf{D}(t,t_0)$.

Similarly as the propagator $\mathbb{R}(t, t_0)$, due to its probability interpretation described in Eq. (2.13), the propagator $\mathbb{G}(w, w_0, t, t_0)$ must also fulfil certain normalisation condition. Specifically, the following formula holds

$$\sum_{i=1}^{N} \int_{-\infty}^{\infty} \mathrm{d}w \, \langle i| \, \mathbb{G}(w, w_0, t, t_0) \, |j\rangle = 1, \quad \forall \, j \ . \tag{2.15}$$

As we said above, the augmented process is, similarly to the process $\mathsf{D}(t, t_0)$, the Markovian one. Thus for the propagator $\mathbb{G}(w, w_0, t, t_0)$ must also hold the Chapman-Kolmogorov equation. Specifically, it obtains the form of integral

$$\mathbb{G}(w, w_0, t, t_0) = \int_{-\infty}^{\infty} \mathbb{G}(w, w', t, t') \mathbb{G}(w', w_0, t', t_0) \, \mathrm{d}w', \quad \forall \, w', \, t' \ . \tag{2.16}$$

Finally, let us suppose that the initial state of the system is described by the vector $|p(t_0)\rangle$. Then, we can calculate the probability density for the work $w - w_0$ done on the system during the time interval (t_0, t), as

$$\begin{aligned} \rho(w, w_0, t, t_0) &= \sum_{i=1}^{N} \sum_{j=1}^{N} \langle i| \, \mathbb{G}(w, w_0, t, t_0) \, |j\rangle \langle j|p(t_0)\rangle = \\ &= \sum_{i=1}^{N} \sum_{j=1}^{N} g_{ij}(w, w_0, t, t_0) p_j(t_0) = \sum_{i=1}^{N} \langle i| \, \mathbb{G}(w, w_0, t, t_0) \, |p(t_0)\rangle \ . \end{aligned} \tag{2.17}$$

We are now finished with the general construction of the suitable theoretical background for our analysis. In the forthcoming chapter, the above probabilistic construction will be incorporated into a specific physical model.

Chapter 3

Specification of the model

From this point, we shall consider just two-level system in contact with thermal reservoir. Thus, if not stated otherwise, in the rest of the work $N = 2$. To complete the specification of the model, we have to do the following two steps:

1. We have to specify the relaxation properties of the system. In the following, the specific relaxation properties will be called as *transition scenario*.

2. We have to specify the time dependence of the state energies $E_i(t)$, $i = 1, 2$. In the following, the specific time dependence of the state energies will be called as *driving scenario*.

In the next section, we shall specify the transition scenario, the driving scenario will be specified in the section after.

3.1 Transition scenario

To specify the transition scenario, we need some explicit prescription for the probabilities $\langle i| \mathbb{K}(t) |j\rangle$, $i, j \in \{1, 2\}$, which form the transition rates in the Pauli equation (2.4). The matrix $\mathbb{K}(t)$ is stochastic [29]. Thus for all j hold $\sum_{i=1}^{N} \langle i| \mathbb{K}(t) |j\rangle = 1$. In other words, the matrix contains only $N - 1$ independent elements in each column. So, in our two-level setting, we have only two independent elements of the matrix $\mathbb{K}(t)$. Let they be the elements $k_{21}(t)$ and $k_{12}(t)$. However, in any physically reasonable situation, these two rates must fulfil an additional requirement, the so-called detailed-balance condition.

We now turn to the description of the condition. Imagine that at an instant t_{inst} the energy levels are suddenly frozen at their instantaneous values, say $E_i(t_{\text{inst}})$,

$i = 1, 2$. The system relaxes towards the equilibrium state compatible with the inverse temperature of the contact reservoir, say β, and the instantaneous position of the energy levels. The equilibrium is described by the Gibbs occupation probabilities of the individual states. Specifically, the equilibrium occupation probability of the ith state is $\pi_i(t_{\mathrm{inst}}) = \exp\left[-\beta E_i(t_{\mathrm{inst}})\right]/Z(t_{\mathrm{inst}})$, $i = 1, 2$. Here $Z(t_{\mathrm{inst}}) = \mathrm{e}^{-\beta E_1(t_{\mathrm{inst}})} + \mathrm{e}^{-\beta E_2(t_{\mathrm{inst}})}$ denotes the State sum. The transition probabilities should guarantee that the system relaxes towards the Gibbs equilibrium if the energies of the states are constant. One of the common ways how to chose such transition probabilities is to suppose that the probabilities fulfil the relation $k_{12}(t)\exp\left[-\beta E_2(t)\right] = k_{21}(t)\exp\left[-\beta E_1(t)\right]$. This relation is referred to as the (time local) detailed-balance condition. It just says that in the equilibrium the system transfers with the same probability from the state 1 to the state 2 and vice versa.

As we said above, considering the detailed balance condition, in the transition matrix remains only one independent parameter, say $k_{21}(t)$. From this point, we shall use the abbreviation $k_{21}(t) = l(t)$. Then $k_{12}(t) = \exp\left[-\beta(E_1(t) - E_2(t))\right]k_{21}(t)$ and the matrix $\mathbb{L}(t) = \mathbb{I} - \mathbb{K}(t)$ from the Pauli equation (2.4) obtains the form

$$\mathbb{L}(t) = \begin{pmatrix} l_1(t) & -l_2(t) \\ -l_1(t) & l_2(t) \end{pmatrix} = l(t) \begin{pmatrix} 1 & -\mathrm{e}^{-\beta[E_1(t)-E_2(t)]} \\ -1 & \mathrm{e}^{-\beta[E_1(t)-E_2(t)]} \end{pmatrix} . \tag{3.1}$$

We were even able to derive the solution of the Pauli equation for the general form of the matrix $\mathbb{L}(t)$, written after the first equals sign. We shall discuss it in detail in Sec. 4.1.

Our last goal in this section is to specify the function $l(t)$. For a specific process, it can be derived by a discretization of the relevant space continuous dynamical equation into its discrete space form, following by the identification of the terms which stands for the transition probabilities in it. Below, we give three examples of choices of the function $l(t)$.

Metropolis scenario $l(t) = 1$. This choice is inspired by Monte Carlo simulations, namely by the so-called *Metropolis algorithm* [30]. In the simulations, the Metropolis algorithm is used for its fast relaxation of the system towards the equilibrium. We shall call this choice of the transition scenario as the *Metropolis scenario*.

Heat bath scenario $l(t) = (1 + \exp\{-\beta[E_1(t) - E_2(t)]\})^{-1}$. This choice is also inspired by the Monte Carlo simulations, namely by the so-called *heat-bath algorithm* [31]. The heat-bath algorithm is often used for simulations of, for example, spin systems [32]. Let us note that the form of the transition rates

$\nu l(t)$, $\nu \mathrm{e}^{-\beta[E_1(t)-E_2(t)]} l(t)$, with hereby defined function $l(t)$, is also often referred to as the *Glauber form* [33]. We shall call this choice of the transition scenario as the *Heat bath scenario*.

Diffusive scenario $l(t) = \exp\{-\beta[E_2(t) - E_1(t)]/2\}$. This form of the transition rates is used for diffusive systems. We shall call this choice of the transition scenario as the *Diffusive scenario*.

Let us consider a driving scenario with linear dependence of the state energies on time, where, moreover, the initial positions of the energy levels coincide. For this driving scenario, it is known the work probability density (i.e., the solution of Eq. (2.17)) for the Metropolis scenario [22] and for the Heat bath scenario [27]. For the Diffusive scenario arises new computational difficulties in comparison with the other two scenarios and we were not able to derive the analytical expression for the work probability density up to the present time. Analysis of such systems shows usefulness of the method of computer simulations proposed in Appendix B.

In the next two chapters, we shall focus only on the heat-bath scenario. Specifically, in Sec. 4.1 we offer the solution of the Pauli equation. In Sec. 5.4 we show how to extend the results of Ref. [27] to the situation when the initial energies differs.

3.2 Generic driving scenario

Let us suppose a linear dependence of the energy levels on time (the linear driving protocol). Without any lose of generality, we will in the rest of this work assume that $E_2(t) = -E_1(t)$. Considering these assumptions, the generic form of the driving scenario is

$$E_2(t) = h + v(t - t_0), \qquad E_2(t) = -h - v(t - t_0) \ . \tag{3.2}$$

Here h and v are arbitrary constants and the time t fulfils the inequality $t \geq t_0$. Finally, let us denote as T the temperature of the contact heat reservoir during the generic evolution. We see that the first state's energy $E_1(t)$ starts from the initial value h and linearly increases (decreases) with the velocity v. Further, we shall call this velocity as the *velocity of the driving*.

3.3 Two stroke engine

The heat engine is the device which is able to convert periodically heat into work. One period of the engine's operation is referred to as the operational cycle of

the engine. The cycle starts in some thermodynamical state and is formed by a sequence of thermodynamical processes which leads the system back to its initial state. The individual thermodynamical processes which form the operational cycle are referred to as strokes of the engine. The minimum number of such strokes is two.

If we consider the two state system, we can design a simple two strokes engine using the following construction. During the first stroke the system evolves isothermally from its initial state S_0 described by the occupation probabilities $p_1(t_0)$ and $p_2(t_0)$ into some state S_+ described by the occupation probabilities $p_1(t_+)$ and $p_2(t_+)$. The temperature of the heat bath during this evolution is T_+. Then, during the second stroke, the system evolves isothermally back into the state $S_- = S_0$ described by the occupation probabilities $p_1(t_+ + t_-) = p_1(t_0)$ and $p_2(t_+ + t_-) = p_2(t_0)$. The temperature of the bath during the second stroke is T_-.

We can obtain such evolution of the system by periodic driving protocol for the two energies supplemented by a specific initial state of the system. We set the periodic driving as follows

$$E_1(t) = \begin{cases} h_1 + \dfrac{h_2 - h_1}{t_+}\, t & \text{for} \quad t \in \langle 0, t_+ \rangle \ , \\ \\ h_2 - \dfrac{h_2 - h_1}{t_-}\, (t - t_+) & \text{for} \quad t \in \langle t_+, t_+ + t_- \rangle \ . \end{cases} \tag{3.3}$$

As mentioned before, $E_2(t) = -E_1(t)$. From the prescription for the energy time dependence above, we see that the energy of the first level starts the first stroke (branch) at the value h_1 and changes linearly until it attains the value h_2. The velocity of the driving within the first branch is $(h_2 - h_1)/t_+$. During the second stroke the energy returns linearly from its initial value h_2 towards its original value h_1. The velocity of the driving within the second branch is $-(h_2 - h_1)/t_-$. The first stroke takes the time t_+, the second one takes the time t_-. We shall designate the period of the cycle $t_+ + t_-$ as t_p. Moreover, as stated above, we shall assume that the temperature of the first stroke contact reservoir is T_+. Similarly, the bath which communicates with the system during the second stroke posses the temperature T_-. We summarise the parameters of the individual strokes in TAB. 3.1. Moreover, in the table, we offer comparison of the parameters of the individual branches with the parameters of the generic scenario EQ. (3.2).

Notice that at the instants $t = t_+$ and $t = t_\mathrm{p}$, the temperature changes immediately from T_+ to T_- and vice versa. Therefore, in these time instants, there is

	Initial time	Driving velocity	Initial value of E_1	Final value of E_1	Contact temperature
The first stroke	0	$\frac{h_2-h_1}{t_+}$	h_1	h_2	T_+
The second stroke	t_+	$-\frac{h_2-h_1}{t_-}$	h_2	h_1	T_-
Generic driving	t_0	v	h_0	-	T

TAB. 3.1: Parameters of the driving scenario within the individual strokes of the cycle and their comparison with parameters of the generic driving scenario.

no possibility for the system to be in the thermal equilibrium with the reservoirs. Not even in the quasi-static limit (i.e., during infinitesimally slow progress of the cycle). From this reason, there exists no true equilibrium limit of global dynamics of the cycle and the whole process is *inherently* irreversible. However, we can call as equilibrium limit the case when $t_\mathrm{p} \to \infty$ and thus the system is in the equilibrium with the contact reservoirs nearly within the whole cycle, only except the two points where we change the reservoirs.

3.4 Limit cycle

Let us designate the special initial occupation probabilities as p_0^{stat} and p_1^{stat}. These probabilities form the initial state vector $|p^{\mathrm{stat}}\rangle$. Let us suppose that we have the propagators $\mathbb{R}(t,t_0)$ for the individual branches of the cycle (we shall calculate them precisely in the next chapter). Say $\mathbb{R}_+(t,0)$, $t \in (0,t_+)$, for the first branch and $\mathbb{R}_-(t,t_+)$, $t \in (t_+,t_\mathrm{p})$, for the second one. Moreover, let us introduce the abbreviations $\mathbb{R}_+(t) = \mathbb{R}_+(t,0)$ and $\mathbb{R}_-(t) = \mathbb{R}_-(t,t_+)$.

The state of the system after the first branch will be described by the vector $|p_+\rangle = \mathbb{R}_+(t_+)|p^{\mathrm{stat}}\rangle$. We now take the terminal state after the first stroke as a new initial condition for the second stroke. Thus the state of the system after one cycle will be $|p_\mathrm{p}\rangle = \mathbb{R}_-(t_\mathrm{p})|p_+\rangle = \mathbb{R}_-(t_\mathrm{p})\mathbb{R}_+(t_+)|p^{\mathrm{stat}}\rangle$. We see that, regardless the different driving within the individual branches, we can still use the Chapman-Kolmogorov equation (2.7) for calculation of the propagator within the limit cycle. Specifically, we get the propagator at the end of the cycle as the product $\mathbb{R}_\mathrm{p}(t_\mathrm{p}) = \mathbb{R}_-(t_\mathrm{p})\mathbb{R}_+(t_+)$.

To close the cycle its final state $|p_\mathrm{p}\rangle$ must coincide with its initial state. Therefore we can obtain the special initial condition for the cycle from the formula

$$|p^{\mathrm{stat}}\rangle = |p_\mathrm{p}\rangle = \mathbb{R}_\mathrm{p}(t_\mathrm{p})|p^{\mathrm{stat}}\rangle \ . \tag{3.4}$$

The initial state is thus the right eigenvector of the matrix $\mathbb{R}_{\mathrm{p}}(t_{\mathrm{p}})$ which belongs to the eigenvalue 1. Because the matrix $\mathbb{R}_{\mathrm{p}}(t_{\mathrm{p}})$ is stochastic, this equation is equivalent with [24, 29]

$$|p^{\mathrm{stat}}\rangle = \lim_{n\to\infty} [\mathbb{R}_{\mathrm{p}}(t_{\mathrm{p}})]^n |p(t_0)\rangle \ , \tag{3.5}$$

where $|p(t_0)\rangle$ is an arbitrary initial state. Physically, the last equation means that the system under the influence of our periodic driving relaxes towards the cycle's initial state $|p^{\mathrm{stat}}\rangle$. From this reason we shall call the operational cycle of our engine as the *limit cycle* and its initial state as its *stationary* state (we have already used the word stationary in the upper index of the abbreviation of it). The limit cycle attracts any evolution, defined by the fixed periodic driving protocol (3.3), starting from an arbitrary initial condition. The specific form of the stationary state is calculated in Sec. 4.3.

For calculation of the propagator $\mathbb{G}(w, w_0, t, t_0)$ at the and of the limit cycle, say $\mathbb{G}_{\mathrm{p}}(w, t_{\mathrm{p}})$, we can adopt the same approach as above. We shall again calculate the propagators for the individual branches, say $\mathbb{G}_{+}(w', 0; t_{+}, 0)$ for the first one and $\mathbb{G}_{-}(w, w'; t_{\mathrm{p}}, t_{+})$ for the second one and then we shall use the Chapman-Kolmogorov equation (2.16). We get immediately the relation for the desired propagator, which is $\mathbb{G}_{\mathrm{p}}(w, t_{\mathrm{p}}) = \int_{-\infty}^{\infty} \mathrm{d}w' \, \mathbb{G}_{-}(w, w'; t_{\mathrm{p}}, t_{+}) \mathbb{G}_{+}(w', 0; t_{+}, 0)$.

We have now finished with the description of general definitions and equations. In further two chapters we will introduce specific form of the above defined functions and we shall proceed further to the analysis of physical attributes of the above defined engine. In Chap. 4 we shall discuss its thermodynamics, while in Chap. 5 we shall discuss the properties of its work and heat probability densities.

Chapter 4

Path-averaged properties

4.1 Generic form of the propagator for the Pauli equation

In this section we will introduce the solution of the Pauli equation (2.4) for the generic driving scenario Eq. (3.2). As we stated above, this solution will be the general solution for any linear driving protocol. Thus we shall easily get from it the specific form of the propagators for the individual strokes of the engine described in previous sections 3.3 and 3.4.

First of all, we shall write the solution of the general Pauli equation, i.e., the solution for the general matrix $\mathbb{L}(t)$ as it is written in Eq. (3.1). Then we will write this solution for our specific form of the transition rates dictated by the heath-bath scenario.

If we insert the matrix $\mathbb{L}(t)$ (3.1) into the Pauli equation (2.4), we get general form of the equation, which is

$$\frac{\mathrm{d}}{\mathrm{d}t}\mathbb{R}(t,t_0) = -\nu \begin{pmatrix} l_1(t) & -l_2(t) \\ -l_1(t) & l_1(t) \end{pmatrix} \mathbb{R}(t,t_0), \qquad \mathbb{R}(t_0,t_0) = \mathbb{I}\ , \tag{4.1}$$

where $l_1(t)$ and $l_2(t)$ are arbitrary functions.

This matrix equation includes two pairs of coupled ordinary differential equations. Thanks to our two-level setting, this coupled equations can be easily untan-

gled and solved [34, 35]. The solution is

$$\mathbb{R}(t,t_0) = \mathbb{I} - \frac{1}{2}\begin{pmatrix} 1 & -1 \\ -1 & 1 \end{pmatrix}\left\{1 - \exp\left[-\nu\int_{t_0}^{t} \mathrm{d}t'\,\alpha_+(t')\right]\right\} + \frac{\nu}{2}\begin{pmatrix} -1 & -1 \\ 1 & 1 \end{pmatrix}\int_{t_0}^{t}\mathrm{d}t'\,\exp\left[-\nu\int_{t'}^{t}\mathrm{d}t''\,\alpha_+(t'')\right]\alpha_-(t')\ , \quad (4.2)$$

where we have used the abbreviations $\alpha_+(t) = l_1(t) + l_2(t)$ and $\alpha_-(t) = l_1(t) - l_2(t)$.

As we stated in SEC. 3.2, our chosen form of the transition rates, i.e., the Glauber form, is

$$\nu l_1(t) = \nu\frac{1}{1+\mathrm{e}^{-\beta[E_1(t)-E_2(t)]}}, \quad \nu l_2(t) = \nu\frac{\mathrm{e}^{-\beta[E_1(t)-E_2(t)]}}{1+\mathrm{e}^{-\beta[E_1(t)-E_2(t)]}}\ . \quad (4.3)$$

Immediately, we see that $\alpha_+(t) = 1$ and $\alpha_-(t) = \tanh\{\beta/2[E_1(t) - E_2(t)]\}$.

Further, in our present setting, the generic driving scenario is given by EQ. (3.3) as $E_1(t) = h + v(t - t_0)$, $E_2(t) = -E_1(t)$. Thus for the difference of the level energies holds $E_1(t) - E_2(t) = 2E_1(t) = 2[h + v(t - t_0)]$. Therefore $\alpha_-(t) = \tanh\{\beta[h + v(t - t_0)]\}$.

Let us denote as $\Omega = 2\beta v$ the temperature-reduced velocity of the driving and $c = \exp(-2\beta h)$ the constant which represents the position of the energies at the time t_0. Moreover, we define the so-called *reversibility parameter* a through the relation $a = \nu/\Omega$. As we will see below, the magnitude of this dimensionless combination dictates how close the process is to the reversible one. More precisely, in the limit $a \to \infty$ is the system during its generic evolution in the Gibbs equilibrium, defined by the temperature of the reservoir T and by the instantaneous values of the energies E_1 and E_2, at any instant.

Now, we can write the generic form of the transition rates (4.3) as

$$\nu l_1(t) = \nu\frac{1}{1+c\mathrm{e}^{-\Omega(t-t_0)}}, \quad \nu l_2(t) = \nu\frac{c\mathrm{e}^{-\Omega(t-t_0)}}{1+c\mathrm{e}^{-\Omega(t-t_0)}}\ . \quad (4.4)$$

Using the current notation the generic solution of the Pauli equation, which immediately follows from EQ. (4.2), is

$$\mathbb{R}(t,t_0) = \mathbb{I} - \frac{1}{2}\begin{pmatrix} 1 & -1 \\ -1 & 1 \end{pmatrix}\left[1 - \mathrm{e}^{-\nu(t-t_0)}\right] + \frac{1}{2}\begin{pmatrix} -1 & -1 \\ 1 & 1 \end{pmatrix}\xi(t,t_0)\ , \quad (4.5)$$

where

$$\xi(t,t_0) = \nu\int_{t_0}^{t}\mathrm{d}t'\mathrm{e}^{-\nu(t-t')}\tanh\{\beta[h + v(t' - t_0)]\}\ . \quad (4.6)$$

This form of the propagator $\mathbb{R}(t,t_0)$ is useful, however it is not fully analytical (the function $\xi(t,t_0)$ is defined as the definite integral). Luckily, due to the normalisation condition (2.6), the equation (4.5) for the propagator could be rewritten [35] into the form

$$\mathbb{R}(t,t_0) = \mathbb{I} - \begin{pmatrix} 1 & 0 \\ -1 & 0 \end{pmatrix} \left[1 - \mathrm{e}^{-\nu(t-t_0)}\right] + \begin{pmatrix} 1 & 1 \\ -1 & -1 \end{pmatrix} \gamma(t,t_0) \ , \tag{4.7}$$

where

$$\gamma(t,t_0) = \nu c \int_{t_0}^{t} \mathrm{d}t' \mathrm{e}^{-\nu(t-t')} \frac{\mathrm{e}^{-\Omega t'}}{1 + c\mathrm{e}^{-\Omega t'}} = ac\mathrm{e}^{-\nu t} \int_{\Omega t_0}^{\Omega t} \mathrm{d}\tau \frac{\mathrm{e}^{(a-1)\tau}}{1 + c\mathrm{e}^{-\tau}} \ . \tag{4.8}$$

Now, in dependence on the given value of the parameter a, the function $\gamma(t,t_0)$ could be calculated analytically. Specifically, we get
for $a \in (0,1)$:

$$\gamma(t,t_0) = \frac{a}{1-a} c\mathrm{e}^{-\nu t} \Big[\mathrm{e}^{(a-1)\Omega t_0} \ {}_2\mathrm{F}_1\left(1, 1-a; 2-a; -c\mathrm{e}^{-\Omega t_0}\right) - \mathrm{e}^{(a-1)\Omega t} \ {}_2\mathrm{F}_1\left(1, 1-a; 2-a; -c\mathrm{e}^{-\Omega t}\right) \Big] \ , \tag{4.9}$$

for $a = 1$:

$$\gamma(t,t_0) = c\mathrm{e}^{-\Omega t} \left[\Omega(t - t_0) + \ln \frac{1 + c\mathrm{e}^{-\Omega t}}{1 + c\mathrm{e}^{-\Omega t_0}} \right] \ , \tag{4.10}$$

and finally for $a \in (1,\infty)$:

$$\gamma(t,t_0) = \ {}_2\mathrm{F}_1\left(1, a; 1+a; -\frac{1}{c\mathrm{e}^{-\Omega t}}\right) - \mathrm{e}^{-a\Omega(t-t_0)} \ {}_2\mathrm{F}_1\left(1, a; 1+a; -\frac{1}{c\mathrm{e}^{-\Omega t_0}}\right) \ . \tag{4.11}$$

Above, the symbol ${}_2\mathrm{F}_1\left(a, b; c; z\right)$ denotes the Gauss hypergeometric function [36].

Now, having in our hands the generic propagator for the Pauli equation, we can proceed further in the analysis of our engine. First of all, in the next section, we shall write the specific form of the propagator $\mathbb{R}(t,t_0) = \mathbb{R}_{\mathrm{p}}(t)$ for its operational cycle as it is described in Sec. 3.3.

4.2 The propagator $\mathbb{R}_{\mathrm{p}}(t)$ within the cycle

As we stated before, having the specific form of the generic propagator $\mathbb{R}(t, t_0)$, we are able to write the propagator for any linear driving scenario immediately. As we also stated, the operational cycles of our engine consists of the two linear strokes (branches). To construct the propagator $\mathbb{R}_{\mathrm{p}}(t)$ within the cycle, we just need to identify the parameters of the individual branches of the cycle with the parameters of our generic process and then use the Chapman-Kolmogorov equation (2.7). From this point, we will denote the parameters and functions for the first branch by the subscript $+$ and for the second branch by the subscript $-$, respectively.

From Tab. 3.1 we immediately get for the first branch: $h = h_+ = h_1$, $v = v_+ = (h_2 - h_1)/t_+$, $t_0 = 0$, $t = t_+$ and $\beta = \beta_+$. Similarly for the second branch: $h = h_- = h_2$, $v = v_- = -(h_2 - h_1)/t_-$, $t_0 = t_+$, $t = t_{\mathrm{p}}$ and $\beta = \beta_-$. If we substitute these constants into Eq. (4.5) and into Eq. (4.6), we easily get the propagators for the individual branches of the cycle, $\mathbb{R}_+(t)$ and $\mathbb{R}_-(t)$, in the form

$$\mathbb{R}_+(t) = \mathbb{I} - \frac{1}{2}\begin{pmatrix} 1 & -1 \\ -1 & 1 \end{pmatrix}\left[1 - \mathrm{e}^{-\nu t}\right] + \frac{1}{2}\begin{pmatrix} -1 & -1 \\ 1 & 1 \end{pmatrix}\xi_+(t) \,, \tag{4.12}$$

$$\mathbb{R}_-(t) = \mathbb{I} - \frac{1}{2}\begin{pmatrix} 1 & -1 \\ -1 & 1 \end{pmatrix}\left[1 - \mathrm{e}^{-\nu(t-t_+)}\right] + \frac{1}{2}\begin{pmatrix} -1 & -1 \\ 1 & 1 \end{pmatrix}\xi_-(t) \,, \tag{4.13}$$

where

$$\xi_+(t) = \nu \int_0^t \mathrm{d}t' \mathrm{e}^{-\nu(t-t')} \tanh\left\{\beta_+\left[h_1 + \frac{h_2 - h_1}{t_+}t'\right]\right\} \,, \tag{4.14}$$

$$\xi_-(t) = \nu \int_{t_+}^t \mathrm{d}t' \mathrm{e}^{-\nu(t-t')} \tanh\left\{\beta_-\left[h_2 - \frac{h_2 - h_1}{t_-}(t' - t_+)\right]\right\} \,. \tag{4.15}$$

Getting the propagator for the limit cycle is now only a question of the simple matrix multiplication

$$\mathbb{R}_{\mathrm{p}}(t) = \begin{cases} \mathbb{R}_+(t) & \text{for} \quad t \in \langle 0, t_+\rangle \,, \\ \\ \mathbb{R}_-(t)\mathbb{R}_+(t_+) & \text{for} \quad t \in \langle t_+, t_{\mathrm{p}}\rangle \,. \end{cases} \tag{4.16}$$

Finally, having the propagator $\mathbb{R}_{\mathrm{p}}(t)$ for the limit cycle, we can calculate the specific form of the initial and final state of the cycle $|p^{\mathrm{stat}}\rangle$ (cf Sec. 3.4).

4.3 Stationary cycle of the engine

As we said in SEC. 3.4, the initial state of the cycle must be also its final state so that the cycle is closed. Therefore it must fulfil the eigenvalue EQ. (3.4), which is $|p^{\mathrm{stat}}\rangle = \mathbb{R}_{\mathrm{p}}(t_{\mathrm{p}})|p^{\mathrm{stat}}\rangle$. Moreover, due to the normalisation condition for probability vectors, we have $\sum_{i=1}^{2}\langle i|p^{\mathrm{stat}}\rangle = 1$. Solving this system of two coupled equations, the occupation probabilities at the beginning and also at the end of the limit cycle (and thus the components of the vector $|p^{\mathrm{stat}}\rangle$) are

$$p_1^{\mathrm{stat}} = \frac{1}{2}\left[1 - \frac{\xi_+ \mathrm{e}^{-\nu t_-} + \xi_-}{1 - \mathrm{e}^{-\nu t_p}}\right], \qquad p_2^{\mathrm{stat}} = \frac{1}{2}\left[1 + \frac{\xi_+ \mathrm{e}^{-\nu t_-} + \xi_-}{1 - \mathrm{e}^{-\nu t_p}}\right] . \tag{4.17}$$

Here we have used the abbreviations $\xi_+ = \xi_+(t_+)$ and $\xi_- = \xi_-(t_p)$ for the functions which are defined by EQ. (4.14) and EQ. (4.15).

The knowledge of the specific form of the propagator $\mathbb{R}_{\mathrm{p}}(t)$ together with the above stated initial condition $|p^{\mathrm{stat}}\rangle$ allows us to calculate the state of the system at an arbitrary time during the limit cycle, say $|p(t)\rangle$, through the obvious relation

$$|p(t)\rangle = \mathbb{R}_{\mathrm{p}}(t)|p^{\mathrm{stat}}\rangle, \qquad t \in \langle 0, t_{\mathrm{p}}\rangle \ . \tag{4.18}$$

Now we have in our hands all analytical results (i.e., the propagator $\mathbb{R}_{\mathrm{p}}(t)$ and the initial state of the cycle $|p^{\mathrm{stat}}\rangle$) needed for the thermodynamic treatment of the engine. In the next section, we shall start this treatment with definitions of basic thermodynamic quantities.

4.4 Basic thermodynamic quantities

State functions $U(t)$ (internal energy of the system at a time t) and $S_{\mathrm{s}}(t)$ (entropy of the system at a time t) are defined as certain mean values over the states of the system. Specifically, the internal energy is the mean value of the energy of the system, i.e.,

$$U(t) = E_1(t)p_1(t) + E_2(t)p_2(t) \ , \tag{4.19}$$

and the entropy is the mean value of the function $-k_{\mathrm{B}} \ln p_i(t)$, i.e.,

$$S_{\mathrm{s}}(t) = -k_{\mathrm{B}}\left[p_1(t)\ln p_1(t) + p_2(t)\ln p_2(t)\right] \ . \tag{4.20}$$

Here and below, for sake of transparency, we use the abbreviation $p_i(t) = p_i(t, t_0)$, $i = 1, 2$ for the occupation probability of the ith state of the system at a time t, under the condition that the system evolves from a state $|p(t_0)\rangle$ at a time t_0. Thus,

unlike the CHAP. 2.1, we omit here to write the initial time of the process. While the equations in this sections are general, in the forthcoming sections the state vector $|p(t)\rangle$ will have the meaning determined by EQ. (4.18). Thus it is possible to identify the state vector $|p(t)\rangle$ as the state of the system at a time t within the limit cycle of the engine.

From very definition of the functions $U(t)$ and $S_{\mathrm{s}}(t)$, it is obvious that their increments within some process depend only on its initial and final state. This sentence doesn't hold for other important thermodynamic quantities which are $Q(t, t_0)$ (mean heat accepted by the system[1] within a time period $t - t_0$) and $W(t, t_0)$ (mean work accepted by the system within a time period $t - t_0$). These two are not the state functions and could be defined as certain mean values over all possible paths which the system can undergoes to get from the state $|p(t_0)\rangle$ to the state $|p(t)\rangle$ (cf sections 2.1, B.4 and EQ. (B.23)).

Considering that our system can change its internal energy only through interchange of heat and work with the environment, we can write for an increment of the internal energy

$$U(t) - U(t_0) = Q(t, t_0) + W(t, t_0) \ , \tag{4.21}$$

or infinitesimally, which is in fact the first law of thermodynamics,

$$\mathrm{d}U(t) = U(t) - U(t - \mathrm{d}t) = đQ(t) + đW(t) \ . \tag{4.22}$$

Here $đQ(t) = Q(t, t - \mathrm{d}t)$ and $đW(t) = W(t, t - \mathrm{d}t)$ are inexact differentials of heat and of work, respectively. Differencing the EQ. (4.19) we get another relation for the quantity $\mathrm{d}U(t)$, which is

$$\mathrm{d}U(t) = p_1(t)\mathrm{d}E_1(t) + p_2(t)\mathrm{d}E_2(t) + E_1(t)\mathrm{d}p_1(t) + E_2(t)\mathrm{d}p_2(t) \ . \tag{4.23}$$

We can thus identify the inexact differential of work as (cf EQ. (2.9))

$$đW(t) = p_1(t)\mathrm{d}E_1(t) + p_2(t)\mathrm{d}E_2(t) = [p_1(t) - p_2(t)]\,\mathrm{d}E_1(t) \ , \tag{4.24}$$

where we have used the relation between the linearly driven energies of the sites $E_2(t) = -E_1(t)$. Consequently, the inexact differential of heat must be

$$đQ(t) = E_1(t)\,\mathrm{d}p_1(t) + E_2(t)\,\mathrm{d}p_2(t) = E_1(t)[\mathrm{d}p_1(t) - \mathrm{d}p_2(t)] \ . \tag{4.25}$$

[1] We use the attribute "accepted" to stress that, in our sign convention, the positive heat flows into the system. More precisely, the hereby defined accepted heat is the difference of absolute values of the heat which flowed into the system and the heat which flowed from the system during the evolution.

Now, by integration of relations (4.24) and (4.25), we can write relations for the work and for the heat accepted by the system within the time interval (t_0, t). They are

$$W(t,t_0) = \int_{E_1(t_0)}^{E_1(t)} [p_1(t') - p_2(t')]\,\mathrm{d}E_1(t') = \int_{t_0}^{t} [p_1(t') - p_2(t')] \frac{\mathrm{d}E_1(t')}{\mathrm{d}t'}\,\mathrm{d}t' \ , \quad (4.26)$$

and

$$Q(t,t_0) = \int_{p_1(t_0)}^{p_1(t)} E_1(t')\,[\mathrm{d}p_1(t') - \mathrm{d}p_2(t')] = \int_{t_0}^{t} E_1(t') \frac{\mathrm{d}}{\mathrm{d}t'} [p_1(t') - p_2(t')]\,\mathrm{d}t' \ . \quad (4.27)$$

If we use the vector form of the Pauli equation $\frac{\mathrm{d}}{\mathrm{d}t}|p(t)\rangle = -\nu \mathbb{L}(t)|p(t)\rangle$ (cf Eq. (2.8)), we can write for the derivative of the difference of occupation probabilities the relation $\frac{\mathrm{d}}{\mathrm{d}t}[p_1(t) - p_2(t)] = -2\nu[l_1(t)p_1(t) - l_2(t)p_2(t)]$. Here we have used a general form of the matrix $\mathbb{L}(t)$ introduced in Eq. (3.1). Therefore the formula (4.27) can be easily worked further into the form

$$Q(t,t_0) = -2\nu \int_{t_0}^{t} E_1(t')[l_1(t')p_1(t') - l_2(t')p_2(t')]\,\mathrm{d}t' \ . \quad (4.28)$$

If we compare our formula for the accepted work (4.24) with the one from the basic course of thermodynamics, i.e., with the relation $đW = -p\,\mathrm{d}V$, we can identify the difference of the occupation probabilities $p_1(t) - p_2(t)$ as some kind of "negative pressure" $p(t) = p_1(t) - p_2(t)$ and the energy of the first level $E_1(t)$ as an equivalent of "volume" $E(t) = E_1(t)$. We can thus construct an analogy of the well-known p–V diagram from which will be obvious the sign of the work accepted by the system within an evolution.

Instead of that, let us first finish the definitions of thermodynamic functions with discussion of entropic quantities. While we have, in Eq. (4.20), already defined the instantaneous entropy of the two-level system $S_\mathrm{s}(t)$, we didn't introduce any corresponding formula for entropy of the bath. Let us suppose that our heat bath can be characterised as a *reversible heat source* [37]. Then we can write for an infinitesimal increment of the heat bath's entropy at an instant t the quasi-static relation $\mathrm{d}S_\mathrm{r}(t) = S_\mathrm{r}(t) - S_\mathrm{r}(t - \mathrm{d}t) = -k_B\beta(t)\,đQ(t)$, where $\beta(t) = 1/[k_B T(t)]$ is instantaneous inverse temperature of the bath. The entropy production of the bath is thus proportional to the heat accepted by the system and, recalling relations (4.25) and (4.28), we can write for an increment of the entropy of the bath within

a time interval (t_0, t)

$$S_{\mathrm{r}}(t) - S_{\mathrm{r}}(t_0) = -k_B \int_{p_1(t_0)}^{p_1(t)} \beta(t') E_1(t') \left[\mathrm{d}p_1(t') - \mathrm{d}p_2(t')\right]$$
$$= 2k_B \nu \int_{t_0}^{t} \beta(t') E_1(t') [l_1(t') p_1(t') - l_2(t') p_2(t')] \, \mathrm{d}t' \ . \quad (4.29)$$

Therefore for calculation of the instantaneous value of the entropy of the bath $S_{\mathrm{r}}(t)$, we must specify its initial value $S_{\mathrm{r}}(t_0)$ (or its value at any other time). Below, we shall always assume that $S_{\mathrm{r}}(t_0) = 0$. Finally, the total entropy of the set {two-level system — heat bath} is given as a simple sum of the individual entropies, thus

$$S_{\mathrm{tot}}(t) = S_{\mathrm{s}}(t) + S_{\mathrm{r}}(t) \ . \quad (4.30)$$

This entropy is an entropy of a closed system and thus, according to the second law of thermodynamics, must be non-decreasing for any possible evolution (while the entropies $S_{\mathrm{s}}(t)$ and $S_{\mathrm{r}}(t)$ of the subsystems can be both increasing and decreasing).

Except for application of the assumption of linear driving of the energy level in Eq. (4.24), the above given definitions are general for any evolution of the two-level system. Now, we shall finally focus on thermodynamic properties of our model engine. We shall start with promised analogy of the well known p–V diagram.

4.5 p–E diagram

In the first subsection, we describe the p–E diagram and develop its analogy with the thermodynamic p–V diagram. We define curves corresponding to thermodynamic isobars, isotherms and isochores. In the second subsection, we investigate possible isothermal realisations of the system's evolution. Finally, in the third section, we describe possible representations of the limit cycle in the p–E diagram and present some examples of the specific cycles.

4.5.1 Description

As we suggested in previous section, if we plot the dependence of the difference of the occupation probabilities $p(t) = p_1(t) - p_2(t)$ as a function of the energy of the first level $E(t) = E_1(t)$ during some evolution of the system (we shall call this plot as a p–E diagram), we get a diagram similar to the p–V diagram from basic

thermodynamics course in the sense that the area under the clockwise followed[2] curve $p(t)$ equals to the work accepted by the system during the evolution (cf EQ. (4.26)). Moreover, every point of the $p-E$ diagram represents some state of the system, because, thanks to the relations $p_1(t) + p_2(t) = 1$ and $E_1(t) = -E_2(t)$, to specify any state of the system it is sufficient to give values of two independent combinations of the functions $p_i(t)$, $E_i(t)$, $i = 1, 2$. We can thus call this diagram as a *state diagram* for our model system. Let us finish this paragraph, inspired by the thermodynamic p–V diagram, by calling lines of constant energy $E(t) = const$ in the $p-E$ plane as "*isochores*" and lines of constant difference of the occupation probabilities $p(t) = const$ in the $p-E$ plane as "*isobars*". Moreover we shall refer to the stroke within which the energy of the first level increases as to an *expansion stroke* and to the stroke within which the energy of the fist level decreases as to a *compression stroke*.

Below, we show that, in the p–E diagram, there exists a set of important curves, which we call as *equilibrium isotherms*. These curves belong to those evolutions of the system within which it is in the Gibbs equilibrium with a contact reservoir on a given inverse temperature $\beta = const$. Thus they are described by the equation

$$p(t) = \pi(t) = \frac{\mathrm{e}^{-\beta E_1(t)} - \mathrm{e}^{-\beta E_2(t)}}{\mathrm{e}^{-\beta E_1(t)} + \mathrm{e}^{-\beta E_2(t)}} = -\tanh\left[\beta E(t)\right] , \tag{4.31}$$

where $\pi(t) = \pi_1(t) - \pi_2(t)$, $\pi_i(t) = \langle i|\pi(t)\rangle = \mathrm{e}^{-\beta E_i(t)}/[\mathrm{e}^{-\beta E_1(t)} + \mathrm{e}^{-\beta E_2(t)}]$, $i = 1, 2$.

As can be seen from the above equation, through every point of the p–E plane (except the line $E(t) = E_1(t) = 0$) passes exactly one equilibrium isotherm. We can thus assign to each such point some "*effective temperature*" T_e determined by the temperature of the passing isotherm. For the effective temperature of the point with coordinates $[p, E]$, we have

$$T_\mathrm{e} = \frac{E}{k_B \,\mathrm{Argtanh}\,(-p)} \ . \tag{4.32}$$

Now, we shall describe possible evolutions in the $p-E$ diagram.

4.5.2 Possible generic evolutions

Below, in three theorems, we will prove that the curve $p(t)$ in the $p-E$ diagram, representing any possible isothermal evolution driven by the Glauber transition rates (4.3), must fulfil following conditions.

[2] In the sense of run of the time parameter t.

1. Whenever the system starts its evolution, it relaxes towards the equilibrium isotherm corresponding to the temperature of the contact reservoir. Only in the irreversible limit it remains in the same state within the whole evolution.

2. If the system starts below the equilibrium isotherm and the energy $E(t)$ is increasing, it can once cross the isotherm and then remains over it for the rest of the evolution (the first level will be overpopulated – $p(t) > \pi(t)$).

3. If the system starts over the equilibrium isotherm and the energy $E(t)$ is decreasing, it can once cross the isotherm and then remains below it for the rest of the evolution (the first level will be underpopulated – $p(t) < \pi(t)$).

4. Consider the evolution with the linear driving scenario for the state energies (cf generic driving EQ. (3.2)). Then the curve $p(t)$, depicting such evolution in the p–E plane, can be formed maximally from two (deformed) arcs. More precisely, the curve has maximally one inflection point.

The points 1-3 follow from the theorems 4.1 and 4.2. The 4th point is a consequence of the theorem 4.3. For the readers convenience, we summarise the conditions for possible realisations of an evolution in the p–E plane in FIG. 4.1. The three theorems follow.

Theorem 4.1 (Non-crossing theorem)**.** *Consider an evolution of the two-level system during a time interval (t_0, t_1), within which the inverse temperature of the contact reservoir, say β, is constant*[3] *and for which, moreover, holds*

1. $p_1(t_0) - p_2(t_0) \gtrless \pi_1(t_0) - \pi_2(t_0) = -\tanh\{\beta[E_1(t_0) - E_2(t_0)]/2\}$

2. $\dfrac{\mathrm{d}}{\mathrm{d}t}[E_1(t) - E_2(t)] \gtrless 0,\ \forall\, t \in (t_0, t_1)$

3. $|p(t)\rangle = \mathbb{R}(t, t_0)|p(t_0)\rangle,\ \forall\, t \in (t_0, t_1)$, *where*

$$\mathbb{R}(t, t_0) = \mathbb{I} - \frac{1}{2}\begin{pmatrix} 1 & -1 \\ -1 & 1 \end{pmatrix}\left[1 - \mathrm{e}^{-\nu(t-t_0)}\right] + \frac{1}{2}\begin{pmatrix} -1 & -1 \\ 1 & 1 \end{pmatrix}\xi(t, t_0)\ ,$$

$$\xi(t, t_0) = \nu\int_{t_0}^{t} \mathrm{d}t' \mathrm{e}^{-\nu(t-t')}\tanh\left\{\frac{\beta}{2}[E_1(t') - E_2(t')]\right\}\ .$$

[3]Further, we shall call such evolutions as *isothermal*.

Then, for all $t \in (t_0, t_1)$ *holds*

$$p_1(t) - p_2(t) \gtrless \pi_1(t) - \pi_2(t) = -\tanh\left\{\beta[E_1(t) - E_2(t)]/2\right\} .$$

Proof. By a simple matrix multiplication we get

$$|p(t)\rangle = \mathbb{R}(t, t_0)|p(t_0)\rangle = \frac{1}{2}\begin{pmatrix} 1 + \mathrm{e}^{-\nu(t-t_0)}[p_1(t_0) - p_2(t_0)] - \xi(t, t_0) \\ 1 - \mathrm{e}^{-\nu(t-t_0)}[p_1(t_0) - p_2(t_0)] + \xi(t, t_0) \end{pmatrix} , \quad (4.33)$$

and thus

$$p_1(t) - p_2(t) = \mathrm{e}^{-\nu(t-t_0)}[p_1(t_0) - p_2(t_0)] - \xi(t, t_0) . \quad (4.34)$$

Thanks to the first assumption, we can decrease/increase the right-hand side of the above equation getting

$$p_1(t) - p_2(t) \gtrless -\mathrm{e}^{-\nu(t-t_0)} \tanh\left\{\frac{\beta}{2}[E_1(t_0) - E_2(t_0)]\right\} - \xi(t, t_0) . \quad (4.35)$$

Integrating the function $\xi(t, t_0)$ by parts, we get

$$\begin{aligned}\xi(t, t_0) = \tanh\left\{\frac{\beta}{2}[E_1(t) - E_2(t)]\right\} - \mathrm{e}^{-\nu(t-t_0)} \tanh\left\{\frac{\beta}{2}[E_1(t_0) - E_2(t_0)]\right\} \\ - \int_{t_0}^{t} \mathrm{d}t' \mathrm{e}^{-\nu(t-t')} \frac{\mathrm{d}}{\mathrm{d}t'}\left(\tanh\left\{\frac{\beta}{2}[E_1(t') - E_2(t')]\right\}\right) . \quad (4.36)\end{aligned}$$

Note that, thanks to the second assumption, the derivative

$$\frac{\mathrm{d}}{\mathrm{d}t'}\left(\tanh\left\{\frac{\beta}{2}[E_1(t') - E_2(t')]\right\}\right) = \frac{\beta}{2} \frac{\frac{\mathrm{d}}{\mathrm{d}t'}[E_1(t') - E_2(t')]}{\cosh^2\left\{\frac{\beta}{2}[E_1(t') - E_2(t')]\right\}} \quad (4.37)$$

is strictly positive/negative and thus also the whole integral from Eq. (4.36) is strictly positive/negative ($\mathrm{e}^{-\nu(t-t')} > 0$). Inserting the last relation for $\xi(t, t_0)$ into the Eq. (4.35) we get

$$\begin{aligned}p_1(t) - p_2(t) \gtrless -\tanh\left\{\frac{\beta}{2}[E_1(t) - E_2(t)]\right\} \\ + \int_{t_0}^{t} \mathrm{d}t' \mathrm{e}^{-\nu(t-t')} \frac{\mathrm{d}}{\mathrm{d}t'}\left(\tanh\left\{\frac{\beta}{2}[E_1(t') - E_2(t')]\right\}\right) . \quad (4.38)\end{aligned}$$

Omitting the positive/negative integral from the above inequality, we shall decrease/increase its right-hand side. Therefore we really have

$$p_1(t) - p_2(t) \gtrless \pi(t) = -\tanh\left\{\frac{\beta}{2}[E_1(t) - E_2(t)]\right\}, \quad \forall\, t \in (t_0, t_1) , \quad (4.39)$$

and our proof is finished. □

First, note that the evolution operator defined in the third assumption of this theorem differs from the generic propagator (4.5) only at the time dependence of the state energies, which is in the theorem arbitrary and in the generic propagator linear. Second, the theorem is defined only for isothermal evolutions. Because, in the operational cycle of our engine (cf SEC. 3.3) the individual strokes are isothermal, we can apply the theorem for the strokes. Let us suppose that the energy of the first state $E(t)$ is increasing/decreasing during a stroke. Moreover, let us suppose that the system departs from a point $p(t_0)$ which lies, in the $p{-}E$ diagram, over/below the equilibrium isotherm which belongs to the temperature of the contact reservoir. Differently speaking, we suppose that the initial state has bigger/lower effective temperature T_e than is the temperature of the reservoir. Then the theorem simply says, that the curve $p(t)$, depicting the evolution of the system, remains over/below the isotherm within the whole stroke.

The next theorem, follows from EQ. (4.33) and EQ. (4.36). First, if we carry out the limit $\nu \to 0$ in these equations, we get the occupation probability vector $|p(t)\rangle$ for the evolution where the system cannot change its state at all, because the probability that an inter-attempt time will occur within a finite time period is zero (cf SEC. 2.1). We shall call this limit scenario as an *irreversible limit*. In the irreversible limit, the difference of the occupation probabilities is constant, i.e., $p(t) = const$. In other words, the system during the irreversible limit evolves along the proper isobar. Second, if we suppose that the energies of the individual levels are frozen at their values at an instant t_0 and we carry out the limit $t \to \infty$ (or the limit $\nu \to \infty$ with any time dependence of the energies) in EQ. (4.33) and EQ. (4.36), we nearly immediately get for the difference of the occupation probabilities the relation $p(t_0) = \pi(t_0)$. Thus, as expected, the system relaxes towards the proper Gibbs equilibrium. We shall call this limit scenario as an *equilibrium limit*. In the $p{-}E$ diagram it will be depicted by the above defined isochores (because of the constant energy).

Theorem 4.2 (Right angle theorem)**.** *Representation of any possible isothermal evolution of the system from any point in the $p{-}E$ plane must lay within the right angle formed by the isobar and the isochore, which runs through the point. This right angle is oriented towards an equilibrium isotherm corresponding to the temperature of the contact reservoir.*

Proof. As can be seen from EQ. (4.33) and EQ. (4.36), the occupation probabilities are continuous functions of the frequency $\nu \in (0, \infty)$. Therefore the difference of the occupation probabilities $p(t)$ is also such function. As we have shown above, for limit values of the frequency 0 and ∞, the system evolves from any point of the

$p-E$ plane along an isobar or along an isochore towards the corresponding equilibrium isotherm. Therefore any possible evolution of the system must lay within the right angle formed by the isobar and the isochore, oriented towards an equilibrium isotherm corresponding to the temperature of the contact reservoir. □

Finally, let us derive the last theorem needed for describing possible realisations of an evolution in the $p-E$ plane.

Theorem 4.3 (Snake theorem)**.** *Representation of any isothermal evolution of the system with constant velocity of the driving* $\frac{\mathrm{d}}{\mathrm{d}t}E_1(t) = v$ *in the* $p-E$ *diagram has maximally one point of inflexion. In other words, the curve* $p(t)$ *for the evolution can change from concave to convex form or vise versa maximally once. Formally, we get the condition that the equation*

$$\frac{\mathrm{d}}{\mathrm{d}E(t)}p(E(t)) = 0$$

has maximally one root.

Proof. Recalling the fact that $\frac{\mathrm{d}E(t)}{\mathrm{d}t} = v$ (cf the generic driving (3.2)) we can write

$$\frac{\mathrm{d}}{\mathrm{d}E(t)}p(E(t)) = \frac{\mathrm{d}t}{\mathrm{d}E(t)}\frac{\mathrm{d}}{\mathrm{d}t}p(t) = \frac{1}{\frac{\mathrm{d}E(t)}{\mathrm{d}t}}\frac{\mathrm{d}}{\mathrm{d}t}p(t) = \frac{1}{v}\frac{\mathrm{d}}{\mathrm{d}t}p(t) = 0\ . \tag{4.40}$$

According to Eq. (4.34) we have from the last equality

$$\nu\int_{t_0}^{t}\mathrm{d}t'\mathrm{e}^{\nu t'}\tanh\left[\beta E(t')\right] + \mathrm{e}^{\nu t_0}p(t_0) + \mathrm{e}^{\nu t}\tanh\left[\beta E(t)\right] = 0\ , \tag{4.41}$$

where we have moreover used that in our model holds $E_1(t) - E_2(t) = 2E_1(t) = 2E(t)$. If we integrate the first therm by parts we get after simple rearrangement

$$\int_{t_0}^{t}\mathrm{d}t'\mathrm{e}^{\nu t'}\frac{\mathrm{d}}{\mathrm{d}t'}\tanh\left[\beta E(t')\right] + \mathrm{e}^{\nu t_0}\left\{\tanh\left[\beta E(t_0)\right] + p(t_0)\right\} = 0\ . \tag{4.42}$$

As we have already discussed in the proof of the Theorem 4.1, the integrated function has a sign of v, so in our case of constant v, it is monotonically increasing or decreasing in time t. The second therm in the equation is constant. Therefore, because of monotonicity of the only therm which depends on t, this equation solves maximally one time, say t_{i}. Thus the curve $p(t)$ has maximally one inflection which is located at the point $E(t_{\mathrm{i}})$. Finally, note that the proof could be done in the same way as above also for more general case when the function $\frac{\mathrm{d}E(t)}{\mathrm{d}t}$ doesn't changes its sign within the evolution. □

4.5.3 Possible forms of the limit cycle

As we stated above, the theorem 4.1 holds for the individual branches of the limit cycle. The validity of the theorems 4.2 and 4.3 for the individual branches is obvious. Therefore, using the theorems, we can specify possible shapes of the limit cycle in the p–E diagram. First, we describe the cycle which operates only with one reservoir on a constant temperature. Second, we describe the possible shapes of the cycle which operates with two different temperatures.

Isothermal cycle. If the cycle operates with the same temperature of the contact reservoir within the both branches, the only possible shape of the cycle in the p–E plane is one clockwise followed loop and thus such cycle can't produce positive work. The proof is given in the theorem 4.4 below.

Theorem 4.4 (Kelvin Statement)**.** *If the temperatures of the contact reservoirs within the both branches of the cycle equals, the engine can't produce positive work.*

Proof. The prove is obvious from FIG. 4.1. Let us suppose that the energy of the first level during the first stroke increases, i.e., $\frac{\mathrm{d}}{\mathrm{d}t}E(t) > 0$. If the system starts over the equilibrium isotherm, i.e., if $p(t_0) > \pi(t_0)$, then the cycle cannot be closed. Because during the first stroke the system evolves as a green point in the figure (we have increasing $E(t)$) and during the second stroke it evolves as a red/black point in the figure (we have decreasing $E(t)$). If the system starts below the equilibrium isotherm, i.e., if $p(t_0) < \pi(t_0)$ it must reach some point $p(t) < p(t_0)$, $t \in (t_0, t_\mathrm{p})$ to close the cycle. To reach such point, the system must cross the isotherm (if not, it shall evolve as the black point and shall never reach the initial state) and then evolves, during the second stroke, as the red point and further as the black point back to its initial state. Therefore the only closed cycle with one temperature during the both branches and increasing $E(t)$ during the first stroke is the one which is followed clockwise. Therefore the work done on the environment during such cycle is negative, or zero. The proof for decreasing $E(t)$ is similar. This result coincides with Kelvin interpretation of the second law of thermodynamics. □

Cycle operating with two temperatures. The possible shapes of the limit cycle which operates with two different temperatures follow.

1. The cycle consists from one clockwise followed loop and thus can't produce positive work on the environment. Such cycle behaves as a refrigerator.

2. The cycle consists from one counterclockwise followed loop and produce positive work on the environment. Such cycle behaves as an engine.

3. The cycle consists from two loops, one followed clockwise and the other followed counterclockwise. The sign of the produced work depends on the areas of the individual loops.

Other shapes of the cycle are forbidden by the theorems 4.1 , 4.2 and 4.3 (this one secures the maximum number of loops). Having the theorems, proofs are nearly immediate. However, they are quite similar to the proof of the theorem 4.4 and we shall omit it here.

Instead of it, we shall present some representative limit cycles from which the correctness of these statements will be obvious (considering the theorems). In all the pictures we take increasing energy of the first state during the first (expansion) stroke. And therefore decreasing energy of the first state during the second (compression) stroke. In other words, in all the figures we take $h_2 > h_1$ (cf SEC. 3.3).

In FIG. 4.2 we show a case where the cycle is followed counterclockwise and a case of the cycle with two loops. In the both subplots in this figure, we consider that the system is in contact with colder reservoir during the first stroke, i.e., $T_+ < T_-$. In the case of the counterclockwise followed cycle has the initial state of the system higher effective temperature than the reservoir (cf EQ. (4.32)), in the second case vise versa. The accepted work during the counterclockwise followed cycle is, of course, negative, i.e., the engine produces positive work outcome. In the case of the cycle with two loops, the area of the clockwise followed loop is larger than the area of the counterclockwise followed loop. Therefore the accepted work is positive and the system behaves like a refrigerator. Details about parameters taken for the figures are written in the caption of FIG. 4.2.

In FIG. 5.3 in the next chapter, we show another four realisations of the limit cycle and besides them also probability densities for work and for heat accepted by the system within the individual evolutions. In the row a) we took the same parameters as for the counterclockwise followed cycle in FIG. 4.2 beside duration of the individual strokes. Here the first stroke lasts much longer than in the mentioned figure and the second one lasts nearly the same time. The curve which belongs to the first stroke thus lies much closer to the equilibrium isotherm T_+. Otherwise are both cycles nearly identical. In the row b) we have just exchanged the temperatures of the contact reservoirs. Interesting fact, resulting from the theorems 4.1 and 4.2, is the change of the sign of the mean work. In opposite to the line a), the cycle is now followed clockwise. Let us mention here that a case where $T_+ > T_-$ is similar to a case $T_+ < T_-$ in a sense that if we have a cycle with $T_+ > T_-$ starting in the fourth quadrant of the $p-E$ diagram, we get a qualitatively similar picture as if we have a cycle with $T_+ < T_-$ starting in the second quadrant. This fact follows from relative positions of equilibrium isotherms, corresponding to the temperatures

of the individual strokes, to the initial point of the cycle. These positions are, according to our theorems, crucial for the shape of the cycle and in the two cases they are quite similar. In the row c) we show the cycle with highly irreversible regime during the both branches. In the row d) we took only one temperature during the whole cycle. As follows from the theorem 4.4, the accepted work within the cycle must be positive and thus it is followed clockwise. Specific parameters taken in the individual figures are written in the caption of FIG. 5.3.

Having described the possible shapes of the limit cycle, we will now proceed to the analysis of thermodynamics of the engine.

4.6 Thermodynamic analysis of the engine

First of all, recalling that we assume that the cycle starts at a time $t_0 = 0$, let us define the work and the heat accepted by the system within the limit cycle as $W(t) = W(t, 0)$ and $Q(t) = Q(t, 0)$, where $W(t, 0)$ and $Q(t, 0)$ are defined in EQ. (4.26) and EQ. (4.27). We want to study a power outcome of the engine, however our work variable $W(t)$ represents the work accepted by the engine. Let us thus define another work variable $W_{\text{out}} = -W(t_{\text{p}})$, which represents the work done by the engine on the environment per cycle. For other thermodynamic quantities, i.e., for the internal energy $U(t)$ and for the entropies $S_{\text{s}}(t), S_{\text{r}}(t)$ and $S_{\text{tot}}(t)$, we use the definitions from SEC. 4.4 (cf EQ. (4.19), EQ. (4.20), EQ. (4.29) and EQ. (4.30)). Finally, let us stress that for calculation of these quantities, we use of course the state vector $|p(t)\rangle$ given by EQ. (4.18) and the protocol for the engine described in SEC. 3.3.

In FIG. 4.3 we show time behaviour of these variables within one chosen limit cycle. Note that in the both panels, the initial and the final values of the state variables of the system, i.e., $U(t)$ and $S_{\text{s}}(t)$, coincide. It is just because the initial and the final state of the cycle are the same. In the left panel, note that within the cycle $U(t) - U(t_0) = W(t) + Q(t)$. Within the first stroke the engine does positive work on the environment and within the second stroke the work is accepted by the engine. Similar time dependence we see for the heat accepted by the engine. However, the work done on the environment per cycle is positive and the heat delivered to the environment per cycle is negative. In the right panel we see that the total entropy of the system is really an increasing function of time. Because the production of the entropy of the system per cycle is zero, the entropy is produced only in the heat bath. Magnitude of this entropy production, i.e., $S_{\text{tot}}(t) - S_{\text{tot}}(0)$, measures the degree of irreversibility of the cycle. The parameters used for the figure are stated in the figure's caption.

According to the second law of thermodynamics, the output work done by the engine can't be bigger than the work done in the equilibrium limit, i.e., then the sum of increments of the Helmholtz free energy per the individual branches of the cycle (because at the time t_+, where we change the bath, the system is necessarily in a nonequilibrium state and we thus can't just take difference of Helmholtz free energies at the beginning and at the end of the cycle). The Helmholtz free energy of a system on a temperature T at a time t is defined as $F(T,t) = U(T,t) - TS_{\mathrm{s}}(T,t)$, where we stress that also the internal energy and the entropy must be calculated for the temperature T. Finally, the maximal work is defined as $W_{\max} = F(T_-,t_{\mathrm{p}}) - F(T_-,t_+) + F(T_+,t_+) - F(T_+,0)$. After some calculations, we find that for the maximum work done by the engine holds

$$W_{\max} = -\frac{1}{\beta_+}\ln\left[\frac{\cosh(\beta_+ h_2)}{\cosh(\beta_+ h_1)}\right] - \frac{1}{\beta_-}\ln\left[\frac{\cosh(\beta_- h_1)}{\cosh(\beta_- h_2)}\right] \ . \tag{4.43}$$

The engine reaches this work output in the equilibrium limit, which is both the case when the cycle is followed infinitely slow, i.e., when $t_{\mathrm{p}} \to \infty$, and the case when for the reversibility parameter holds $a \to \infty$ (we shall discuss this case in the next chapter). Finally, let us note that more precisely must be valid the inequality $|W(t_{\mathrm{p}})| < |W_{\max}|$, so the value of the maximum work also bounds the work which we can deliver to the engine.

Important characteristics of an engine are its power output P_{out} and its efficiency μ. The power output is defined as the work done by the engine per cycle divided by the duration of the cycle, i.e.,

$$P_{\mathrm{out}} = \frac{W_{\mathrm{out}}}{t_{\mathrm{p}}} \ . \tag{4.44}$$

The efficiency is defined as quotient of the work done by the engine per cycle and the heat accepted by the engine per cycle[4], which we denote as Q_{in}, i.e.,

$$\mu = \frac{W_{\mathrm{out}}}{Q_{\mathrm{in}}} \ . \tag{4.45}$$

From the equation for the maximum work (4.43), we immediately see that the power output in this case is zero (we divide a finite quantity by the infinite time). On the other hand, the efficiency is in this case maximal (because the accepted heat is proportional to the entropy production of the bath, which is in equilibrium limit

[4]Here we talk really about the heat which flowed into the system during the evolution. Thus this quantity doesn't equal to the accepted heat $Q(t,t_0)$ defined in Sec. 4.4!

minimal). In [35] is shown that for given temperatures of the baths T_+, T_-, $T_+ < T_-$ and given boundary values of the energy of the first level h_1, h_2, $0 < h_1 < h_2$ is this maximum efficiency $\mu_{\max}$ given as

$$\mu_{\max} = \frac{\frac{1}{\beta_+}\ln\left[\frac{\cosh(\beta_+ h_2)}{\cosh(\beta_+ h_1)}\right] + \frac{1}{\beta_-}\ln\left[\frac{\cosh(\beta_- h_1)}{\cosh(\beta_- h_2)}\right]}{h_2\tanh(\beta_+ h_2) - h_1\tanh(\beta_- h_1) + \frac{1}{\beta_-}\ln\left[\frac{\cosh(\beta_- h_1)}{\cosh(\beta_- h_2)}\right]} \ . \tag{4.46}$$

Interestingly enough, this rather complicated formula reduces to the Carnot efficiency $\mu_{\mathrm{C}} = 1 - T_+/T_-$ in a limit $h_2 \to \infty \wedge h_1 \to 0$.

We illustrate the facts stated in the previous paragraph in FIG. 4.4. Moreover, we show in this figure dependences of the output work, output power, efficiency and entropy production on the duration of the cycle, when we take equal durations of the individual branches ($t_\pm = t_{\mathrm{p}}/2$). In the figure we see that the output work, the power output, the efficiency and the entropy production converges to its limit values, while the output work and the efficiency increases with t_{p} and the power output and the entropy production decreases with t_{p}. Positive value of the entropy production in the equilibrium limit follows from the fact that, for the limit cycle with different temperatures during the both branches, the true equilibrium limit doesn't exist. As we stated in SEC. 3.3, around the instants where we change the reservoirs, the cycle is always highly irreversible. The value of the entropy production around these instants is exactly the limit value of the entropy. Remarkable thing in panels b) and d) is the fact that, for certain (and different) values of the period durations, the output power and the entropy production reaches its maximal values. In panel a) we also offer the dispersion of the output work $\sigma(-\mathsf{W}(t))$ calculated from the work probability density within the cycle $\rho_{\mathrm{p}}(w, t_{\mathrm{p}})$ (cf EQ. (5.39) and adjacent text). Note that for maximal output power is this fluctuation comparatively high. Interestingly enough, in panels b) and c), for certain value of the cycle duration, the power output and the efficiency changes its sign. For this value of t_{p}, the direction in which the limit cycle is followed is changing. And thus also the sign of the work delivered by the engine changes. Finally, let us note that for the given inverse temperatures, $\beta_+ = 0.5\ \mathrm{J}^{-1}$ and $\beta_- = 0.1\ \mathrm{J}^{-1}$, the Carnot efficiency equals $\mu_{\mathrm{C}} = 0.8$ and the efficiency of our engine converges to the value $\mu_{\max} = 0.6$. The parameters used for the figure are stated in the figure's caption.

In FIG. 4.4 we see that for certain value of cycle duration, the power output reaches its maximum value. However, this figure was constructed for a case where durations of the individual strokes equals. Therefore, in the next FIG. 4.5, we offer dependence of variables μ, P_{out} and $S_{\mathrm{tot}}(t_{\mathrm{p}}) - S_{\mathrm{tot}}(0)$ on a parameter which describes allocation of duration of the cycle between the individual strokes for a fixed period

t_p. We call this parameter as *allocation parameter* and we define it as

$$\Delta = \frac{t_+ - t_-}{t_\mathrm{p}} \ . \tag{4.47}$$

From its definition is clear that $\Delta \in \langle -1, 1\rangle$, $\Delta = 1$ when $t_\mathrm{p} = t_+$ and $\Delta = -1$ when $t_\mathrm{p} = t_-$. Negative values of this parameter thus belongs to those cycles where $t_+ < t_-$ and vice versa. Panels a1)–c1) illustrate the situation where the bath corresponding to the expansion stroke is colder than that of the compression stroke. The Curzon-Ahlborn efficiency in this case equals approximately $\mu_\mathrm{CP} = 0.55$ and the efficiency at maximum power output in the figure is lower. Notice that the maximum efficiency doesn't correspond to the maximum output power. The dotted curves in the panels b1) and b2) show the dispersion of the output power $\sigma(-\mathsf{W}(t))/t_\mathrm{p}$ as calculated from the probability density for the work $\rho_\mathrm{p}(w, t_\mathrm{p})$ (cf Eq. (5.39) and adjacent text). The parameters used for the figure are stated in the figure's caption.

In closing this chapter, let us note that quite similar discussion of thermodynamics of the engine is also done in [35]. In the next chapter we shall concentrate on calculation and discussion of probability densities for hereby defined variables, namely for the accepted heat $Q(t)$ and for the accepted work $W(t)$.

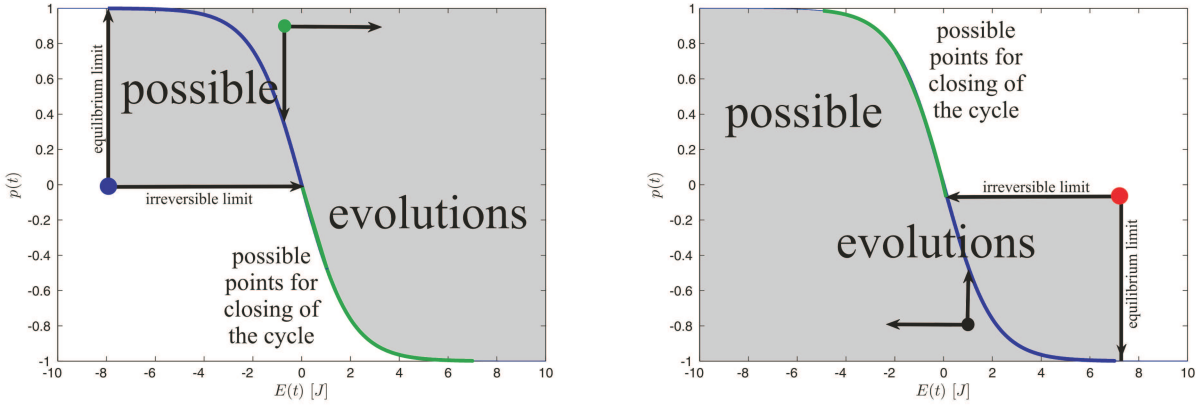

FIG. 4.1: Possible isothermal evolutions in the p–E diagram. In the both panels, the blue-green curve depicts the equilibrium isotherm corresponding to the isothermal process. In the left panel the energy $E(t)$ increases during the evolution (expansion), in the right one contrarywise (compression). In all points in the figure are depicted right angles, within which must, according to the right angle theorem 4.2, lay any possible evolution starting from the points. The evolution starting from the blue point below the isotherm (in the left panel) and the evolution starting from the red point over the isotherm (in the right panel), respectively, are driven towards the isotherm. After the isotherm is crossed, the system reaches the state which fulfils conditions of the non-crossing theorem 4.1 (for example the green and the black point) and remains over/below the isotherm for the rest of its evolution. The grey area containing the sign "possible evolutions" in the left panel represents the set of points accessible by possible evolutions from the blue point. Similar meaning has the grey area in the right panel for the evolutions departing from the red point. Let us now describe possible realisation of an isothermal cycle (the same temperature of the contact reservoir within the both strokes). Imagine that, during the expansion stroke, the system evolves from the blue point, crosses the isotherm an stops, at the end of the expansion, in some point over the isotherm. Then, during the compression stroke, the system departs from this point, relaxes towards the equilibrium isotherm and crosses it in some point. Finally the system returns back to the blue point, so the cycle is closed. The green part of the isotherm shows possible points where the isotherm must be crossed in order to the cycle can be closed. Similarly in the right panel. Obviously, the cycle must be followed clockwise and thus the work done by the engine on the environment can't be positive (cf theorem 4.4).

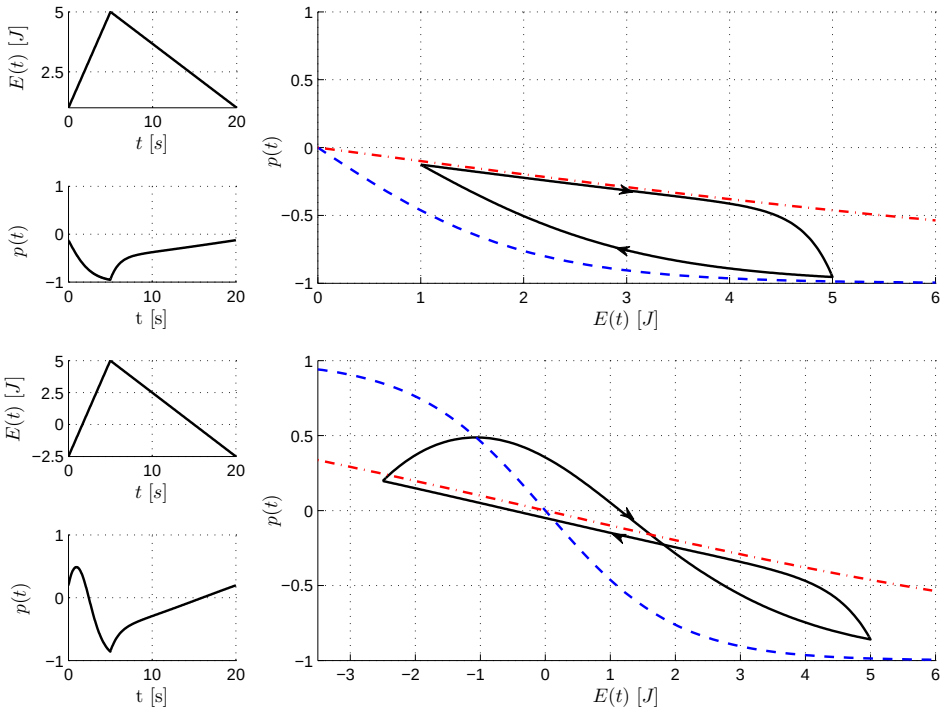

FIG. 4.2: Limit cycle for the two-stroke engine using as the working medium a two-level system. The upper three panels illustrate the case where $h_2 > h_1 > 0$. Therefore the energy levels do not cross during their driving. We first give the energy of the first level $E(t)$ as the function of time. Below this panel, we plot the system response, i.e. the time dependence of the occupation difference $p(t)$. The right panel then gives the parametric plot of the limit cycle in the p–E plane. The cycle starts in the upper vertex and proceeds counterclockwise, c.f. the arrows. The dashed (the dot-dashed) curve shows the equilibrium isotherm corresponding to the bath which communicates with the system during the first (the second) stroke. The parameters used are: $h_1 = 1$ J, $h_2 = 5$ J, $t_+ = 5$ s, $t_- = 15$ s, $\beta_+ = 0.5$ J^{-1}, $\beta_- = 0.1$ J^{-1}, $\nu = 1$ s^{-1}. The lower three panels depict the case where $h_1 < 0 < h_2$ and therefore the energies cross twice during the cycle. We have taken $h_1 = -2.5$ J, all other parameters are the same as above. The two-loop shape follows from the general rules as explained in the main text.

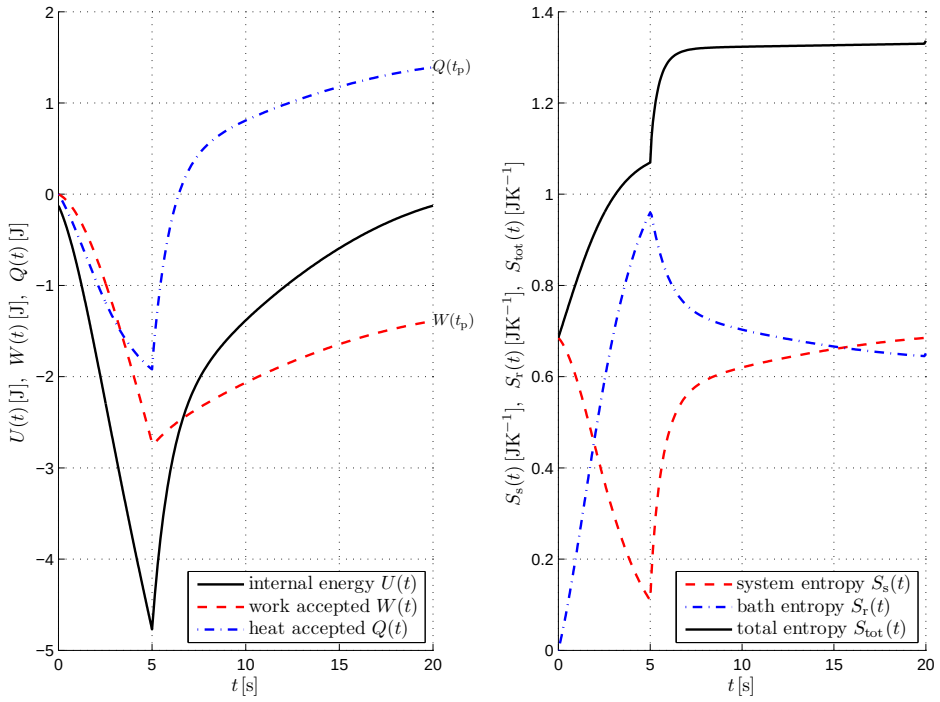

FIG. 4.3: The left panel shows the internal energy, the work done on the system, and the heat accepted from the both reservoirs as the function of time within the limit cycle $t \in (0, t_\mathrm{p})$. The final position of the work curve indicates the work done on the system per cycle $W(t_\mathrm{p})$. For the parameter used here (the same set as in FIG. 4.2 with positive h_1) the accepted work per cycle is negative and hence the positive work $W_\mathrm{out} = -W(t_\mathrm{p})$ was done on the environment. The internal energy returns to its original value and, after completion of the cycle, the accepted heat equals the negative accepted work. The right panel shows the entropy of the system, the entropy of the bath, and their sum as the function of time. After completing the cycle, the system entropy reassumes its initial value. The difference $S_\mathrm{tot}(t_\mathrm{p}) - S_\mathrm{tot}(0)$ equals the new entropy added to the baths, it is always positive and it measures the degree of irreversibility of the cycle.

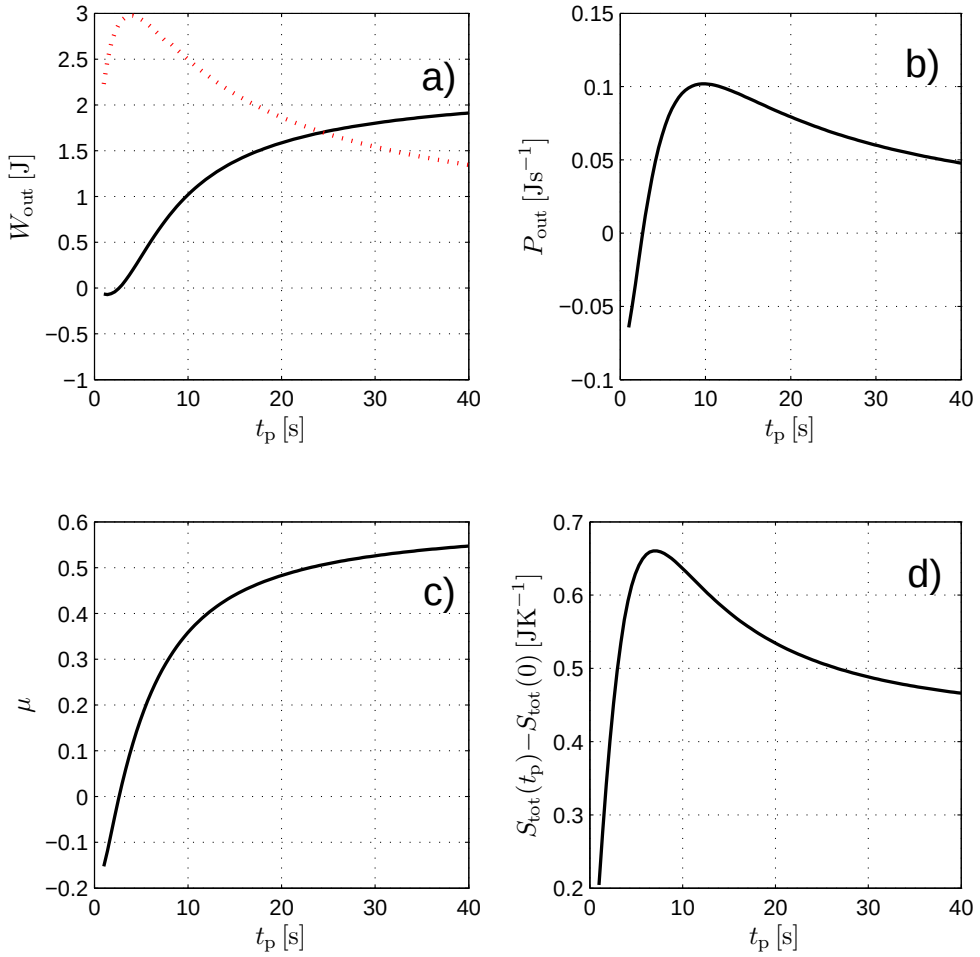

FIG. 4.4: The engine performance versus the duration of the limit cycle $t_{\rm p}$. For a given period, the both branches have equal lengths, $t_{\pm} = \frac{1}{2}t_{\rm p}$. Other parameters assume the same values as in FIG. 4.2 with positive h_1. If $t_{\rm p}$ increases then both the output work (panel a)) and the efficiency (panel c)) also increase. However, the output power (panel b)) assumes a maximum at a special cycle duration. The dotted line in the panel a) gives the dispersion of the output work as calculated from the probability density $\rho_{\rm p}(w, t_{\rm p})$. Notice that the work fluctuation in the vicinity of the maximal output power is comparatively high. In the long-period limit, the cycle still represents a nonequilibrium process and hence the entropy production $S_{\rm tot}(t_{\rm p}) - S_{\rm tot}(0)$ (panel d)) remains positive, approaching a specific asymptotic value.

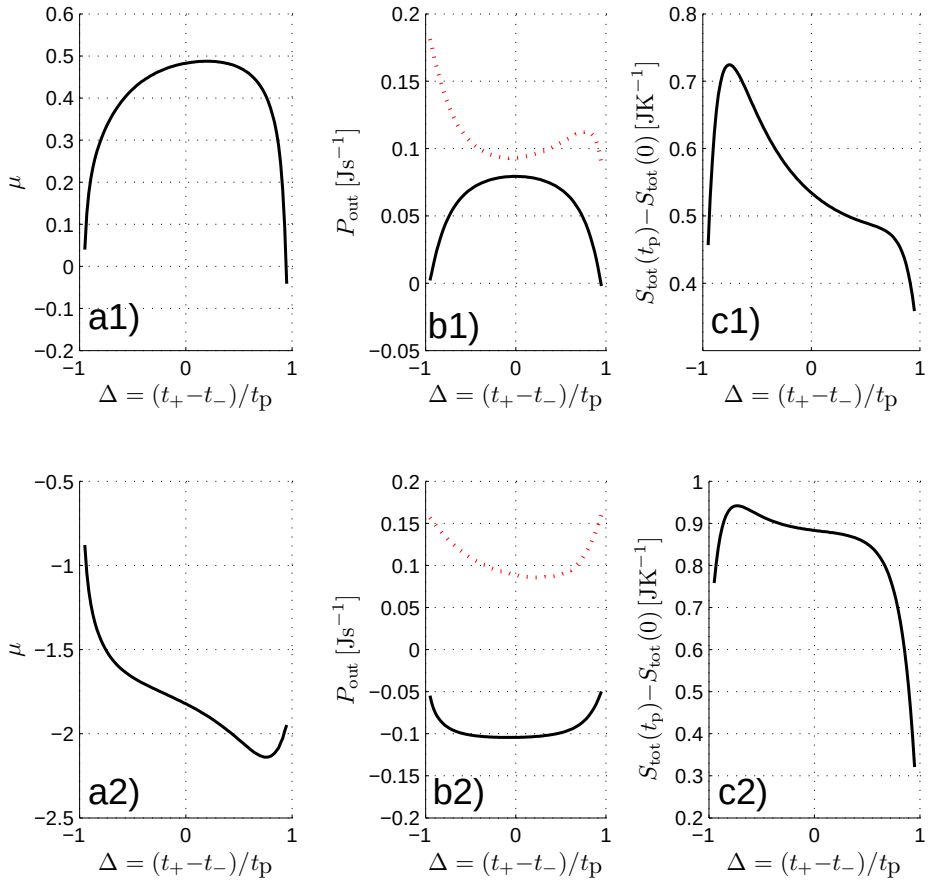

FIG. 4.5: The engine performance versus the allocation parameter Δ. We have taken the fixed period $t_{\mathrm{p}} = 20$ s and the parameters h_1, h_2, and ν equal those in FIG. 4.2. The panels a1)–c1) illustrate the situation where the bath corresponding to the expansion stroke is colder than that of the compression stroke: $\beta_{+} = 0.5\ \mathrm{J}^{-1}$ and $\beta_{-} = 0.1\ \mathrm{J}^{-1}$. Notice that the maximum efficiency doesn't correspond to the maximum output power. In the panels a2)–c2) we have taken the opposite disposition of the bath temperatures: $\beta_{+} = 0.1\ \mathrm{J}^{-1}$ and $\beta_{-} = 0.5\ \mathrm{J}^{-1}$. The dotted curves in the panels b1) and b2) show the dispersion of the output power as calculated from the probability density for the work $\rho_{\mathrm{p}}(w, t_{\mathrm{p}})$.

Chapter 5

Path-resolved properties

5.1 Generic propagator for the work probability density

In this section, similarly as in Sec. 4.1, we will derive the propagator for the augmented process (2.13) for the generic driving scenario (3.2). As we stated before, this solution will be the general solution for any linear driving protocol. Thus we shall easily get from it the specific form of the propagators for the individual strokes of the engine described in the previous Sec. 3.3.

For our generic driving scenario (3.2), the matrix $\mathbb{H}(t)$, the time derivative of which appears in the equation for the work probability density, has the form $\mathbb{H}(t) = \mathrm{diag}\{h + v(t - t_0), -h - v(t - t_0)\}$. Thus for its time derivative we get $\frac{\mathrm{d}}{\mathrm{d}t}\mathbb{H}(t) = v\,\mathrm{diag}\{1, -1\}$. Note that thanks to the linear driving, we have, in the resulting equation, the time variable t only in the arguments of exponential functions (of course except the propagator itself). This fact is, as we will see below, crucial for usableness of our calculation method of the work probability density propagator. Inserting this matrix $\frac{\mathrm{d}}{\mathrm{d}t}\mathbb{H}(t)$ together with the Glauber form of the transition probabilities (4.4) into Eq. (2.12), we get the equation for the Laplace transform of the generic work probability density for any linear driving scenario, say $\mathbb{G}(u, t, t_0)$. This equation is

$$\frac{\mathrm{d}}{\mathrm{d}t}\mathbb{G}(u,t,t_0) = -\left[\frac{\nu}{1 + c\mathrm{e}^{-\Omega(t-t_0)}}\begin{pmatrix} 1 & -c\mathrm{e}^{-\Omega(t-t_0)} \\ -1 & c\mathrm{e}^{-\Omega(t-t_0)} \end{pmatrix} + vu\begin{pmatrix} 1 & 0 \\ 0 & -1 \end{pmatrix}\right]\mathbb{G}(u,t,t_0), \qquad \mathbb{G}(u,t_0,t_0) = \mathbb{I}\,. \quad (5.1)$$

Performing the inverse Laplace transformation with respect to the variable u, we could get partial differential equation for the work probability density propagator $\mathbb{G}(w, w_0, t, t_0)$, which we wish to calculate. Instead of solving this differential equation directly, we shall rather find the function $\mathbb{G}(u, t, t_0)$ first and than transform it back to its original variables.

In the computation below, we will suppose that the parameter v is strictly positive, i.e., $v > 0$, and hence also $\Omega = 2\beta v > 0$ (we suppose the finite temperature). The propagator for the case $\Omega = 0$ can be calculated easily, because in this case is the time dependence in our dynamic equation trivial. The resulting propagator is proportional to the work done in the equilibrium limit, which is given by difference of the Helmholtz free energies at the end and in the beginning of the evolution. We will be also able to obtain this result from our general solution in the limit $\Omega \to 0$ (or $a \to \infty$). The solution for the case $v < 0$ we shall obtain by simple trick. Knowing that the energy of the 2nd state is defined as $E_2(t) = -E_1(t)$, we see that the parameter $-v$, which denotes the velocity of changing the energy of the 2nd state, is positive when $v < 0$. Therefore, in the case of negative v, we can just rename the states $1 \leftrightarrow 2$ and calculate the propagator for this setting. Let us stress that we have to redefine our constants in correspondence with the definition of the second energy level as $\Omega = -2\beta v$ and $c = \mathrm{e}^{2\beta h}$. Thus if we calculate the functions $g_{ij}(w, w_0; t, t_0)$ according to the procedure further with this new Ω and c, and if we interchange the indices $i \leftrightarrow j$, we get the desired propagator for the case $v < 0$.

Now we shall finally proceed in the calculations. Our approach will be very similar to that performed in [27], the only difference is the presence of the function c which stands, as stated before, for the arbitrary position of the energy levels on the beginning of the evolution. First of all, we introduce the substitution $s = u/(2\beta)$. This means that for the variable conjugated with s through the inverse Laplace transformation, say η, holds $\eta = 2\beta(w - w_0)$ (here we already suppose, as stated in Sec. 2.3, that the initial value of the accepted work is with certainty w_0). Further we shall call the variable η as the *dimensionless* work. Moreover we introduce the dimensionless time $\tau = \Omega(t - t_0)$. Note that since $t \geq t_0$, is $\tau \geq 0$ (for now we have $\Omega > 0$). Inserting this substitutions into the equation (5.1), we get

$$\frac{\mathrm{d}}{\mathrm{d}\tau}\mathbb{G}(s,\tau) = -\left[s\begin{pmatrix} 1 & 0 \\ 0 & -1 \end{pmatrix} + \frac{a}{1+c\mathrm{e}^{-\tau}}\begin{pmatrix} 1 & -c\mathrm{e}^{-\tau} \\ -1 & c\mathrm{e}^{-\tau} \end{pmatrix}\right]\mathbb{G}(s,\tau)\ , \tag{5.2}$$

with the initial condition given as $\mathbb{G}(s, 0) = \mathbb{I}$. The dimensionless combination $a = \nu/\Omega$ is nothing but the *reversibility parameter* from Sec. 4.1.

We shall advance with another substitution $\mathbb{F}(2s, \tau) = \mathrm{e}^{-s\tau}\mathbb{G}(s, \tau)$. Then our

dynamical equation obtains the form

$$\frac{\mathrm{d}}{\mathrm{d}\tau}\mathbb{F}(s,\tau) = -\left[s\begin{pmatrix} 1 & 0 \\ 0 & 0 \end{pmatrix} + \frac{a}{1+c\mathrm{e}^{-\tau}}\begin{pmatrix} 1 & -c\mathrm{e}^{-\tau} \\ -1 & c\mathrm{e}^{-\tau} \end{pmatrix}\right]\mathbb{F}(s,\tau)\ , \tag{5.3}$$

with the initial condition given as $\mathbb{F}(s,0) = \mathbb{I}$. This matrix equation splits into two independent systems of two coupled ordinary differential equations. Let us first consider the second pair, i.e.,

$$\begin{aligned}\frac{\mathrm{d}}{\mathrm{d}\tau}f_{12}(s,\tau) =& -\frac{a}{1+c\mathrm{e}^{-\tau}}f_{12}(s,\tau) + \frac{ac\mathrm{e}^{-\tau}}{1+c\mathrm{e}^{-\tau}}f_{22}(s,\tau) - sf_{12}(s,\tau)\ , \\ & f_{12}(s,0) = 0\ , \end{aligned} \tag{5.4}$$

$$\begin{aligned}\frac{\mathrm{d}}{\mathrm{d}\tau}f_{22}(s,\tau) =& \frac{a}{1+c\mathrm{e}^{-\tau}}f_{12}(s,\tau) - \frac{ac\mathrm{e}^{-\tau}}{1+c\mathrm{e}^{-\tau}}f_{22}(s,\tau)\ , \\ & f_{22}(s,0) = 1\ . \end{aligned} \tag{5.5}$$

Let us now carry out the three following steps. First, we multiply Eq. (5.4) by the expression $(1+c\mathrm{e}^{-\tau})$. Then we carry out the *direct* Laplace transformation in the variable τ on both sides of the resulting equation. The Laplace variable conjugated to τ we shall denote as z. During this step, the product $\mathrm{e}^{-\tau}f_{22}(s,\tau)$ is transformed into $f_{22}(s,z+1)$ and similarly for the product $\mathrm{e}^{-\tau}f_{12}(s,\tau)$. If the driving wasn't linear, we would have to deal with products like $\psi(t)f_{22}(s,\tau)$, where $\psi(t) \sim \frac{\mathrm{d}}{\mathrm{d}t}E_1(t)$, which would be probably very difficult. Secondly, we want to eliminate the unknown function $f_{22}(s,z)$. For this purpose one could use the Laplace transformation of Eq. (5.5). Instead of that, and perhaps more conveniently, we will sum the original equations (5.4), (5.5) and carry out the direct Laplace transformation of the emerging sum. In this way, we get the relation $(z+s)f_{12}(s,z) + zf_{22}(s,z) = 1$. Finally, in the third step, we use the last relation to eliminate the function $f_{22}(s,z)$ from the equation obtained in the first step. On the whole, we arrive at the single *difference* equation for the function $f_{12}(s,z)$. It is

$$f_{12}(s,z) + c\frac{(z+a+1)(z+s+1)}{(z+1)(z+s+a)}f_{12}(s,z+1) = c\frac{a}{(z+1)(z+s+a)}\ . \tag{5.6}$$

Similar equations emerge if we replace on both sides of this equation the variable z with $z+n$, $n = 1,2,\ldots$. Hence we arrive at an infinite system of linear algebraic equations for the functions $f_{12}(s,z+n)$, $n = 0,1,\ldots$. This system can be rewritten in the matrix form. The matrix of the coefficients having the nonzero elements just on the main diagonal and above it. Using standard algebraic methods (it is

sufficient to calculate the first line of the matrix inverse to the coefficient matrix), we solve the infinite system and the function $f_{12}(s,z)$ emerges in the form

$$f_{12}(s,z) = ca\sum_{n=0}^{\infty}(-c)^n \frac{(z+s+1)_n}{(z+s+a)_{n+1}} \frac{(z+a+1)_n}{(z+1)_{n+1}} \ . \tag{5.7}$$

Here and below, $(z)_n = z(z+1)(z+2)\ldots(z+n-1)$ is the Pochhammer symbol [38]. We want to find the double inverse Laplace transformation of this function.

In order to accomplish our goal,we introduce an important auxiliary function

$$H(a;s,z) = \sum_{n=0}^{\infty}(-c)^n \frac{(s+b)_n}{(s)_{n+1}} \frac{(z+a)_n}{(z)_{n+1}} \ , \tag{5.8}$$

where $b = 1-a$. Its fundamental role stems from the following two observations. First, we have succeeded in calculation of its double inverse Laplace transformation. While we present the details of the calculations in Appendix A, the result is

$$H(a;\eta,\tau) = \Theta(\eta)\Theta(\tau)\frac{1}{(1+c\mathrm{e}^{-\eta})^a}\frac{1}{(1+c\mathrm{e}^{-\tau})^{1-a}} \times \ {}_2\mathrm{F}_1\left(a,1-a;1;-c\frac{1-\mathrm{e}^{-\eta}}{1+c\mathrm{e}^{-\eta}}\frac{1-\mathrm{e}^{-\tau}}{1+c\mathrm{e}^{-\tau}}\right) \ , \tag{5.9}$$

where $\Theta(\eta)$ denotes the unit step function. Second, as follows from comparison of Eq. (5.7) and Eq. (5.8), we have that

$$f_{12}(s,z) = acH(a;s+z+a,z+1) \ . \tag{5.10}$$

Knowing the double inverse Laplace transformation of the function $H(a;s,z)$, we can easily transform the function $f_{12}(s,z)$. We first carry out the inverse Laplace transformation of the function $H(a;s+z+a,z+1)$ with respect to the variable s. The result is $\mathrm{e}^{-\eta(z+a)}H(a;\eta,z+1)$. Thereupon, we perform the inverse Laplace transformation with respect to the variable z. Here the combination $\mathrm{e}^{-\eta z}H(a;\eta,z+1)$ is transformed into $\mathrm{e}^{-(\tau-\eta)}H(a;\eta,\tau-\eta)$. Summing up, the functions $f_{12}(\eta,\tau)$ and $H(a;\eta,\tau)$ are related through the formula

$$f_{12}(\eta,\tau) = ac\mathrm{e}^{-(a-1)\eta}\mathrm{e}^{-\tau}H(a;\eta,\tau-\eta) \ . \tag{5.11}$$

Let us turn our attention to the function $f_{22}(\eta,\tau)$. It is coupled with the function $f_{12}(\eta,\tau)$ by the system of differential equations (5.6) and (5.5). We now use the standard rules of the operational calculus [39] and carry out the inverse Laplace

transformation with respect to the variable s on both sides of Eq. (5.4). We obtain the relation between the functions $f_{22}(\eta,\tau)$ and $f_{12}(\eta,\tau)$

$$f_{22}(\eta,\tau)=\frac{1+c\mathrm{e}^{-\tau}}{ac\mathrm{e}^{-\tau}}\left(\frac{\partial}{\partial\eta}f_{12}(\eta,\tau)+\frac{\partial}{\partial\tau}f_{12}(\eta,\tau)\right)+\frac{1}{c\mathrm{e}^{-\tau}}f_{12}(\eta,\tau)\ . \tag{5.12}$$

Repeating the same steps, as for the functions $f_{12}(s,z)$ and $f_{22}(s,z)$, for the remaining two functions $f_{21}(s,z)$ and $f_{11}(s,z)$, we obtain the relations

$$f_{12}(\eta,\tau)=a\mathrm{e}^{-a\eta}H(a+1;\eta,\tau-\eta)\ . \tag{5.13}$$

and

$$f_{11}(\eta,\tau)=\frac{1+c\mathrm{e}^{-\tau}}{a}\frac{\partial}{\partial\tau}f_{12}(\eta,\tau)+c\mathrm{e}^{-\tau}f_{12}(\eta,\tau)\ . \tag{5.14}$$

Let us stress that during the calculation of the functions $f_{22}(\eta,\tau)$ and $f_{11}(\eta,\tau)$ from equations (5.12) and (5.14), the partial derivative of the unit step function (cf (5.9)) produces a term proportional to the Dirac delta function. We won't to show here the specific form of the matrix elements $f_{ij}(\eta,\tau)$, $i,j=1,2$. Instead of it, we shall write directly the elements of the desired matrix $\mathbb{G}(w,w_0,t,t_0)$. First, we will consider the above stated relation $\mathbb{F}(2s,\tau)=\mathrm{e}^{-s\tau}\mathbb{G}(s,\tau)$ and perform therein the inverse Laplace transformation with respect to the variable s, we obtain $\mathbb{G}(\eta,\tau)=\frac{1}{2}\mathbb{F}(\frac{\tau+\eta}{2},\tau)$. Let us besides remind that $\eta=\eta(w,w_0)=2\beta(w-w_0)$ and $\tau=\tau(t,t_0)=\Omega(t-t_0)$. Thus we finally have $\mathbb{G}(w,w_0,t,t_0)=2\beta\mathbb{G}(\eta,\tau)$.

As we stated before, for negative velocity of the driving v we have to redefine the constants c and Ω and interchange the matrix indices of $\mathbb{G}(w,w_0,t,t_0)$ to get the correct result. We shall therefore define the general form of the constants through the relations $c=\exp(-2\beta h|v|/v)$ and $\Omega=2\beta|v|$. Moreover, we introduce the following abbreviations

$$x=x(w,w_0,t,t_0)=\exp\left(-\frac{\tau+\eta}{2}\right)\ , \tag{5.15}$$

$$y=y(w,w_0,t,t_0)=\exp\left(-\frac{\tau-\eta}{2}\right)\ , \tag{5.16}$$

$$\phi=\phi(w,w_0,t,t_0)=-c\frac{1-x}{1+cx}\frac{1-y}{1+cy}\ . \tag{5.17}$$

Finally, we are prepared to write the crucial result of this section, the generic form of the propagator for the augmented process. For the case $v>0$, its matrix

elements are

$$
\begin{aligned}
g_{11}(w,w_0,t,t_0) &= 2\beta\left[\frac{(1+c)\exp(-\tau)}{1+c\exp(-\tau)}\right]^a \delta(\tau-\eta) - \Theta(\tau+\eta)\Theta(\tau-\eta)ac\beta \\
&\times\ x^a(1-x)y\left[\frac{{}_2\mathrm{F}_1\left(1+a,-a;1;\phi\right)}{(1+cx)^{1+a}(1+cy)^{1-a}} - (1+a)(1+c)\right. \\
&\times\ \left.(1+cxy)\frac{{}_2\mathrm{F}_1\left(2+a,1-a;2;\phi\right)}{(1+cx)^{2+a}(1+cy)^{2-a}}\right], \qquad (5.18)\\
g_{12}(w,w_0,t,t_0) &= \Theta(\tau+\eta)\Theta(\tau-\eta)\,ac\beta x^a y\frac{{}_2\mathrm{F}_1\left(a,1-a;1;\phi\right)}{(1+cx)^a(1+cy)^{1-a}}, \qquad (5.19)\\
g_{21}(w,w_0,t,t_0) &= \Theta(\tau+\eta)\Theta(\tau-\eta)\,a\beta x^a\frac{{}_2\mathrm{F}_1\left(1+a,-a;1;\phi\right)}{(1+cx)^{1+a}(1+cy)^{-a}}, \qquad (5.20)\\
g_{22}(w,w_0,t,t_0) &= 2\beta\left[\frac{1+c\exp(-\tau)}{1+c}\right]^a \delta(\tau+\eta) + \Theta(\tau+\eta)\Theta(\tau-\eta)\,ac\beta \\
&\times\ x^a(1-y)\left[\frac{{}_2\mathrm{F}_1\left(a,1-a;1;\phi\right)}{(1+cx)^{1+a}(1+cy)^{1-a}} - (1-a)(1+c)\right. \\
&\times\ \left.(1+cxy)\frac{{}_2\mathrm{F}_1\left(1+a,2-a;2;\phi\right)}{(1+cx)^{2+a}(1+cy)^{2-a}}\right]. \qquad (5.21)
\end{aligned}
$$

As we stated before, if $v<0$, we just interchange the subscripts 1 and 2 in order to get the right result.

Now, having in our hands the generic propagator for the augmented process, we can proceed further in the analysis of our engine. First of all, in the next section, we shall write the specific form of the propagator $\mathbb{G}(w,w_0,t,t_0)=\mathbb{G}_{\mathrm{p}}(w,t)$ for its operational cycle as it is described in Sec. 3.4.

5.2 The work probability density within the cycle

Similarly as in Sec. 4.2 we shall now nearly immediately write the propagators for the individual branches of the operational cycle of our engine. We repeat ones more the constants for the individual branches of the cycle (cf Tab. 3.1), they are for the first branch: $h=h_+=h_1$, $v=v_+=(h_2-h_1)/t_+$, $t_0=0$, $t=t_+$ and $\beta=\beta_+$. For the second branch we get: $h=h_-=h_2$, $v=v_-=-(h_2-h_1)/t_-$, $t_0=t_+$, $t=t_{\mathrm{p}}$ and $\beta=\beta_-$. If we substitute these constants into the equations (5.18) – (5.21) (and considering the text around them, especially about the sign of v), we easily get the propagators for the individual branches of the cycle, $\mathbb{G}_+(w',0;t_+,0)$ and

$\mathbb{G}_-(w, w'; t_\mathrm{p}, t_+)$. We shall not write its specific form here, because the equations are to huge.

Instead of it, we shall directly write the propagator for the limit cycle

$$\mathbb{G}_\mathrm{p}(w,t) = \begin{cases} \mathbb{G}_+(w,0,t,0) & \text{for} \quad t \in \langle 0, t_+ \rangle \ , \\ \\ \displaystyle\int_{-\infty}^{-\infty} \mathrm{d}w' \, \mathbb{G}_-(w,w',t,t_+)\mathbb{G}_+(t_+,0,w',0) & \text{for} \quad t \in \langle t_+, t_\mathrm{p} \rangle \ . \end{cases} \tag{5.22}$$

Having this propagator, we can easily calculate the probability density for the work done on the engine within the cycle by the simple formula (similar to Eq. (2.17))

$$\rho_\mathrm{p}(w,t) = \sum_{i=1}^{N} \langle i | \, \mathbb{G}_\mathrm{p}(w,t) \, | p^\mathrm{stat} \rangle \ , \tag{5.23}$$

Here $|p^\mathrm{stat}\rangle$ is our known vector representing the initial state of the limit cycle with the components given by (4.17). Before we shall introduce some examples of the work probability densities, we shall, moreover, introduce the probability density for heat accepted by the system.

5.3 The heat probability density within the cycle

First, we shall define two new random variables. Specifically, we designate as $\mathsf{Q}(t, t_0)$ the heat accepted by the system during an evolution which starts at a time t_0 and finishes at a time t and as $\mathsf{U}(t)$ the internal energy of the system at an instant t. The first law of thermodynamics must hold for any trajectory and thus we can write an equivalent of Eq. (4.21) for this random variables

$$\mathsf{U}(t) - \mathsf{U}(t_0) = \mathsf{W}(t, t_0) + \mathsf{Q}(t, t_0) \ . \tag{5.24}$$

We get a relation between the random variables $\mathsf{U}(t) - \mathsf{U}(t_0)$, $\mathsf{W}(t, t_0)$ and $\mathsf{Q}(t, t_0)$. From this relation, we can easily get the relation between the probability densities for the individual random variables. Instead of direct calculation, we shall first define a generic propagator for heat $\mathbb{Q}(\omega, \omega_0, t, t_0)$ by the relation quite similar to that for $\mathbb{G}(w, w_0, t, t_0)$ (cf Eq. (2.13))

$$\begin{aligned} &q_{ij}(\omega, \omega_0; t, t_0) \, \mathrm{d}\omega = \langle i | \, \mathbb{Q}(\omega, \omega_0, t, t_0) \, | j \rangle \, \mathrm{d}\omega \\ &= \mathrm{Prob}\left\{ \mathsf{Q}(t,0) \in (\omega, \omega + \mathrm{d}\omega) \ \wedge \ \mathsf{D}(t) = i \mid \mathsf{Q}(t_0,0) = \omega_0 \ \wedge \ \mathsf{D}(t_0) = j \right\} . \end{aligned} \tag{5.25}$$

In other words, quantity $q_{ij}(\omega, \omega_0; t, t_0)\,\mathrm{d}\omega$ is the probability that the system, which starts with certainty from the state j and stops with certainty in the state i, accepted during its evolution an amount of heat ω.

The change of internal energy of the system depends only on its initial and final state and thus, if we know them, it is no longer the random variable. If we designate as $u_{ij}(t, t_0)$ a change of the internal energy of the system during an evolution from a state j to a state i and similarly $\mathsf{Q}_{ij}(t, t_0)$ and $\mathsf{W}_{ij}(t, t_0)$ accepted heat by the system during this evolution and accepted work by the system during this evolution, respectively, we can write the relation

$$u_{ij}(t, t_0) = u_{ij} = E_i(t) - E_j(t_0) = \mathsf{W}_{ij}(t, t_0) + \mathsf{Q}_{ij}(t, t_0) \ , \tag{5.26}$$

and thus

$$\mathsf{Q}_{ij}(t, t_0) = u_{ij}(t, t_0) - \mathsf{W}_{ij}(t, t_0) \ . \tag{5.27}$$

Therefore we can write

$$\text{Prob}\,\{\mathsf{Q}_{ij} \in (u_{ij} - w, u_{ij} - w + \mathrm{d}w)\} = \text{Prob}\,\{\mathsf{W}_{ij} \in (w, w + \mathrm{d}w)\} \ , \tag{5.28}$$

where we have omit to write the time dependence of the variables. The probability densities for Q_{ij} and W_{ij} are the functions $q_{ij}(\omega, \omega_0; t, t_0)$ and $g_{ij}(w, w_0; t, t_0)$ (cf equations (2.13) and (5.25)). According to Eq. (5.28) we can immediately write

$$q_{ij}(u_{ij} - w, \omega_0; t, t_0)\,\mathrm{d}w = g_{ij}(w, w_0; t, t_0)\,\mathrm{d}w \ . \tag{5.29}$$

Here $\omega_0 = w_0$. After a simple substitution $u_{ij} - w = \omega$, we get

$$q_{ij}(\omega, \omega_0; t, t_0)\,\mathrm{d}\omega = g_{ij}(u_{ij} - \omega, w_0; t, t_0)\,\mathrm{d}\omega \ . \tag{5.30}$$

Note that from Eq. (5.30) follows by simple substitution $x = \omega + u_{ij}/2$ that for the functions $q_{ij}(\omega, w_0; t, t_0)$ and $g_{ij}(w, w_0; t, t_0)$ holds $g_{ij}(u_{ij}/2 + x, w_0; t, t_0) = q_{ij}(u_{ij}/2 - x, \omega_0; t, t_0)$, i.e., the functions with the subscript (ij) are symmetric around the point $u_{ij}/2$. For the propagator for heat we finally get

$$\mathbb{Q}(\omega, \omega_0, t, t_0) = \begin{pmatrix} g_{11}(u_{11} - \omega, w_0; t, t_0) & g_{12}(u_{12} - \omega, w_0; t, t_0) \\ g_{21}(u_{21} - \omega, w_0; t, t_0) & g_{22}(u_{22} - \omega, w_0; t, t_0) \end{pmatrix} \ , \tag{5.31}$$

where, recalling Eq. (3.2), the functions $u_{ij} = u_{ij}(t, t_0)$ are given as

$$u_{11}(t, t_0) = E_1(t) - E_1(t_0) = v(t - t_0) \ , \tag{5.32}$$

$$u_{12}(t, t_0) = E_1(t) - E_2(t_0) = 2h + v(t - t_0) \ , \tag{5.33}$$

$$u_{21}(t, t_0) = E_2(t) - E_1(t_0) = -2h - v(t - t_0) \ , \tag{5.34}$$

$$u_{22}(t, t_0) = E_2(t) - E_2(t_0) = -v(t - t_0) \ , \tag{5.35}$$

$\omega_0 = w_0$, and the functions $g_{ij}(w, w_0; t, t_0)$ are given by equations (5.18)-(5.21).

Therefore, to calculate the heat probability density within the cycle, $\chi_{\rm p}(\omega, t)$, it is sufficient to calculate the work propagator $\mathbb{G}_{\rm p}(w, t)$ from Eq. (5.22), and than transform it according to matrix Eq. (5.31) obtaining the heat propagator $\mathbb{Q}_{\rm p}(\omega, t)$. Heaving the heat propagator, the heat probability density can be calculated through the simple formula

$$\chi_{\rm p}(\omega, t) = \sum_{i=1}^{2} \langle i| \, \mathbb{Q}_{\rm p}(\omega, t) \, |p^{\rm stat}\rangle \ , \tag{5.36}$$

where the initial state of the system $|p^{\rm stat}\rangle$ is given by Eq. (4.17).

In the next section, we shall discuss properties both of the work probability density and the heat probability density.

5.4 Properties of the probability densities

First, let us stress that in further analysis we, similarly as in the discussion of thermodynamic properties of the engine, suppose that the first stroke is the expansion stroke and the second one is the compression stroke, i.e., that $h_2 > h_1$ (cf Sec. 3.3) and thus $v_+ > 0$ and $v_- < 0$ (cf Sec. 5.2).

Description of main features of the work probability density for the generic scenario (cf Sec. 5.1) is given in [27]. Here we shall directly proceed to analysis of the work probability density for the limit cycle, $\rho_{\rm p}(t, w)$, given by Eq. (5.23). Within the expansion stroke the work probability density is given by linear combination of the functions $g_{ij}(w, 0, t, 0)$. As we see from equations (5.18)-(5.21) for the generic probability density for work, these functions has (common) finite support located within the interval $\langle -\tau, \tau\rangle$, i.e., $\langle -v_+ t, v_+ t\rangle$, which grows linearly with time t. Diagonal elements $g_{ii}(w, 0, t, 0)$ contain, in addition to continuous part located within the support, a singular part represented by delta functions located at the borders of the support. These delta functions correspond to those evolutions within which the system stays in one state. Specifically, weight of the delta function located at $\eta = \tau$ represents the probability that the system starts in the 1st state and remains there up to time t and similarly for the second delta function. The weight of the delta functions thus decrease with increasing time t. Actually, the delta function corresponding to the first level intuitively vanishes (the first level energy increases) and the weight of the second one reaches the asymptotic value $2\beta/(1+c)^a$. Within the compression stroke, the propagator which forms the work probability density is given by the integral of the propagators for the individual strokes (cf Eq. (5.22)).

After the integration the singular part of the propagator remains, however the delta functions are now located within the borders of the support at the positions $w = -v_+t_+ - v_-(t - t_+)$ and $w = v_+t_+ + v_-(t - t_+)$. The support is changed to $\langle -v_+t_+ + v_-(t - t_+), v_+t_+ - v_-(t - t_+)\rangle$. Interestingly, but not surprisingly, the probability density at the end of the limit cycle, $\rho_{\rm p}(t, w)$, contains only one delta function located at the point $w = 0$. The energies of the levels have simply returned to their initial values. Hand in hand with presence of the delta functions within the borders of the support is the non-singular part of the density no more continuous. The discontinuities are located just in the positions of the delta functions and their magnitudes correspond to the weights of the delta functions. FIG. 5.1, where we show the work probability density in four times within the limit cycle, demonstrates hereby described properties of the density.

Let us now discuss behaviour of the work probability density related to values of the reversibility parameters a_+ and a_-. If the both a_+ and a_- are small, the both branches of the cycle are strongly irreversible. There are three different reasons for small values of the reversibility parameters. For the readers convenience, we repeat the definitions $a = \nu/\Omega$, $\Omega = 2\beta v$. The reversibility parameter a is thus small in the following cases:

1. ν is small — the inter-attempt times are long and the occupation probabilities are effectively frozen.

2. β is big — the temperature of the contact reservoir is small and the occupation probabilities are again effectively frozen – the thermal fluctuations aren't big enough to disrupt any state of the system.

3. v is big — the energy levels are moving rapidly, the system lags behind the equilibrium state, and again, the occupation probabilities are effectively frozen.

As we stated in the preceding paragraph. The weights of the delta functions correspond to the probabilities of those trajectories which never change their initial state within the evolution. Because the occupation probabilities of the levels are nearly frozen for small values of a, we expect large weights of the delta functions in this irreversibility limit. Actually, from the equations (5.18)-(5.21) for a generic density immediately follows that in the limit $a \to 0$ the weights of the delta functions reach their maximum values and the non-singular part of the density vanishes.

If the both a_+ and a_- are big, the both branches of the cycle are close to equilibrium limit. It has been shown in [11] that, if the general process approaches its equilibrium limit, the work probability density assumes the Gaussian shape.

In our setting, the sharpness of the Gaussian shape growth with the reversibility parameters and in the equilibrium limit, the work probability density collapses into the delta function located at the reversible work, i.e.,

$$\lim_{a_+,a_-\to\infty} \rho_{\mathrm{p}}(t,w) = \delta(w - W_{\max}(t)) \ , \tag{5.37}$$

where (cf Eq. (4.43) and adjacent text)

$$W_{\max}(t) = \begin{cases} F(T_+,t) - F(T_+,0) & \text{for} \quad t \in \langle 0, t_+ \rangle \ , \\ \\ F(T_-,t) - F(T_-,t_+) + W_{\max}(t_+) & \text{for} \quad t \in \langle t_+, t_+ + t_- \rangle \ . \end{cases} \tag{5.38}$$

As we have seen in the previous section, the propagator for heat comes from the work propagator by a simple similarity transformation. Therefore the properties of the heat probability density must be similar to the properties of the density for work. However, there are some interesting differences.

Vaguely said, the work is done on the system when it sists on some energy level, the energy of which is changing (cf Eq. (4.24)). On the other hand, the heat is produced in the system when it jumps between the energy levels, when the amount of produced heat is proportional to the difference of the level energies at the instant of the jump (cf Eq. (4.25)). We didn't write exact equations for the heat propagator, however, using these ideas, we can easily describe the support of the density and also its singular and non-singular parts. First, the support of the heat density is determined by the biggest difference of the level energies during the evolution. Within the expansion stroke the energy difference growth and thus also the support expanses linearly with time as $\langle -2h_1 - 2v_+t, 2h_1 2v_+t \rangle$ up to its maximum value at the end of the stroke $\langle -2h_2, 2h_2 \rangle$. Within the compression stroke, the energy difference is decreasing and therefore the support remains the same as that at the end of the first stroke. Second, the delta functions in the work probability density correspond to those evolutions when the system doesn't change its state. Therefore, within such evolutions, couldn't be created any heat. Consequently, the singular part of the heat density consist from a single delta function located at the origin. The weight of this delta function equals to the sum of the weights of the delta functions form the work density. Another difference from the work density is that the non-singular part of the heat density isn't continuous in any time, i.e., not even within the first stroke. There is five discontinuities and four

of them lies in different points than the delta function. The non-singular part of the heat density therefore consists of six continuous parts separated by the discontinuities. The discontinuities corresponds to the borders of supports of the individual matrix elements of the heat propagator $\mathbb{Q}_{\mathrm{p}}(\omega, t)$. The fact that these elements have different supports is obvious from the transformation (5.31), because the elements of the work propagator have identical supports and every element is transformed with different shift function $u_{ij}(t)$ (cf Eq. (5.32)–Eq. (5.35)). This property of the supports can be also seen immediately from the definition of the matrix elements, linear driving scenario for the state energies and above described intuitive definition of heat. For example, the support of the density $q_{12}(\omega, 0, t, 0)$ necessarily begins at a point $E_1(0) - E_2(0)$ (minimal energy difference between the levels 1 and 2) and ends at a point $E_1(t) - E_2(t)$ (maximal energy difference between the levels 1 and 2). Similarly, we get the supports for other elements. Within the compression stroke, after the integration, the functional values of the matrix elements at the borders of the supports decrease. Therefore, within the first stroke, the discontinuities are pronounced better than within the second one. The only discontinuity which remains is the one located, with the delta function, at zero. This discontinuity is induced by the discontinuity of the work probability density. We show hereby described properties of the heat probability density in Fig. 5.2. This figure somehow supplements Fig. 5.1 where we show the work probability density calculated for the same parameters.

Behaviour of the heat probability density connected with values of the reversibility parameter a is also similar to the above described behaviour of the work density. In a case close to equilibrium (large a), each element of the work propagator $\mathbb{G}_{\mathrm{p}}(w, t)$ exhibits Gaussian shape and in the equilibrium limit $a \to \infty$ collapses into the delta function located at the position of the reversible work $W_{\max}(t)$. Therefore the individual elements of the heat propagator $\mathbb{Q}_{\mathrm{p}}(\omega, t)$ also exhibit Gaussian shapes for large values of a (but they have still different supports), and in the equilibrium limit, the elements collapse into delta functions located at the positions $u_{ij}(t) - W_{\max}(t)$. Thus, in the limit $a \to \infty$, the heat probability density consists only from the singular part represented by the four delta functions, while the mean value of the accepted heat is $U(t) - U(0) - W_{\max}(t)$. In the irreversible case the weight of the delta function located at the origin growth, and in the irreversible limit $a \to 0$ the density collapses into the single delta function, with the weight 1, located at zero.

In Fig. 5.3 we show the work and the heat probability densities for four representative shapes of the limit cycle, which are also included in the figure. In the row a) we chose that the bath of the expansion stroke is colder than that of

the compression stroke ($T_+ < T_-$). The reversibility parameters for both branches equals, $a_+ = a_- = 12.5$, and the both branches are, as can be seen from the shape of the limit cycle (the curves which forms the cycle are close to the equilibrium isotherms), not so far from equilibrium. In the row b) we have just exchanged the temperatures of the baths. Notice the change of the sign of the mean values of work and heat accepted by the engine per cycle. Oppositely to the row a), the cycle is now followed clockwise. The reversibility parameter for the first branch is big, $a_+ = 62.5$, and thus the system is within the first branch close to equilibrium. The parameter for the second branch is small, $a_- = 2.5$, and the system is within this stroke far from equilibrium. This facts can be again seen from the included p–E diagram. The row c) shows a strongly irreversible regime during the both branches ($a_+ = 1.25$, $a_- = 2.5$). The cycle is followed clockwise and the mean accepted work is positive (so the mean heat is negative). Finally, in the row d), we take a large difference in the duration of the strokes and the system communicates during the both strokes with the same bath. As follows from the theorem 4.4, the representative point follows the cycle clockwise and the accepted work is necessarily positive. The reversibility parameters within the branches are $a_+ = 25$ and $a_- = 1.25$, thus the system is close to equilibrium within the first branch and far from it within the second one.

Having in our hands the exact expressions for the probability densities, we are able to immediately calculate all one-time characteristics of the stochastic processes $\mathsf{W}(t)$ and $\mathsf{Q}(t)$ measuring the heat and the work accepted by the engine within the evolution. For example, all moments $\langle \mathsf{W}^n(t) \rangle$, $\langle \mathsf{Q}^n(t) \rangle$, $n = 1, 2, \ldots$, are accessible through a single integration

$$\langle \mathsf{W}^n(t) \rangle = \int_{-\infty}^{\infty} w^n \, \rho_{\mathrm{p}}(t, w) \, \mathrm{d}w \ , \tag{5.39}$$

$$\langle \mathsf{Q}^n(t) \rangle = \int_{-\infty}^{\infty} \omega^n \, \chi_{\mathrm{p}}(t, \omega) \, \mathrm{d}w \ . \tag{5.40}$$

As an example, we plot in figures 4.3–4.5 dependences of the variables $W(t) = \langle \mathsf{W}(t) \rangle$, $\sigma(-\mathsf{W}(t)) = -[\langle \mathsf{W}^2(t) \rangle - \langle \mathsf{W}(t) \rangle^2]$ and $\sigma(-\mathsf{W}(t))/t_{\mathrm{p}}$ on time t.

As we noted in Sec. 4.6, the mean work must, according to the second law of thermodynamics, fulfil the inequality $|W_{\max}(t)| > |W(t)|$. However, there of course exists some trajectories which violent this inequality (the second law of thermodynamics is often introduced by words: "For the system holds with big probability that ...", in the sense that this probability is big in the thermodynamic limit which isn't fulfilled in our setting). Using our exact work probability density, we can calculate the weight of those trajectories which violates the second law.

Specifically, in a case when $W_{\max}(t) > 0$ they can be calculated by the simple integration

$$\text{Prob}\,\{|\mathsf{W}(t)| > |W_{\max}(t)|\} = \int_{W_{\max}(t)}^{\infty} \rho_{\mathrm{p}}(t,w)\,\mathrm{d}w\ . \tag{5.41}$$

In a case when $W_{\max}(t)$ is negative, we just change the interval of integration to $(-\infty, W_{\max}(t))$.

In closing this chapter, we would like to describe few ways for testing correctness of our resulting work probability density $\rho_{\mathrm{p}}(t,w)$. We use four different methods. Three of them are obvious:

1. The normalisation condition. For the probability density obviously holds $\int_{-\infty}^{\infty} \rho_{\mathrm{p}}(t,w)\,\mathrm{d}w = 1\ \forall\, t \in (0,t_{\mathrm{p}})$.

2. The mean accepted work calculated from Eq. (4.26) (i.e., from the Pauli equation, which we can solve easily) must equals to that calculated as $\langle \mathsf{W}(t)\rangle = \int_{-\infty}^{\infty} w\,\rho_{\mathrm{p}}(t,w)\,\mathrm{d}w$.

3. The densities calculated by computer simulations, described in Appendix B, must agree with the exact ones.

The forth method uses the modern fluctuation theorems [4, 5, 6, 7, 8, 9, 10, 11, 12, 13, 14]. Specifically, our probability density must fulfil the so-called *Jarzynski relation* (for example [40, 27]) which holds for any isothermal nonequilibrium evolution under the condition that the system starts from the Gibbs equilibrium state corresponding to the inverse temperature of the reservoir β. The relation is

$$\left\langle \mathrm{e}^{-\beta \mathsf{W}(t)} \right\rangle = \mathrm{e}^{-\beta[F(t)-F(0)]}\ . \tag{5.42}$$

Here $F(t)$ is the Helmholtz free energy of the system at a time t. Therefore, if we consider only the generic work propagator Eq. (5.18)-Eq. (5.21) and the Gibbs equilibrium state $|\pi(t_0)\rangle$ as the initial state of the evolution, and we calculate the probability density from the equation $\rho(w,0,t,t_0) = \sum_{i=1}^{2} \langle i|\, \mathbb{G}(w,0,,t,t_0)\,|\pi(t_0)\rangle$, this density must fulfil

$$\int_{-\infty}^{\infty} \mathrm{e}^{-\beta w}\,\rho(w,0,t,t_0)\,\mathrm{d}w = \mathrm{e}^{-\beta[F(t)-F(t_0)]}\ . \tag{5.43}$$

Our exact solution of course passed through all above described test.

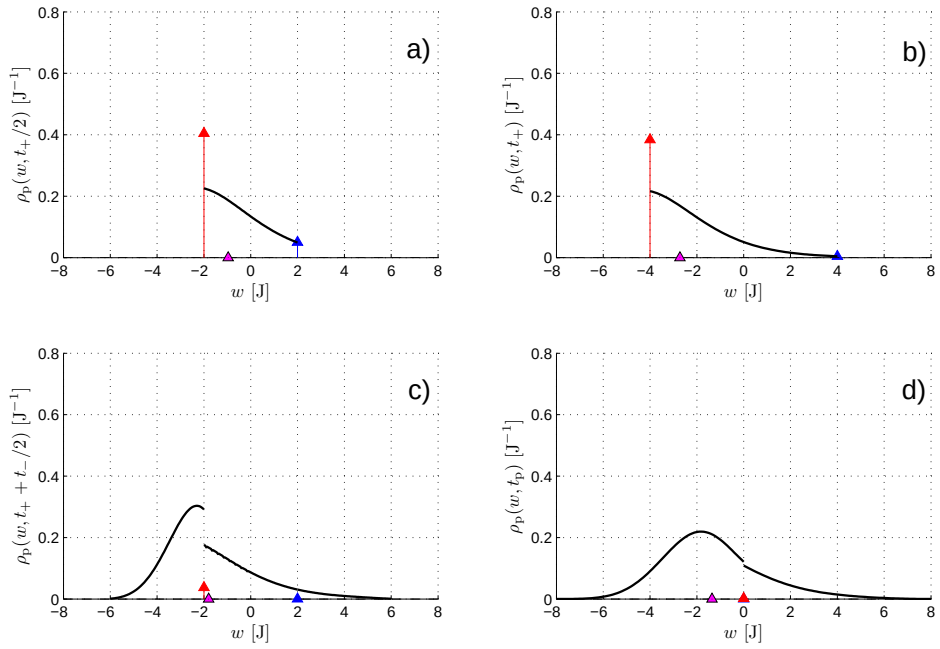

FIG. 5.1: The probability density for the work $\rho_{\rm p}(w,t)$ as the function of the work variable w and for four values of the observation time t. We have used the same parameters as in FIG. 4.2 with positive h_1. The panel a) illustrates the density at the middle of the expansion stroke, i.e. at $t = \frac{1}{2}t_+$. The panel b) shows the density at the end of the expansion stroke, at $t = t_+$. The panel c) depicts the density at one half of the compression stroke, i.e. at $t = t_+ + \frac{1}{2}t_-$. Finally, in the panel d), we observe the work probability density at the end of the limit cycle. The triangle situated on the work axis within the support indicates the instantaneous mean work $W(t)$ at the corresponding times. The singular parts of the density are depicted by the arrows and the heights of the arrows equal to the weight of the corresponding delta functions. For example, in the panel a), the height of the left arrow indicates the probability that the occupation of the lower level has not been changed from the beginning of the cycle to the observation time $t = \frac{1}{2}t_+$. This is also the probability that the accepted work assumes the negative value $-\frac{1}{2}(h_2 - h_1)$.

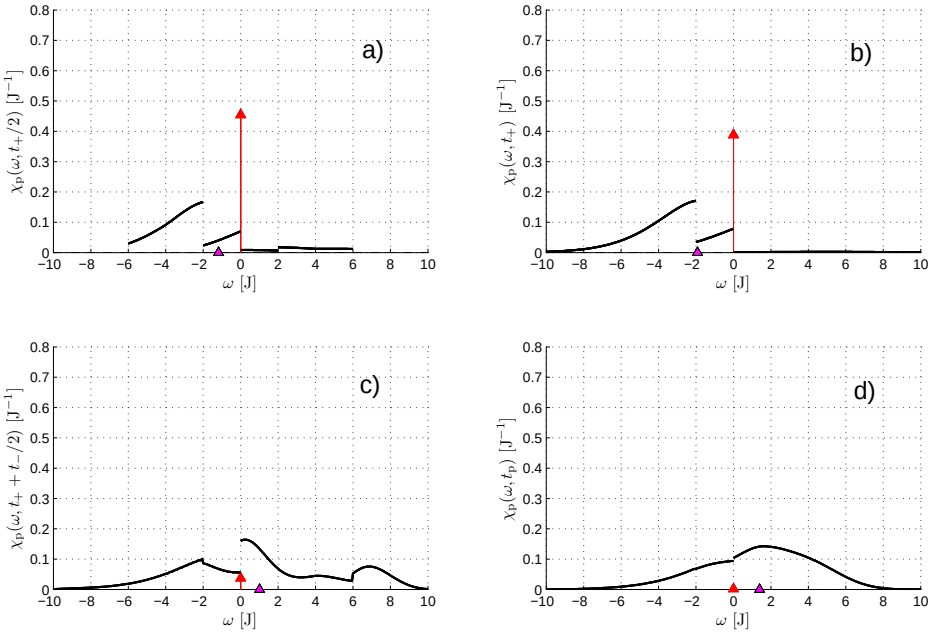

FIG. 5.2: The probability density for the heat $\chi_{\rm p}(w,t)$ as the function of the heat variable ω and for four values of the observation time t. For comparison with the work probability densities from FIG. 5.1, we have used the same parameters as in this figure. The panel a) illustrates the density at the middle of the expansion stroke, i.e. at $t = \frac{1}{2}t_+$. The panel b) shows the density at the end of the expansion stroke, at $t = t_+$. The panel c) depicts the density at one half of the compression stroke, i.e. at $t = t_+ + \frac{1}{2}t_-$. Finally, in the panel d), we observe the heat probability density at the end of the limit cycle. The triangle situated on the heat axis within the support indicates the instantaneous mean heat $Q(t)$ at the corresponding times. The singular part of the density is depicted by the arrow and the height of the arrow equals to the weight of the delta functions. For example, in the panel a), the height of the arrow indicates the probability that the occupation of the levels has not been changed from the beginning of the cycle to the observation time $t = \frac{1}{2}t_+$. This is also the probability that the accepted heat assumes the value 0.

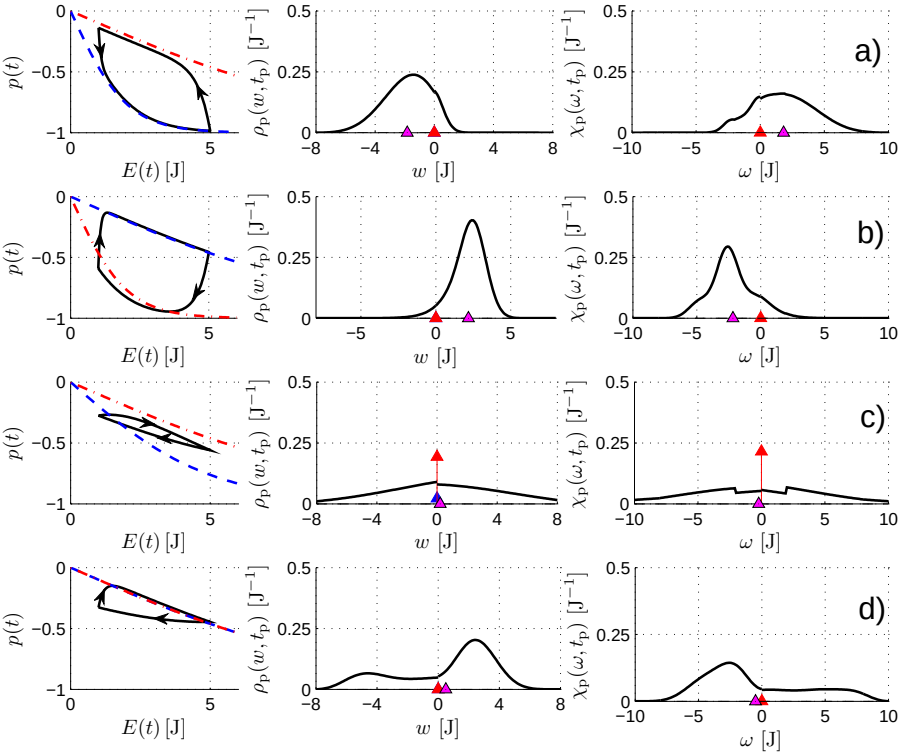

FIG. 5.3: The probability densities $\rho_{\mathrm{p}}(w, t_{\mathrm{p}})$ and $\chi_{\mathrm{p}}(\omega, t_{\mathrm{p}})$ as the functions of the work variable w and of the heat variable ω, respectively, for four representative sets of the engine parameters. For every set we also show the limit cycle in the $p-E$ plane. In all rows, we take $h_1 = 1$ J, $h_2 = 5$ J, and $\nu = 1\ \mathrm{s}^{-1}$. Further, the row a) has $t_+ = 50$ s, $t_- = 10$ s, $\beta_+ = 0.5\ \mathrm{J}^{-1}$, and $\beta_- = 0.1\ \mathrm{J}^{-1}$. Hence the bath of the expansion stroke is colder than that of the compression stroke. In the row b) we have just exchanged the temperatures of the baths: $t_+ = 50$ s, $t_- = 10$ s, $\beta_+ = 0.1\ \mathrm{J}^{-1}$, and $\beta_- = 0.5\ \mathrm{J}^{-1}$. Notice the change of the sign of the mean values. The cycle is now followed clockwise. The row c) shows a strongly irreversible regime during the both branches. The cycle is followed clockwise and the mean accepted work is positive (the mean heat is negative). The parameters are $t_+ = 2$ s, $t_- = 2$ s, $\beta_+ = 0.2\ \mathrm{J}^{-1}$, and $\beta_- = 0.1\ \mathrm{J}^{-1}$. Finally, in the row d), we take a large difference in the duration of the strokes and the system communicates during the both strokes with the same bath: $t_+ = 20$ s, $t_- = 1$ s, $\beta_+ = 0.1\ \mathrm{J}^{-1}$, and $\beta_- = 0.1\ \mathrm{J}^{-1}$. The representative point follows the cycle clockwise and the accepted work is necessarily positive.

Chapter 6

Conclusion and outlook

We have investigated a simple example of the microscopically based heat engine which is both physically transparent and exactly solvable. Specifically, we have investigated the engine performance characterised by the mean values which can be calculated from the Pauli equation. Moreover, we have calculated the work and the heat probability densities for the cycle which allow us to calculate also fluctuations of the mean values. Our resulting exact probability densities represent, as far as we know, first results of a kind in accessible literature and are, after recently discovered fluctuations theorems, the next step in investigations in the field of nonequilibrium thermodynamics. In Appendix B we also described simple method of computer simulations of time nonhomogeneous Markov process based on our path approach.

The present setting can be expanded in various directions. One can follow the time-dependent entropy and the entropy production. One can formulate various problems concerning the thermodynamic optimization. Another option would be the embodiment of additional (e.g., adiabatic) branches. The role of the working medium can be assigned to the more complicated systems (e.g., the particles diffusing on the semi-infinite line with the time-dependent drift) with a more complicated dynamics (e.g., a variant of the generalized master equation).

Another interesting field of possible research are the so-called "reward processes". Within these processes are measured waiting (inter-event) times for the individual states along individual trajectories of the system. From these waiting times are then calculated some quantities (the rewards). Actually, the work in our model with linearly driven energy levels is a kind of such reward process, with the rewards linearly dependent on the waiting times. However, studying of such processes gives nontrivial results even with the frozen, i.e., time independent, energy levels. Of course it would be interesting to investigate processes with a different

than the linearly dependent rewards on the waiting times. If the time dependence of the driving of the energy levels would be the same as the dependence of the rewards on the waiting times, we would get again probability density for work. However, as we have discussed in SEC. 5.1, this calculation could be very difficult.

Important goal is of course to generalise our calculations for transition rates which describe stretching of biomolecules, where the histogram of work is experimentally measurable. Important quantity measured within these stretching experiments is the so-called "counting statistics", which measures the probability of number of hoops folded-unfolded and back during the stretching experiments. Recently, there were published two articles [41, 42] where the counting statistics is, in some approximations, calculated. We believe that, using our path approach, we will be able to give at least for a two-level model exact result. This calculation is of our nearest interest. Some of the ensuing calculations are in progress and the results will be reported elsewhere.

Appendix A

The detailed calculation of the function $H(a;\eta,\tau)$

The fact that we could carry out the double inverse Laplace transformation of the auxiliary function (5.8) was crucial in calculation of the generic work probability density in Sec. 5.1. In this part we present details on the inversion procedure.

First of all, for the reader's convenience, we repeat the equation (5.8)

$$H(a;s,z)=\sum_{n=0}^{\infty}(-c)^n\frac{(s+b)_n}{(s)_{n+1}}\frac{(z+a)_n}{(z)_{n+1}}\ , \tag{A.1}$$

where $b=1-a$. In order to performing the inverse Laplace transformation, we try firstly to expand the rational functions $(s+b)_n/(s)_{n+1}$ and $(z+a)_n/(z)_{n+1}$ into the corresponding partial fractions. We obtain the expression

$$H(a;s,z)=\sum_{n=0}^{\infty}(-c)^n\sum_{k=0}^{n}\frac{(b-k)_n}{k!(n-k)!}\frac{(-1)^k}{s+k}\sum_{l=0}^{n}\frac{(a-l)_n}{l!(n-l)!}\frac{(-1)^l}{z+l}\ . \tag{A.2}$$

Now, the double inverse Laplace transformation is straightforward. the fractions $1/(s+k)$ and $1/(z+l)$ are transformed into $\Theta(\eta)\mathrm{e}^{-k\eta}$ and $\Theta(\tau)\mathrm{e}^{-l\tau}$, respectively. Thus the explicit form of the function $H(a;\eta,\tau)$ is

$$H(a;\eta,\tau)=\Theta(\eta)\Theta(\tau)\sum_{n=0}^{\infty}(-c)^n\sum_{k=0}^{n}\frac{(b-k)_n}{(n-k)!}\frac{(-\mathrm{e}^{-\eta})^k}{k!}\sum_{l=0}^{n}\frac{(a-l)_n}{(n-l)!}\frac{(-\mathrm{e}^{-\tau})^l}{l!}\ . \tag{A.3}$$

In principle, this complicated formula already represents an accomplishment of our goal. However, as we shall show further, this result can be written in a much more elegant form.

We start with following two steps. First, we take into account the factorization

$$H(a;\eta,\tau) = \Theta(\eta)\Theta(\tau)F(a;\eta,\tau) \ , \tag{A.4}$$

and, we focus on the calculation of the function $F(a;\eta,\tau)$. Second, noting that the function $F(a;\eta,\tau)$ depends on its variables only through the combinations $\mathrm{e}^{-\eta}$ and $\mathrm{e}^{-\tau}$, we denote them, for demands of this appendix, as x and y, respectively (don't mix up with the abbreviations (5.15) and (5.16) from the main text).

The detailed analysis of the summation on the right-hand side of (A.3) reveals the possibility to write the whole expression as a single matrix element of a certain infinite order matrix. More precisely, we introduce the so-called shift operators $\mathbb{E}_+$ and $\mathbb{E}_-$ with the matrix elements $\langle i|\,\mathbb{E}_+\,|j\rangle = \delta_{ij+1}$ and $\langle i|\,\mathbb{E}_-\,|j\rangle = \delta_{i+1j}$, $i,j = 0,1,\ldots$. In other words, the operator $\mathbb{E}_+$ ($\mathbb{E}_-$) has nonzero matrix elements only just below (above) the main diagonal. The shift operators don't commute and fulfil the following obvious relations

$$(\mathbb{E}_+)^i|0\rangle = |i\rangle, \qquad (\mathbb{E}_-)^i|j\rangle = \begin{cases} |j-i\rangle & \text{for } i \geq j \\ 0 & \text{for } i < j \end{cases} \qquad \text{with } i,j = 0,1,\ldots \ . \tag{A.5}$$

Finally, using the shift operators, the function $F(a;\eta,\tau)$, defined by the relations (A.3) and (A.4), can be written in the form

$$F(a;\eta,\tau) = \langle 0|\,\frac{1}{(1-d\mathbb{E}_-)^a}\frac{1}{(1-dy\mathbb{E}_-)^b}\frac{1}{(1+dx\mathbb{E}_+)^a}\frac{1}{(1+d\mathbb{E}_+)^b}\,|0\rangle \ , \tag{A.6}$$

where we have denoted $d = \sqrt{c}$. After a rather lengthy but purely algebraic rearrangement, we obtain an equivalent expression

$$F(a;\eta,\tau) = \frac{1}{x^a}\frac{1}{y^b}\langle 0|\frac{1}{1-d\mathbb{E}_-}\frac{1}{\{1-[(y-1)/y][1/(1-d\mathbb{E}_-)]\}^b} \times \frac{1}{\{1-[(x-1)/x][1/(1+d\mathbb{E}_+)]\}^a}\frac{1}{1+d\mathbb{E}_+}|0\rangle \ . \tag{A.7}$$

In the next step, we expand the second and the third operator into the corresponding power series, i.e., we use the formal expansions

$$\frac{1}{\{1-[(y-1)/y][1/(1-d\mathbb{E}_-)]\}^b} = \sum_{n=0}^{\infty}\frac{(b)_n}{n!}\left(\frac{y-1}{y}\right)^n\frac{1}{(1-d\mathbb{E}_-)^n} \ , \tag{A.8}$$

and

$$\frac{1}{\{1-[(x-1)/x][1/(1+d\mathbb{E}_+)]\}^a} = \sum_{m=0}^{\infty} \frac{(a)_m}{m!} \left(\frac{x-1}{x}\right)^m \frac{1}{(1+d\mathbb{E}_+)^m} \ . \qquad \text{(A.9)}$$

After substituting these expansions back into Eq. (A.7), we arrive at the formula

$$F(a;\eta,\tau) = \frac{1}{x^a}\frac{1}{y^b} \sum_{n=0}^{\infty}\sum_{m=0}^{\infty} \frac{(b)_n (a)_m}{n!m!} \times \left(\frac{y-1}{y}\right)^n \left(\frac{x-1}{x}\right)^m \langle 0| \frac{1}{(1-d\mathbb{E}_-)^{n+1}} \frac{1}{(1+d\mathbb{E}_+)^{m+1}} |0\rangle \ . \qquad \text{(A.10)}$$

We are faced with the matrix elements

$$\kappa_{mn}(v) = \langle 0| \frac{1}{(1-d\mathbb{E}_-)^{n+1}} \frac{1}{(1+d\mathbb{E}_+)^{m+1}} |0\rangle \ . \qquad \text{(A.11)}$$

We again expand the inverse operators in this equation into the corresponding power series. After this step we have

$$\kappa_{mn}(v) = \sum_{k=0}^{\infty}\sum_{l=0}^{\infty} \frac{(m+1)_k}{k!} \frac{(n+1)_l}{l!} d^k (-d)^l \langle 0| \left(\mathbb{E}_-\right)^k \left(\mathbb{E}_+\right)^l |0\rangle \ . \qquad \text{(A.12)}$$

Using the property $\langle 0| \left(\mathbb{E}_-\right)^k \left(\mathbb{E}_+\right)^l |0\rangle = \delta_{kl}$, $k,l = 0,1,\ldots$, which follows immediately from Eq. (A.5), the double summation in Eq. (A.12) reduces to the single one. The remaining summation can be identified with the Gauss hypergeometric series [38]. Using the standard notation, the explicit form of the functions (A.11) are

$$\kappa_{mn}(d) = \sum_{k=0}^{\infty} \frac{(m+1)_k}{k!} \frac{(n+1)_k}{k!} (-d^2)^k = \ {}_2\mathrm{F}_1\left(m+1, n+1; 1; -d^2\right) \ . \qquad \text{(A.13)}$$

All three parameters of the Gauss hypergeometric series are integers and thus it reduces into a polynomial in a more complicated variable. Actually, applying first the Euler transformation [38], we get

$$\kappa_{mn}(d) = {}_2\mathrm{F}_1\left(m+1, n+1; 1; -d^2\right) = \frac{1}{(1+d^2)^{n+1}} \ {}_2\mathrm{F}_1\left(-m, n+1; 1; \frac{d^2}{1+d^2}\right) = \frac{1}{(1+d^2)^{n+1}} \mathrm{P}_m^{(0,n-m)}\left(\frac{1-d^2}{1+d^2}\right) \ . \qquad \text{(A.14)}$$

Remembering that $d^2 = c$ and denoting $w = (1-c)/(1+c)$, we can insert this expression for the matrix elements (A.11) back into Eq. (A.10). We get the function $F(a;\eta,\tau)$ in the form

$$F(a;\eta,\tau) = \frac{1}{x^a}\frac{1}{y^b}\sum_{n=0}^{\infty}\sum_{m=0}^{\infty}\frac{(b)_n(a)_m}{n!\,m!}\left(\frac{y-1}{y}\right)^n\left(\frac{x-1}{x}\right)^m \times \frac{1}{(1+c)^{n+1}}\mathrm{P}_m^{(0,n-m)}(w)\ . \quad \text{(A.15)}$$

In this point, we profitably use known fact that the numbers $\mathrm{P}_m^{(0,n-m)}(w)$ can be represented as integrals in the complex plane [38]. In this representation the Jacobi polynomial $\mathrm{P}_m^{(0,n-m)}(w)$ is

$$\mathrm{P}_m^{(0,n-m)}(w) = \frac{1}{2\pi\mathrm{i}}\frac{1}{(1+w)^{n-m}}\oint\left[\frac{z^2-1}{2(z-w)}\right]^m\frac{(1+z)^{n-m}}{z-w}\,\mathrm{d}z\ , \quad \text{(A.16)}$$

where we integrate along the positively oriented closed contour around the point $z = w$, $w \in \langle 0,1\rangle$. Inserting the last expression into Eq. (A.15), changing the order of summation and integration, and further rearranging the terms, we obtain

$$F(a;\eta,\tau) = \frac{1}{(1+cx)^a}\frac{1}{(1+cy)^b}\frac{1}{2\pi\mathrm{i}}\oint\sum_{n=0}^{\infty}\sum_{m=0}^{\infty}\frac{(b)_n(a)_m}{n!\,m!} \times\left(\frac{1}{z-w}\right)^{n-m+1}\left(\frac{1-y}{1+cy}\frac{2c}{1+c}\right)^n\left(-\frac{1-x}{1+cx}\frac{1+c}{2}\right)^m\mathrm{d}z\ . \quad \text{(A.17)}$$

We now integrate the double series term by term. Invoking the residue theorem in the form $\oint(z-w)^{m-n-1}\,\mathrm{d}z = 2\pi\mathrm{i}\delta_{nm}$, all summands with $m \neq n$ vanish and the surviving terms yield

$$F(a;\eta,\tau) = \frac{1}{(1+cx)^a}\frac{1}{(1+cy)^b}\sum_{n=0}^{\infty}\frac{(a)_n(b)_n}{n!\,n!}\left(-c\frac{1-x}{1+cx}\frac{1-y}{1+cy}\right)^n\ . \quad \text{(A.18)}$$

On the right-hand side we again recognise the Gauss hypergeomtric series. Thus we have

$$F(a;\eta,\tau) = \frac{1}{(1+cx)^a}\frac{1}{(1+cy)^b}\ {}_2\mathrm{F}_1\left(a,b;1;-c\frac{1-x}{1+cx}\frac{1-y}{1+cy}\right)\ . \quad \text{(A.19)}$$

Remembering that $x = \mathrm{e}^{-\eta}$, $y = \mathrm{e}^{-\tau}$ and $b = 1 - a$, the final expression is

$$H(a;x,y) = H(a;\eta,\tau) = \Theta(\eta)\Theta(\tau)\frac{1}{(1+c\mathrm{e}^{-\eta})^a}\frac{1}{(1+c\mathrm{e}^{-\tau})^{1-a}} \\ \times\ {}_2\mathrm{F}_1\left(a,1-a;1;-c\frac{1-\mathrm{e}^{-\eta}}{1+c\mathrm{e}^{-\eta}}\frac{1-\mathrm{e}^{-\tau}}{1+c\mathrm{e}^{-\tau}}\right)\ . \quad \text{(A.20)}$$

This expression is used in main text and, for the reader's convenience, we repeat it in Eq. (5.9).

In closing the appendix, we would like to mention an alternative way to get the result (A.19). First notice that the variable of the Gauss function vanishes both at $x = 1$ ($\eta = w - w_0 = 0$) and $y = 1$ ($\tau = t - t_0 = 0$) and thus the whole Gauss function reduces to 1. In other words, our solution fulfils the boundary conditions

$$H(a;x,y)\Big|_{x\uparrow 1} = \frac{1}{(1+c)^a}\frac{1}{(1+cy)^b},\quad H(a;x,y)\Big|_{y\uparrow 1} = \frac{1}{(1+cx)^a}\frac{1}{(1+c)^b}\ , \quad \text{(A.21)}$$

where the arrows $\uparrow$ denote that the limits are taken from lower values. This conditions must be already incorporated in the system of equations (5.3).

On the other hand, one can perform the inverse Laplace transformation with respect to the variable s directly in the original system of equations (5.3). Then, considering the relations between the auxiliary function $H(a,x,y)$ and the elements f_{ij} (for example (5.11)) and performing some algebra, we can isolate a single hyperbolic partial differential equation [43] for the function $H(a,x,y)$. Specifically, the equation is

$$\left[(1+cxy)\frac{\partial}{\partial x}\frac{\partial}{\partial y} + cbx\frac{\partial}{\partial x} + cay\frac{\partial}{\partial y} + cab\right]H(a;x,y) = 0\ . \quad \text{(A.22)}$$

To get the solution of our problem, the equation must be supplemented by the boundary conditions (A.21). Thus we are looking for a function which both solves the hyperbolic differential Eq. (A.22) and fulfils the boundary conditions (A.21). Such problem is often referred to as *Gursa problem*. We have verified by direct substitution that our function (A.19) (and thus the function (A.20) as well) actually represents the (unique) solution of the boundary problem thereby formulated.

Appendix B

Computer simulation of a time nonhomogeneous Markov process

Simulation methods of time nonhomogeneous Markov processes are still insufficiently described in the present literature. In this chapter, we describe in detail two different methods. One of them was already suggested by Gillespie [44], however we offer new view into the method. The other one originates in our workshop.

The cornerstone of the derivation of the methods will be general form of the Pauli equation, which describes any time nonhomogeneous N-state Markov process. We shall introduce two different perturbative solutions of this equation. In the perturbative solutions, we will be able to identify terms corresponding to the probability density for the inter-event times of the Markov process and also terms corresponding to the transition probabilities between the individual states of the process. Having the probability density for the inter attempt times and the probabilities of the individual transitions, the simulation procedure is straightforward. First, we generate the inter-event time using the probability density. And than we decide the new state of the process using the transition probabilities at the generated inter-event time. The two simulation methods differs just in the specific realisation of these two points (see TAB. 2.1).

Actually, in EQ. (2.3), we have already stated one of the perturbative solutions of the Pauli equation. However, in the SEC. 2.1, we derived the Pauli equation from known probabilistic construction of the Markov process, i.e., from known probabilities of the inter-event times and of the individual transitions between the states. Now we will proceed reversely.

The general form of the Pauli equation 2.4 is

$$\frac{\mathrm{d}}{\mathrm{d}t}\mathbb{R}(t,t_0) = -\mathbb{M}(t)\mathbb{R}(t,t_0), \qquad \mathbb{R}(t_0,t_0) = \mathbb{I}\ . \tag{B.1}$$

Here the matrix $\mathbb{M}(t)$ is the transition rates matrix.

Let us consider the assumption that the probability is conserved during the evolution described by the Pauli equation (B.1), i.e., that $\sum_{i=1}^{N}\langle j|\,\mathbb{R}(t)\,|i\rangle = 1$, $\forall\, j,t$. We thus don't consider processes with traps and so on, where this assumption don't have to be valid. Then the rate matrix $\mathbb{M}(t)$ have the general form

$$\mathbb{M}(t) = \begin{pmatrix} \lambda_1(t) & \alpha_{12}(t) & \dots & \alpha_{1N}(t) \\ \alpha_{21}(t) & \lambda_2(t) & \ddots & \vdots \\ \vdots & \ddots & \ddots & \alpha_{N-1N}(t) \\ \alpha_{N1}(t) & \dots & \alpha_{NN-1}(t) & \lambda_N(t) \end{pmatrix}\ , \tag{B.2}$$

where $\lambda_j(t) = -\sum_{i\neq j}\alpha_{ij}(t) \geq 0$ and $\alpha_{ij}(t) \leq 0$, $\forall\, i \neq j$.

Let us now introduce the individual perturbative solutions of the Pauli equation. First, we offer method suggested by Gillespie [44].

B.1 Gillespie method

Consider the following decomposition of the rate matrix $\mathbb{M}(t) = \mathbb{D}(t) - \mathbb{O}(t)$. Here the matrix $\mathbb{D}(t) = \mathrm{diag}\{\lambda_1(t), \lambda_2(t), \dots, \lambda_N(t)\}$ contains the diagonal elements of the matrix $\mathbb{M}(t)$. And the matrix $\mathbb{O}(t)$ has zeros on the main diagonal and contains negatively taken off-diagonal elements of the matrix $\mathbb{M}(t)$, i.e., $\langle i|\,\mathbb{O}(t)\,|j\rangle = (\delta_{ij}-1)\alpha_{ij}$. The symbol δ_{ij} denotes the Kronecker delta. Obviously, all elements of elements of the matrices $\mathbb{D}(t)$ and $\mathbb{O}(t)$ are nonnegative. Moreover, we have $\lambda_i(t) = \sum_{j=1}^{N}\langle i|\,\mathbb{O}(t)\,|j\rangle$.

Now, we insert the decomposition of the rate matrix $\mathbb{M}(t)$ into the Pauli equation B.1. We get

$$\frac{\mathrm{d}}{\mathrm{d}t}\mathbb{R}(t,t_0) = [-\mathbb{D}(t) + \mathbb{O}(t)]\mathbb{M}(t)\mathbb{R}(t,t_0), \qquad \mathbb{R}(t_0,t_0) = \mathbb{I}\ . \tag{B.3}$$

Let us now suppose, for a moment, that the off-diagonal matrix $\mathbb{O}(t)$ vanishes. Then we get the equation $\frac{\mathrm{d}}{\mathrm{d}t}\mathbb{F}_{\mathrm{G}}(t,t_0) = -\mathbb{D}(t)\mathbb{F}_{\mathrm{G}}(t,t_0)$, $\mathbb{F}_{\mathrm{G}}(t_0,t_0) = \mathbb{I}$. The matrix $\mathbb{D}(t)$ is diagonal and thus we can immediately write the solution

$$\mathbb{F}_{\mathrm{G}}(t,t_0) = \exp\left[-\int_{t_0}^{t}\mathbb{D}(t')\,\mathrm{d}t'\right]\ . \tag{B.4}$$

Note that, because the matrix $\mathbb{D}(t)$ is nonnegative, the matrix $\mathbb{F}_{\mathrm{G}}(t,t_0)$ has all elements from the interval $\langle 0,1\rangle$, for all $t > t_0$. Moreover, for $t_1 > t_2$, we can write

$$\mathbb{F}_{\mathrm{G}}(t_1,t_2) = \mathbb{F}_{\mathrm{G}}(t_1,t_0)\mathbb{F}_{\mathrm{G}}^{-1}(t_2,t_0) = \exp\left[-\int_{t_2}^{t_1}\mathbb{D}(t')\,\mathrm{d}t'\right]. \tag{B.5}$$

Now, we proceed with the substitution $\mathbb{R}(t,t_0) = \mathbb{F}_{\mathrm{G}}(t,t_0)\mathbb{R}_{\mathrm{G}}(t,t_0)$, which we insert into the Pauli equation (B.1). We obtain the equation

$$\frac{\mathrm{d}}{\mathrm{d}t}\mathbb{R}_{\mathrm{G}}(t,t_0) = \mathbb{F}_{\mathrm{G}}^{-1}(t,t_0)\mathbb{O}(t)\mathbb{F}_{\mathrm{G}}(t,t_0)\mathbb{R}_{\mathrm{G}}(t,t_0), \qquad \mathbb{R}_{\mathrm{G}}(t_0,t_0) = \mathbb{I}\,. \tag{B.6}$$

This equation is equivalent with the integral formula

$$\mathbb{R}_{\mathrm{G}}(t,t_0) = \mathbb{I} + \int_{t_0}^{t}\mathrm{d}t_1\,\mathbb{F}_{\mathrm{G}}^{-1}(t_1,t_0)\mathbb{O}(t_1)\mathbb{F}_{\mathrm{G}}(t_1,t_0)\mathbb{R}_{\mathrm{G}}(t_1,t_0)\,. \tag{B.7}$$

This equation can be solved iteratively. The solution is

$$\begin{aligned}\mathbb{R}_{\mathrm{G}}(t,t_0) &= \mathbb{I} + \int_{t_0}^{t}\mathrm{d}t_1\,\mathbb{F}_{\mathrm{G}}^{-1}(t_1,t_0)\mathbb{O}(t_1)\mathbb{F}_{\mathrm{G}}(t_1,t_0)\\ &+ \int_{t_0}^{t}\mathrm{d}t_1\int_{t_0}^{t_1}\mathrm{d}t_2\,\mathbb{F}_{\mathrm{G}}^{-1}(t_1,t_0)\mathbb{O}(t_1)\mathbb{F}_{\mathrm{G}}(t_1,t_0)\mathbb{F}_{\mathrm{G}}^{-1}(t_2,t_0)\mathbb{O}(t_2)\mathbb{F}_{\mathrm{G}}(t_2,t_0) + \dots\,.\end{aligned} \tag{B.8}$$

Therefore the solution of the original Eq. (B.1) is

$$\begin{aligned}\mathbb{R}(t,t_0) = \mathbb{F}_{\mathrm{G}}(t,t_0) &+ \int_{t_0}^{t}\mathrm{d}t_1\,\mathbb{F}_{\mathrm{G}}(t,t_1)\mathbb{O}(t_1)\mathbb{F}_{\mathrm{G}}(t_1,t_0)\\ &+ \int_{t_0}^{t}\mathrm{d}t_1\int_{t_0}^{t_1}\mathrm{d}t_2\,\mathbb{F}_{\mathrm{G}}^{-1}(t,t_1)\mathbb{O}(t_1)\mathbb{F}_{\mathrm{G}}(t_1,t_2)\mathbb{O}(t_2)\mathbb{F}_{\mathrm{G}}(t_2,t_0) + \dots\,,\end{aligned} \tag{B.9}$$

where we have used Eq. (B.5). As we said before, the matrices $\mathbb{F}_{\mathrm{G}}(t',t'')$ has all elements from the interval $\langle 0,1\rangle$. Therefore the elements can be interpreted as probabilities. Our last task is to normalise the matrices $\mathbb{O}(t')$, $t' \in \langle t_0,t\rangle$ so their elements can be also interpreted as probabilities.

If we divide the elements in the individual columns of the matrix $\mathbb{O}(t)$ by the sum of the elements in the corresponding column, the resulting matrix will certainly be normalised. However, the matrix $\mathbb{D}(t)$ already contains the sums over the columns of the matrix $\mathbb{O}(t)$. Therefore, if we rewrite the matrix $\mathbb{O}(t)$ in the form $\mathbb{O}(t) = \mathbb{O}(t)\mathbb{D}^{-1}(t)\mathbb{D}(t)$, we can identify the product of the first two matrices

on the right-hand side as a matrix which has all elements in the unit interval. The matrix is

$$\mathbb{K}_{\mathrm{G}}(t) = \mathbb{O}(t)\mathbb{D}^{-1}(t) = \mathbb{I} - \mathbb{M}(t)\mathbb{D}^{-1}(t) \ . \tag{B.10}$$

Here we have used the definition of the original decomposition of the matrix $\mathbb{H}(t) = \mathbb{D}(t) + \mathbb{O}(t)$. After insertion of the matrix $\mathbb{O}(t) = \mathbb{K}_{\mathrm{G}}(t)\mathbb{D}(t)$ into the formula (B.9), we finally obtain the desired perturbative solution of the Pauli equation (B.1)

$$\begin{aligned}\mathbb{R}(t,t_0) = \mathbb{F}_{\mathrm{G}}(t,t_0) + \sum_{n=1}^{\infty} \int_{t_0}^{t} \mathrm{d}t_n \ldots \int_{t_0}^{t_2} \mathrm{d}t_1 \, \mathbb{F}_{\mathrm{G}}(t,t_n)\mathbb{K}_{\mathrm{G}}(t_n)\mathbb{T}_{\mathrm{G}}(t_n,t_{n-1}) \\ \times \mathbb{K}_{\mathrm{G}}(t_{n-1}) \ldots \mathbb{T}_{\mathrm{G}}(t_2,t_1)\mathbb{K}_{\mathrm{G}}(t_1)\mathbb{T}_{\mathrm{G}}(t_1,t_0) \ .\end{aligned} \tag{B.11}$$

Here we have denote as $\mathbb{T}_{\mathrm{G}}(t,t_0)$ the product

$$\mathbb{T}_{\mathrm{G}}(t,t_0) = \mathbb{D}(t)\mathbb{F}_{\mathrm{G}}(t,t_0) = \mathbb{D}(t) \exp\left(- \int_{t_0}^{t} \mathbb{D}(t') \, \mathrm{d}t' \right) \ . \tag{B.12}$$

The decomposition of the propagator $\mathbb{R}(t,t_0)$ is similar to that given in Eq. (2.3). We thus suppose that the corresponding terms in the equations (2.3) and (B.11) have similar interpretation. Really, according to Ref. [26], the elements of the diagonal matrix $\mathbb{T}_{\mathrm{G}}(t,t_0)$ can be interpreted as probability densities for inter-event times of time nonhomogeneous Poisson processes with intensities contained in the matrix $\mathbb{D}(t)$. More precisely,

$$\langle i| \, \mathbb{T}_{\mathrm{G}}(t,t_0) \, |i\rangle \, \mathrm{d}t = \mathrm{Prob} \, \{ \mathsf{T}_n - \mathsf{T}_{n-1} \in (t, t+\mathrm{d}t) \, | \, \mathsf{D}(t') = i \, \forall \, t' \in (t_0,t) \} \ . \tag{B.13}$$

Here and below, we recall the mark $\mathsf{D}(t)$ denoting the random variable "state of the Markov process at a time t" and the mark T_n denoting the random variable "time of the nth event of the Markov process" from Sec. 2.1.

Noting that the matrix $\mathbb{F}_{\mathrm{G}}(t,t_0)$ follows from the matrix $\mathbb{T}_{\mathrm{G}}(t,t_0)$ according to the simple formula $\mathbb{F}_{\mathrm{G}}(t,t_0) = 1 - \int_{t_0}^{t} \mathrm{d}t' \, \mathbb{T}_{\mathrm{G}}(t',t_0)$, the interpretation of the matrix $\mathbb{F}_{\mathrm{G}}(t,t_0)$ is immediate. Its elements just denote the probabilities that the Markov process remains during the time interval (t_0,t) in the same state. Finally, using the analogy with the Eq. (2.3), we can interpret the matrix $\mathbb{K}_{\mathrm{G}}(t)$ as the matrix that contains the probabilities of the transitions between the individual states of the Markov chain at the event time $\mathsf{T}_n = t$. Note that, because of the matrix $\mathbb{K}_{\mathrm{G}}(t)$ has zeros on the main diagonal, the chain changes its state at any attempt time with certainty.

The equations (B.10), (B.11) and (B.12) are the main results of this section. They represent the decomposition of the time nonhomogeneous Markov process into

the time nonhomogeneous Poisson point process described by the matrix $\mathbb{T}_{\mathrm{G}}(t, t_0)$ and the time nonhomogeneous Markov chain described by the matrix $\mathbb{K}_{\mathrm{G}}(t)$.

B.2 Chvosta–Holubec method

Having the rate matrix $\mathbb{M}(t)$ (Eq. (B.2)), our goal is to find the simulating method which allows us to simulate the evolution of the nonhomogeneous Markov process during a time interval $I_{\mathrm{obs}} = (t_0, t_{\mathrm{obs}})$. Above, we have seen that the elements of the rate matrix fulfil the relations $\lambda_j(t) = -\sum_{i \neq j} \alpha_{ij}(t) \geq 0$ and $\alpha_{ij}(t) \leq 0$, $\forall\, i \neq j$. Thus they are not bounded and their absolute values can't be interpreted as probabilities. Let us denote the largest element of the matrix $\mathbb{M}(t)$ within the evolution during the time interval I_{obs} as

$$\lambda = \max_{t \in I_{\mathrm{obs}}} \{m_{ij}(t)\}_{i,j=1}^{N} \ . \tag{B.14}$$

The matrix $\mathbb{M}(t)/\lambda$ has, during the time interval I_{obs}, already all elements from the interval $\langle -1, 1\rangle$. Therefore we can write $\mathbb{M}(t) = \lambda \mathbb{M}(t)/\lambda = \lambda[\mathbb{I} - \mathbb{K}_{\mathrm{P}}(t)]$. Here we have introduced the matrix

$$\mathbb{K}_{\mathrm{P}}(t) = \mathbb{I} - \frac{1}{\lambda}\mathbb{M}(t) \ . \tag{B.15}$$

Therefore, recalling the sings of the diagonal and off-diagonal elements of the matrix $\mathbb{M}(t)$, the elements of the matrix $\mathbb{K}_{\mathrm{P}}(t)$ are from the interval $\langle 0, 1\rangle$.

Let us insert the matrix $\mathbb{M}(t) = \lambda[\mathbb{I} - \mathbb{K}_{\mathrm{P}}(t)]$ into the Pauli equation (B.1). We obtain

$$\frac{\mathrm{d}}{\mathrm{d}t}\mathbb{R}(t, t_0) = [-\lambda\mathbb{I} + \lambda\mathbb{K}_{\mathrm{P}}(t)]\mathbb{M}(t)\mathbb{R}(t, t_0), \qquad \mathbb{R}(t_0, t_0) = \mathbb{I} \ . \tag{B.16}$$

From this point, we will proceed similarly as in Sec. B.1. The solution of the equation without the matrix $\lambda\mathbb{K}_{\mathrm{P}}(t)$ is

$$\mathbb{F}_{\mathrm{P}}(t, t_0) = \exp\left[-\lambda(t - t_0)\mathbb{I}\right] = \exp\left[-\lambda(t - t_0)\right]\mathbb{I} \ . \tag{B.17}$$

The matrix $\mathbb{F}_{\mathrm{G}}(t, t_0)$ has all elements from the interval $\langle 0, 1\rangle$. Moreover, for $t_1 > t_2$, we get

$$\mathbb{F}_{\mathrm{P}}(t_1, t_2) = \mathbb{F}_{\mathrm{P}}(t_1, t_0)\mathbb{F}_{\mathrm{P}}^{-1}(t_2, t_0) = \exp\left[-\lambda(t_1 - t_2)\right]\mathbb{I} \ . \tag{B.18}$$

Now, we proceed with the substitution $\mathbb{R}(t, t_0) = \mathbb{F}_{\mathrm{P}}(t, t_0)\mathbb{R}_{\mathrm{P}}(t, t_0)$, which we insert into the Pauli equation (B.1). We obtain the equation

$$\frac{\mathrm{d}}{\mathrm{d}t}\mathbb{R}_{\mathrm{P}}(t, t_0) = \mathbb{F}_{\mathrm{P}}^{-1}(t, t_0)\mathbb{K}_{\mathrm{P}}(t)\mathbb{F}_{\mathrm{P}}(t, t_0)\mathbb{R}_{\mathrm{P}}(t, t_0), \qquad \mathbb{R}_{\mathrm{P}}(t_0, t_0) = \mathbb{I} \ . \tag{B.19}$$

This equation is equivalent with the integral formula

$$\mathbb{R}_{\mathrm{P}}(t,t_0) = \mathbb{I} + \int_{t_0}^{t} \mathrm{d}t_1\, \mathbb{F}_{\mathrm{P}}^{-1}(t_1,t_0)\lambda\mathbb{K}_{\mathrm{P}}(t_1)\mathbb{F}_{\mathrm{P}}(t_1,t_0)\mathbb{R}_{\mathrm{P}}(t_1,t_0)\ . \tag{B.20}$$

The iterative solution of the above equation is

$$\mathbb{R}(t,t_0) = \mathbb{F}_{\mathrm{P}}(t,t_0) + \sum_{n=1}^{\infty}\int_{t_0}^{t}\mathrm{d}t_n \ldots \int_{t_0}^{t_2}\mathrm{d}t_1\, \mathbb{F}_{\mathrm{P}}(t,t_n)\mathbb{K}_{\mathrm{P}}(t_n)\mathbb{T}_{\mathrm{P}}(t_n,t_{n-1}) \times \mathbb{K}_{\mathrm{P}}(t_{n-1})\ldots\mathbb{T}_{\mathrm{P}}(t_2,t_1)\mathbb{K}_{\mathrm{P}}(t_1)\mathbb{T}_{\mathrm{P}}(t_1,t_0)\ . \tag{B.21}$$

Here we have denote as $\mathbb{T}_{\mathrm{P}}(t,t_0)$ the product

$$\mathbb{T}_{\mathrm{P}}(t,t_0) = \lambda\mathbb{F}_{\mathrm{P}}(t,t_0) = \lambda\exp\left[-\lambda(t-t_0)\right]\mathbb{I}\ . \tag{B.22}$$

The decomposition of the propagator $\mathbb{R}(t,t_0)$ is exactly the same as that given in Eq. (2.3). We have just changed the notation: $f(t-t_0)\,\mathbb{I} \leftrightarrow \mathbb{F}_{\mathrm{P}}(t,t_0)$, $\phi(t-t_0)\,\mathbb{I} \leftrightarrow \mathbb{T}_{\mathrm{P}}(t,t_0)$ and $\mathbb{K}(t) \leftrightarrow \mathbb{K}_{\mathrm{P}}(t)$. Thus the matrix $\mathbb{T}_{\mathrm{P}}(t,t_0)$ represents the probability density for the inter-event (inter-attempt) times for the time homogeneous Poisson process multiplied by the unite matrix. The matrix $\mathbb{F}_{\mathrm{P}}(t,t_0)$ represents the probability that no event occurs within the time interval (t_0,t) again multiplied by the unite matrix. And finally, the matrix $\mathbb{K}_{\mathrm{P}}(t)$ contains the probabilities for the transitions between the individual states of the Markov process at an event time $\mathsf{T}_n = t$.

The equations (B.15), (B.21) and (B.22) are the main results of this section. They represent the decomposition of the time nonhomogeneous Markov process into the time homogeneous Poisson point process described by the matrix $\mathbb{T}_{\mathrm{P}}(t,t_0)$ and the time nonhomogeneous Markov chain described by the matrix $\mathbb{K}_{\mathrm{P}}(t)$.

There are two main difference between the Gillespie method and the Chvosta–Holubec method. First, the inter-event times in the first method are generated by the nonhomogeneous Poisson process, which intensity, moreover differs for the individual states. Whereas in the Chvosta–Holubec method, the inter-event times are generated by the homogeneous Poisson process with the same intensity for all states. Second, having generated the inter-event time, in the Gillespie method the system changes its state with certainty. Whereas in the Chvosta–Holubec method, the system can remain in its present state (the matrix $\mathbb{K}_{\mathrm{P}}(t)$ can have nonzero diagonal elements). For the readers convenience, we summarise the main difference of the two methods in Tab. B.1.

	Inter-event time	Transition prob. matrix
Gillespie	Time nonhomomogen. Poisson point proc.	$\mathbb{K}_{\mathrm{G}}(t)$ – Eq. (B.10)
Ch.–H.	Time homogen. Poisson point proc.	$\mathbb{K}_{\mathrm{P}}(t)$ – Eq. (B.15)

Tab. B.1: Possible decompositions of the time nonhomogeneous Markov process. For the first decomposition see Eq. (B.11), for the second one see Eq. (B.21).

B.3 Algorithms

B.3.1 Gillespie algorithm

Description: In this subsection, we present the algorithm supposed by Gillespie [44]. The presented algorithm is actually a little bit different, however the main features of the original method remain preserved.

As a preparation for transparent description of the algorithm, let us describe briefly the two main steps of the simulation. First, the durations of the inter-event times in the individual states of the Markov process are dictated by the nonhomogeneous Poisson processes. These processes have intensities described by the elements of the matrix $\mathbb{D}(t)$ (cf Eq. (B.12)). The matrix $\mathbb{D}(t)$ contains the diagonal elements of the matrix $\mathbb{M}(t)$ (B.2). Specifically, $\mathbb{D}(t) = \mathrm{diag}\{\lambda_1(t), \lambda_2(t), \ldots, \lambda_N(t)\}$. Thus the intensity of the nonhomogeneous Poisson process which dictates the duration of the inter-event time in the ith state of the Markov process is $\lambda_i(t)$. According to Ref. [45], the inter-event time t for the process which is in the state i can be generated as $\int_{t_0}^{t} \lambda_i(t')\,\mathrm{d}t' = \ln(1/U)$. Here U is a random number from the unit-interval uniform distribution. Second, the transitions between the individual states are driven by the matrix $\mathbb{K}_{\mathrm{G}}(t)$ (cf Eq. (B.10)). Let us suppose that the generated transition time t is shorter than the time t_{obs}, when we want to stop the simulation. Moreover, let us suppose that the process is in the state i. Then the probability that the process changes its state to j is $\langle j|\,\mathbb{K}_{\mathrm{G}}(t)\,|i\rangle = [\mathbb{K}_{\mathrm{G}}(t)]_{ji}$. The simulation algorithm follows.

Algorithm:

1. Initialization. Set the variable j (the current state index) to the prescribed initial value $n_0 \in \{1, \ldots, N\}$, and set the variable t (the current time) to t_0. Set the variable t_{obs} (observation time) to some prescribed value.

2. Generate two random numbers U_1 and U_2 from the unit-interval uniform distribution [45].

3. Inter-event time generation. If the inequality $\ln(1/U_1) < \int_{t_0}^{\infty} \lambda_j(x)\,\mathrm{d}x$ is satisfied, then choose t' so that $\int_{t_0}^{t'} \lambda_j(x)\,\mathrm{d}x = \ln(1/U_1)$. Otherwise choose $t' = \infty$.

4. Transition generation. If $t' < t_{\mathrm{obs}}$, then choose n so that $\sum_{n'=1}^{n-1} [\mathbb{K}_{\mathrm{G}}(t')]_{n'j} < U_2 \leq \sum_{n'=1}^{n} [\mathbb{K}_{\mathrm{G}}(t')]_{n'j}$.

5. If $t' > t_{\mathrm{obs}}$, terminate the random walk in the level j. Otherwise replace t and j by $t + t'$ and n, respectively; then return to step 2.

As is seen from this procedure, the main difficulty appears in the step 4, where could be very difficult to find the time t' (particularly in the cases where the integral couldn't be calculated analytically and thus also the inter-event time t' must be obtained numerically).

B.3.2 Chvosta–Holubec algorithm

Description: As we stated above, this algorithm follows the same main steps as the previous one. We also generate the inter-event time and then we decide whether the system changes its state or not. The only difference is in the specific realisation of the individual steps (cf TAB. B.1).

Similarly to the previous subsection, let us now briefly describe the two main steps of the simulation. First, the durations of the inter-event times in the individual states of the Markov process are dictated by the homogeneous Poisson process. The intensity of the Poisson process is λ defined by EQ. (B.14) (cf EQ. (B.22)). According to REF. [45], the inter-event time t for the time homogeneous Poisson process with intensity λ can be generated as $t = -\ln(U)/\lambda$. Here U is a random number from the unit-interval uniform distribution. Second, the transitions between the individual states are driven by the matrix $\mathbb{K}_{\mathrm{P}}(t)$ (cf EQ. (B.15)). Let us suppose that the generated transition time t is shorter than the time t_{obs}, when we want to stop the simulation. Moreover, let us suppose that the process is in the state i. Then the probability that the process changes its state to j is $\langle j|\,\mathbb{K}_{\mathrm{P}}(t)\,|i\rangle = [\mathbb{K}_{\mathrm{P}}(t)]_{ji}$. The simulation algorithm follows.

Algorithm:

1. Initialization. Set the variable j (the current state index) to the prescribed initial value $n_0 \in \{1, \ldots, N\}$, and set the variable t (the current time) to t_0. Set the variable t_{obs} (observation time) to some prescribed value.

2. Generate two random numbers U_1 and U_2 from the unit-interval uniform distribution [45].

3. Inter-event time generation. Choose t' so that $t' = -\ln(U_1)/\lambda$.

4. Transition generation. If $t' < t_{\text{obs}}$, then choose n so that $\sum_{n'=1}^{n-1}[\mathbb{K}_{\text{P}}(t')]_{n'j} < U_2 \leq \sum_{n'=1}^{n}[\mathbb{K}_{\text{P}}(t')]_{n'j}$.

5. If $t' > t_{\text{calc}}$, terminate the random walk in the level j. Otherwise replace t and j by $t + t'$ and n, respectively; then return to step 2.

Note that the difficulty, which appeared in the 4th step of the Gillespie algorithm, isn't present here. Specifically, in the Chvosta–Holubec method, the inter-event times are generated by the time homogeneous Poisson process and therefore they can be obtained without any difficulties.

B.4 Applications and examples

Using the above described algorithms, we can simulate an evolution of the system for arbitrary time dependence of the transition rates Eq. (B.2), and thus also for any transition and driving scenario. The result of each such simulation will be an unique sequence of states and transition times, the path which the system can undergoes during its evolution. By repeating the simulation many times, we can obtain approximate values of probabilities of the individual paths (cf Eq. (2.1)). The accuracy of the results increases with the number of the simulations executed, say N_{MC}. In other words, for $N_{\text{MC}} \to \infty$ we get exact results.

Having the probabilities of all possible paths during the evolution, we can calculate the mean value for any path dependent variable, say $\mathsf{X}(t)$, using the obvious formula

$$\langle \mathsf{X}(t) \rangle = \sum_{\text{all trajectories}} \begin{pmatrix} \text{probability for} \\ \text{a trajectory} \end{pmatrix} \times \begin{pmatrix} \text{the value of the variable} \\ \mathsf{X}(t) \text{ for this trajectory} \end{pmatrix} . \quad \text{(B.23)}$$

For example, we can calculate the work probability density (here $\mathsf{X}(t) = \delta(\mathsf{W}(t, t_0) - w)$, cf Sec. 2.1). Vaguely said, we just "measure" (calculate) the accepted work along the individual trajectories and than sum up the probabilities for separate values of the work.

If we separate the individual paths into for subgroups according to their initial and final states, and than sum up all probabilities of the paths in the subgroups, we

get the probabilities that the system undergoes an evolution which departs from a given state and resides in another given state. In other words, we get the solution of the Pauli equation $\mathbb{R}(t, t_0)$, (cf Eq. (2.2)). If we measure the work along the individual trajectories separated in the subgroups, we get the propagator for work $\mathbb{G}(w, w_0, t, t_0)$, (cf Eq. (2.13)), and so on.

In the first example, we used the both simulation approaches for calculation of the solution of the Pauli equation (2.4). In this case, it is possible to get analytical relation for the time of the next step in the point 4 of the Gillespie algorithm. Thus the both algorithms don't differ a lot. The strength of the Chvosta–Holubec algorithm became visible in the cases when can't be solved the equation for the time of the next transition in the 4th step of the Gillespie algorithm and we thus would have to find this time also numerically. In this case, the Chvosta–Holubec method would be certainly the faster one. In further examples we use only the Chvosta–Holubec method.

In figures B.1 and B.2, we show results of simulations of the work probability density. For comparison with our exact results (cf Eq. (5.23)), we take in the both figures same parameters as in Fig. 5.3. The figures B.1 and B.2 differs just in its accuracy, i.e., in the number of runs of the simulations N_{MC}. Specifically, in Fig. B.1 we took $N_{\mathrm{MC}} = 10^4$ and in Fig. B.2 we took $N_{\mathrm{MC}} = 10^6$. Obviously, the line in the figure with lower accuracy is much less smother than the line in the more accurate figure. However, if we compare the simulated work probability densities with those exactly calculated in Fig. 5.3, we see that our exact results are sufficiently checked even with the less accurate simulation.

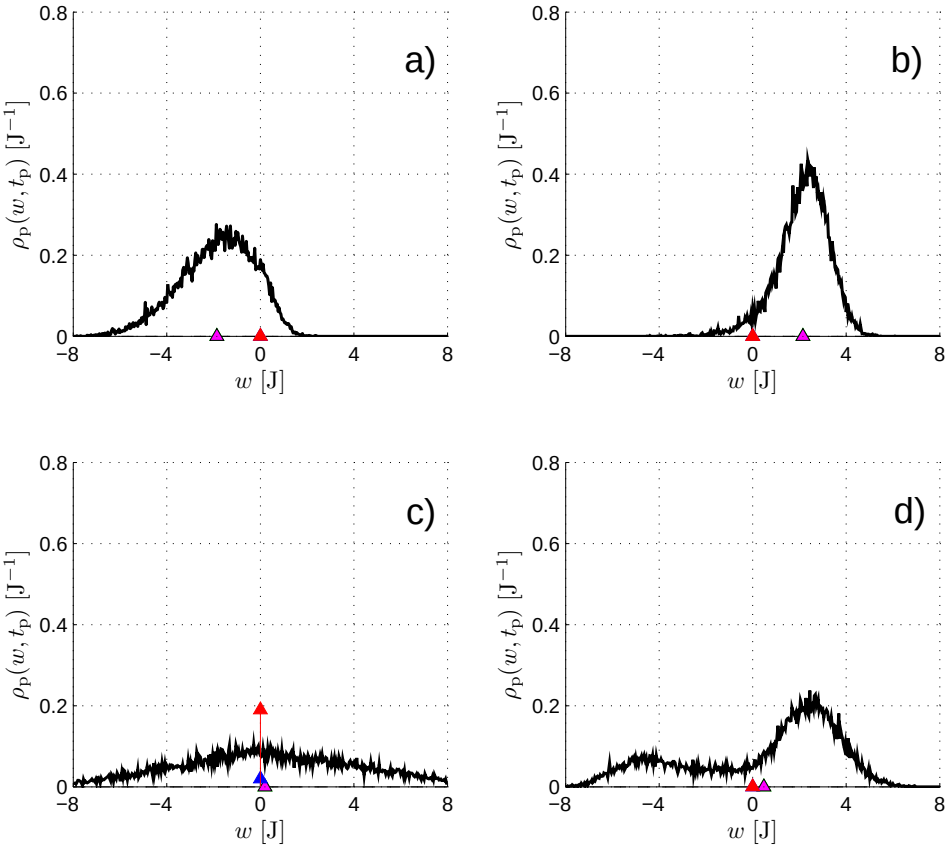

FIG. B.1: The simulated probability densities $\rho_{\mathrm{p}}(t, w)$ of the work accepted by the system during the cycle as the functions of the work variable w. For comparison with the exact results (cf EQ. (5.23)), we have used the same parameters as in FIG. 5.3. In these calculations, we have used relatively small number of Monte Carlo runs $N_{\mathrm{MC}} = 10^4$, but the resulting densities are still sufficiently accurate at least for the first check of the exact ones. For comparison, we offer results of more accurate simulations in FIG. B.2.

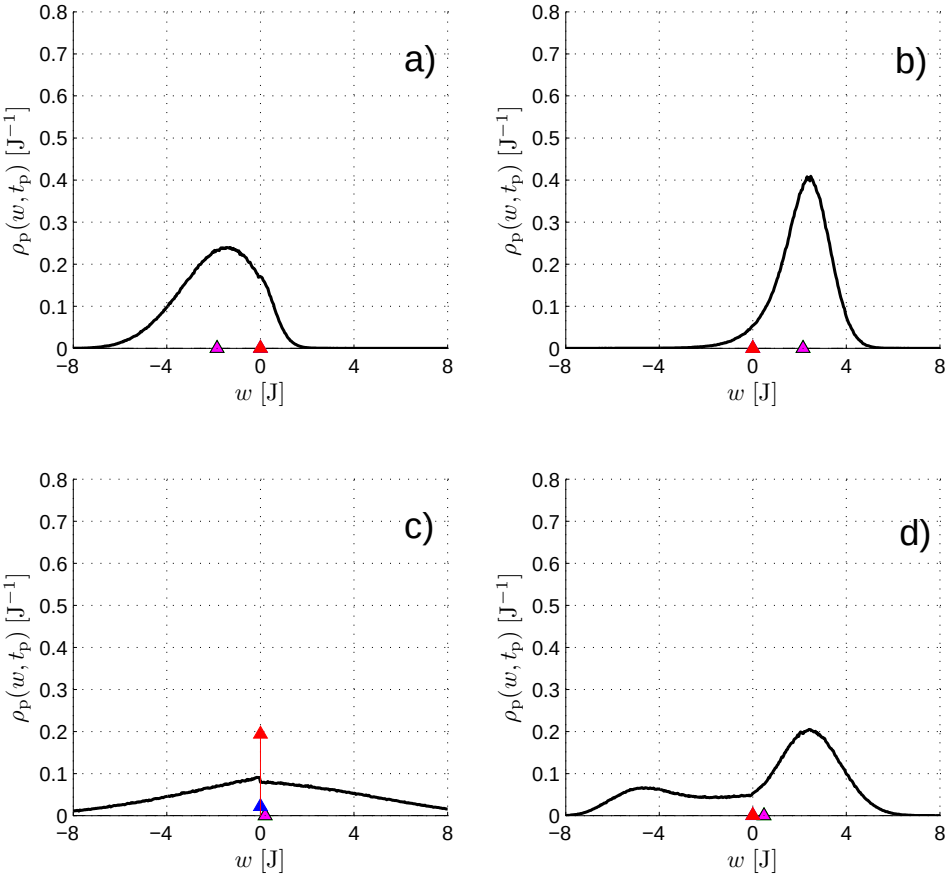

FIG. B.2: The simulated probability densities $\rho_{\mathrm{p}}(t, w)$ of the work accepted by the system during the cycle as the functions of the work variable w. For comparison with the exact results (cf EQ. (5.23)), we have used the same parameters as in FIG. 5.3. In these calculations, we have used big number of Monte Carlo runs $N_{\mathrm{MC}} = 10^6$. The resulting densities are definitely sufficiently accurate for checking of the exact ones. On a first look, one wouldn't recognise any difference. For comparison, we offer results of less accurate simulations in FIG. B.1.

Bibliography

[1] D. J. Evans and D. J. Searles, Adv. Chem. Phys. **51**, 1529 (2002).

[2] F. Ritort, Adv. Chem. Phys. **137**, 31 (2008).

[3] U. Seifert, Eur. Phys. J. B **51** (2008).

[4] G. N. Bochkov and Y. E. Kuzovlev, Physica A **106**, 443 (1981).

[5] D. J. Evans, E. G. D. Cohen, and G. P. Morriss, Phys. Rev. Lett. **71**, 2401 (1993).

[6] G. Gallavotti and E. G. D. Cohen, Phys. Rev. Lett. **74**, 2401 (1995).

[7] C. Jarzynski, Phys. Rev. Lett. **78**, 2690 (1997).

[8] G. E. Crooks, J. Stat. Phys. **90**, 1481 (1998).

[9] C. Maes, Sém. Poincaré **2**, 29 (2003).

[10] T. Hatano and S. Sasa, Phys. Rev. Lett. **86**, 3463 (2001).

[11] T. Speck and U. Seifert, Phys. Rev. E **70**, 066112 (2004).

[12] U. Seifert, Phys. Rev. Lett. **95**, 040602 (2005).

[13] S. Schuler, T. Speck, C. Tietz, J. Wachtrup, and U. Seifert, Phys. Rev. Lett. **94**, 180602 (2005).

[14] M. Esposito and S. Mukamel, Phys. Rev. E **73**, 046129 (2006).

[15] K. Sekimoto, F. Takagi, and T. Hondou, Phys. Rev. E **62**, 7759 (2000).

[16] C. van den Broeck, R. Kawai, and P. Meurs, Phys. Rev. Lett. **93**, 090601 (2004).

[17] T. Schmiedl and U. Seifert, Europhys. Lett. **81**, 20003 (2008).

[18] M. J. Henrich, F. Rempp, and G. Mahler, Eur. Phys. J. Special Topics **151**, 157 (2007).

[19] A. E. Allahverdyan, R. S. J. Johal, and G. Mahler, Phys. Rev. E **77**, 041118 (2008).

[20] F. L. Curzon and B. Ahlborn, Am. J. Phys. **43**, 22 (1975).

[21] N. G. van Kampen, *Stochastic Processes in Physics and Chemistry* (North Holland, Amsterdam, 1992).

[22] P. Chvosta, P. Reineker, and M. Schulz, Phys. Rev. E **75**, 041124 (2007).

[23] P. Chvosta and P. Reineker, Physica A **268**, 103 (1999).

[24] W. Feller, *An Itroduction to Probability Theory and its Applications Vol.1* (Wiley, New York, 1970).

[25] D. R. Cox, *Renewal Theory* (Wiley, New York, 1962).

[26] L. D. Snyder, *Random Point Processes* (Wiley, New York, 1975).

[27] E. Šubrt and P. Chvosta, J. Stat. Mech., P09019 (2007).

[28] G. E. Crooks, Phys. Rev. E **61**, 2361 (2000).

[29] L. Motl and M. Zahradník, *Pěstujeme Lineární Algebru* (Karolinum, Praha, 2003).

[30] N. Metropolis, A. W. Rosenbluth, M. N. Rosenbluth, A. H. Teller, and E. Teller, J. Chem. Phys. **21**, 1087 (1953).

[31] M. Creutz, L. Jacobs, and C. Rebbi, Phys. Rev. Lett. **42**, 1390 (1979).

[32] C. Michael, Phys. Rev. B **33**, 7861 (1986).

[33] R. J. Glauber, J. Math. Phys. **4**, 294 (1963).

[34] J. J. Bray and A. Prados, Phys. Rev. B **43**, 8350 (1991).

[35] A. Ryabov, Energetika molekulárních motorů, Bachelor Thesis, MFF UK, 2008.

[36] L. J. Slater, *Confluent Hypergeometric Functions* (Cambridge University Press, 1960).

[37] H. B. Callen, *Thermodynamics and an Introduction to Themostatistics* (John Wiley and Sons, New York, 1985).

[38] M. Abramovitz and I. A. S. (ed), *Handbook of Mathematical Functions* (New York, Dover, 1997).

[39] D. Voelker and G. Doetsch, *Die Zweidimensionale Laplace-transformation* (Birkhäuser, Basel, 1950).

[40] T. Speck and U. Seifert, J. Stat. Mech., L09002 (2007).

[41] A. Mossa, M. Manosas, N. Forns, J. M. Huguet, and F. Ritort, J. Stat. Mech., P02060 (2009).

[42] M. Manosas, A. Mossa, N. Forns, J. M. Huguet, and F. Ritort, J. Stat. Mech., P02061 (2009).

[43] N. S. Koshlyakov, M. M. Smirnov, and E. B. Gliner, *Differential Equations of Mathematical Physics* (North-Holland, Amsterdam, 1964).

[44] D. T. Gillespie, J. Comput. Phys. **28**, 395 (1978).

[45] D. E. Knuth, *The Art of Computer Programming II.* (Addison-Wesley, 1997).